# EXAMINATION OF IRRADIATED NEUROBLASTOMA AND NEUROEPITHELIAL CELL LINES FOR THE INTERRELATIONSHIP BETWEEN CELL SURVIVAL, MICRONUCLEATION, APOPTOSIS AND DNA REPAIR

**John Mbabuni Akudugu**


Dissertation submitted in fulfillment of the requirements for the degree of Doctor of Philosophy in Medical Sciences at the University of Stellenbosch.

June 2000

Supervisor:

Professor ELJF Böhm
Department of Radiation Oncology
Faculty of Medicine
University of Stellenbosch
South Africa

Co-Supervisor:

Dr. JP Slabbert
Radiobiology Section
National Accelerator Centre
Cape Town, South Africa

# Declaration

I, the undersigned, hereby declare that the work in this dissertation is my own original work and has not previously in its entirety or in part been submitted at any university for a degree.

Signature Date

# ABSTRACT

Predictive assays are of key importance in clinical radiotherapy, chemotherapy and toxicology. Prior to exposing malignant tissues to irradiation or drugs in the clinic, a good understanding of the damage response to the cytotoxic agent is required. Such information is necessary for effective planning and treatment. Regrettably however the methods which detect DNA damage, namely micronucleus, apoptosis and DNA repair assays do not rank cells according to their intrinsic survival response to cytotoxic agents. The application of predictive assays based on micronuclei and apoptosis in the clinic therefore remains unreliable. Using a panel of 7 neuroblastoma and 6 neuroepithelial cell lines, it is shown that damage assays also do not rank cell lines according to cell survival. However, radiosensitivity can be reconstructed from micronuclei formation and apoptosis, and a new parameter, cell death due to small deletions, chromosome aberrations and misrepair. The interrelationships between radiation-induced micronuclei, apoptosis and repair is complex and varies between cell lines. Micronuclei formation and apoptosis are exponentially interrelated. This suggests that these cell inactivation pathways are strongly correlated. Evidence exists to show that the expression of apoptosis and micronuclei is influenced by the extent of DNA double-strand break repair within the first 2 hours after irradiation. Cell lines which repair more damage in the first 2 hours express more micronuclei and less apoptosis. Micronuclei formation and apoptosis and are not significantly correlated with the 20 hours slow repair component. There is however a strong correlation

between 20 hours of repair and radiosensitivity, with the more radioresistant cell lines being more repair proficient. This suggests that the 2 hours (fast) DNA repair component is more error prone, and that cells lines repairing more damage late after irradiation tend to show better survival. In conclusion, micronuclei formation, apoptosis and DNA repair are strictly cell type specific and are not suitable for predicting radiosensitivity in terms of cell survival. However, these assays are very useful for studies on the influences of dose modifying agents i.e. oxygen tension, radiation modality, pH, cytotoxic sensitisers and radiation protectors which alter cellular responses and provide insight into damage mechanisms.

# OPSOMMING

Toetse wat kliniese gevolge kan voorspel is van uiterse beking in stralingsterapie, chemoterapie en toksikologie. Voordat kwaadaardige weefsels aan bestraling of chemise middels blootgestel can word in die kliniek, moet daar 'n goeie begrip van die skade weerstand wees van die selgiftige middel. Hierdie inligting is noodsaaklik vir effektiewe beplanning en behandeling. Ongelukkig stem die metodes wat DNS skade, apoptose en DNS hersteltoetse, nie ooreen met die selle se inherente straling sensitiwiteit nie. Die aanwending van voorspelbare toetse gebaseer op mikrokerne en apoptose in die kliniek bly dus onbetroubaar. Deur gebruik te maak van 'n paneel van 13 neurologiese sellyne, is daar bewys dat DNS skade toetse nie sellyne rangskik volgens sel oorlewing nie. Radiosensitiwiteit kan herbou word deur 'n neiging om mikrokerne te vorm, apoptose, en sel sterftes weens klein vermiste DNS volgordes, chromosoom aberrasies en verkeerd herstelde DNS. Die verhouding tussen straling-geïnduseerde mikrokerne, apoptose en sel-genees is kompleks en varieer tussen sellyne. Die ontstaan van mikrokerne en apoptose is eksponensiel verbind. Dit dui aan dat hierdie seltraagheidsbane streng gekorreleer word. Daar is bewys dat die uitdrukking van apoptose en mikrokerne deur die mate van herstel van die DNS dubbelstring-breuke binne die eerste 2 ure na bestraling beïnvloed is. Daar is gevind dat sellyne wat meer skade herstel binne die eerste 2 ure meer mikrokerne en minder apoptose toon. Die ontstaan van mikrokerne en

apoptose is nie betekenisvol gekorreleer met die 20-uur stadige herstel komponent nie. Daar is inderdaad 'n sterk korrelasie tussen die 20-uur herstel komponent en radiosensitiwiteit, en die meer radioweerstandbiedende sellyne net 'n hoër herstel bekwaamheid. Dit laat mens dink dat die 2 uur (vinnige) DNS herstel komponent meer geneig is om foutief te wees, en dat sellyne wat meer skade, laat na bestraling herstel, beter oorlewing toon. Ten slotte, die ontstaan van mikrokerne, apoptose en DNS herstel is strenggesproke seltipe spesifiek en is nie toepaslik om radiosensitiviteit, in terme van seloorlewing, te voorspel nie. Hierdie toetse is nuttig vir studies waar die invloed van dosismodifiseringsagente, soos suurstof-spanning, straling-tipe, pH, sitotoksieke sensiteerders en stralingsbeskermers, wat sellulêre gevoeligheid verander en insig gee tot skade meganismes.

# Dedication

I dedicate this study to →my wife Rose
→my daughter Elizabeth
→my son Elijah

# Acknowledgements

God does it all and I am very thankful for having been made His instrument to successfully carry out this research.

Sincere thanks to my wife, Rose, and our children, Elizabeth and Elijah, for maintaining my strength through motivating pictures, cards and letters, despite the distance of over 5000 km that separated us during this work. Their smiles and prayers really kept me going.

I thank my employer, the Ghana Atomic Energy Commission, for granting me a study leave to undertake this work.

I wish to extend my sincere gratitude to my colleagues Mr A Serafin, Dr A Binder, Mr WP Roos, Ms T Theron, Dr F Verheye-Dua, Dr J Michie and Mrs D Janssens for creating a fun and friendly atmosphere for the smooth execution of my work. Special thanks go to Mr A Serafin, Dr A Binder, Ms T Theron and Dr F Verheye-Dua for advice on experiments.

Dr JP Slabbert of the South African National Accelerator Centre (NAC) played an important role in providing methodology and for encouraging this study. The help of Mr BS Smit, Dr DTL Jones, Mr AN Schreuder, Mr JE Symons, Mr EA de Kock and the Radiographers of NAC is also acknowledged.

My sincere gratitude goes to my GNLD friends, especially Mr and Mrs Vorster, Mr and Mrs van Vuuren, Ms A Musah, Mr and Mrs van Zyl and Ms L Mboyi. The positive atmosphere that prevailed at our regular meetings always energized the light in me when everything seemed so bleak. Staying around these positive friends really made the seemingly rough journey enjoyable.

The encouragement from Prof F Dakorah (Department of Botany, UCT) and the family of Dr N Biekpe (University of Stellenbosch Business School) is greatly appreciated.

Last but not least, I am deeply indebted to my supervisor Prof ELJF Böhm for suggesting this topic and for his constructive guidance and criticisms. His constant motivation to obtain financial support is also acknowledged. This work was supported by grants and fellowships to Prof Böhm from the South African National Research Foundation (NRF), the Cancer Association of South Africa (CANSA) and VW Stiftung (Germany). A fellowship made available by Prof Sharpey-Schaefer of the South African National Accelerator Centre (NAC) is also acknowledged.

# Contents

# LIST OF TABLES

# LIST OF FIGURES

# LIST OF ABBREVIATIONS

$\alpha_\gamma$: linear coefficient of inactivation after $^{60}$Co $\gamma$-irradiation.

$\alpha_n$: linear coefficient of inactivation after p(66/Be$^+$) neutron irradiation.

$\beta_\gamma$: quadratic coefficient of inactivation after $^{60}$Co $\gamma$-irradiation.

$\beta_n$: quadratic coefficient of inactivation after p(66/Be$^+$) neutron irradiation.

$(\alpha/\beta)_\gamma$: ratio of the linear to the quadratic coefficients of inactivation for $^{60}$Co $\gamma$-irradiation.

$(\alpha/\beta)_n$: ratio of the linear to the quadratic coefficients of inactivation for p(66/Be$^+$) neutron irradiation.

BNC: binucleated cell(s).

$\overline{D}_\gamma$: mean inactivation dose after $^{60}$Co $\gamma$-irradiation.

$\overline{D}_n$: mean inactivation dose after p(66/Be$^+$) neutron irradiation.

EDTA: ethylene diamine tetra-acid (disodium salt).

$\xi$: coefficient for cell inactivation via apoptosis after $^{60}$Co $\gamma$-irradiation.

GABA: $\gamma$-amino-n-butyric acid.

LET: linear energy transfer.

$-\ln SF_\gamma$: number of lethal lesions induced by $^{60}$Co $\gamma$-irradiation.

L-Q: linear-quadratic.

MN: micronucleus/micronuclei.

$MNF2_\gamma$: micronuclei frequency at 2 Gy of $^{60}$Co $\gamma$-irradiation.

$\mu_\gamma$: coefficient for cell inactivation via micronuclei formation after $^{60}$Co $\gamma$-irradiation.

$NNDF_\gamma$: normal nuclear division fraction upon $^{60}$Co $\gamma$-irradiation.

$NNDF_n$: normal nuclear division fraction upon p(66/Be$^+$) neutron irradiation.

$\overline{NDF}$: area under NNDF-dose response curves.

PBL: peripheral blood lymphocytes.

PENT: pentoxifylline.

$P_{oe}$: probability for reproductive cell death.

RBE: relative biological effectiveness.

$RBE_{SF2}$: RBE calculated from SF2 values.

$RBE_{\alpha}$: RBE calculated from $\alpha$-coefficients.

$RBE_{\alpha/\beta}$: RBE calculated from $\alpha/\beta$ ratios.

$RBE_{\overline{D}}$: RBE calculated from $\overline{D}$ values.

$RBE_{\overline{NDF}}$: RBE calculated from the areas under the NNDF-dose response curves.

$SF2_{\gamma}$: surviving fraction at 2 Gy of $^{60}Co$ $\gamma$-irradiation.

$SF_{MA}$: surviving fraction derived from micronucleation and apoptotic data.

$SF_{col}$: surviving fraction derived from colony forming data.

TP53: tumour-suppressor protein 53.

# CHAPTER 1

# INTRODUCTION

## 1.1 Relevance of Radiobiological Studies on Tumour Cell Lines

Radiotherapy produces a wide variety of local and systemic responses in normal tissues. The radiation response consists of acute and late components. Malignant tissues are more radioresistant than the surrounding normal tissues. The degree to which normal tissue is spared in radiotherapy would, therefore, be influenced by the radiosensitivity of the malignant tissue. The need to spare normal tissue has led to the use of differential radiosensitivity as a prognostic factor for the radiotherapy of cancer (Hall *et al.* 1986, Weichselbaum *et al.* 1989, West *et al.* 1993). Presumably, the treatment of a more sensitive tumour would lead to a higher level of normal tissue sparing and vice versa.

*In vitro* studies on different tumour cells show a wide variation in radiation response ranging from the radiosensitive lymphomas, seminomas and neuroblastomas to the resistant melanomas and glioblastomas (Arlett *et al.* 1980, Fertil *et al.* 1984, 1985, Peacock *et al.* 1988, Weichselbaum *et al.* 1989).

Glioblastomas tend to be refractory to radiotherapy as reflected by their poor prognosis in clinical trials (Loeffler *et al.* 1990, Hartsell *et al.* 1997). These clinical results have been supported by *in vitro* studies which show high radiation resistance in glioblastoma cell lines (Fertil and Malaise 1984, Budach *et al.* 1997). The high rate of recurrence in brain tumours, especially astrocytomas, has been attributed to tumour cell migration (Halperin *et al.* 1988, Giese *et al.* 1994). Metastasis is one of the main reasons for the poor clinical outcome in the treatment of head and neck tumours with radiation.

Cellular resistance to irradiation either *in vitro* or in clinical radiotherapy has been known to depend on several factors. The susceptibility of a cell line or tissue to express the so-called programmed cell death or apoptosis is known to influence its radiosensitivity (Stephens *et al.* 1991, Tauchi and Sawada 1994, Olive *et al.* 1996, Hu and Hill 1996). A tissue's ability to adequately repair damage also determines its overall response to irradiation (Fertil and Malaise 1981, 1985, Wlodek and Hittelman 1988b, Durante *et al.* 1998, Dolling *et al.* 1998). The proliferative state of any cell type or tissue would influence its response to radiation damage and its subsequent survival level (Fowler 1986, Begg *et al.* 1990, Budach *et al.* 1997).

Other factors which regulate the cellular response to radiation damage are the bioenergetics and the level of oxygenation (Pettersen *et al.* 1977, Höchel *et al.* 1991, 1993, Zywietz *et al.* 1995, Nordsmark *et al.* 1996). It has been suggested that the high irradiation resistance in neuroepithelial tumours could arise from

low oxygen concentration and low levels of lipid peroxidation in the target tissue, since high levels of these factors facilitate neuronal death (Busciglio and Yankner 1995). Vaupel and co-workers, however, found no significant differences between the distribution of oxygen in normal brain and brain tumours (Vaupel *et al.* 1996).

Environmental and growth factors can also influence radiosensitivity. The presence of a platelet-derived growth factor has been found to modify the expression of radiation-induced apoptosis in human prostate cancer cells (Kim *et al.* 1997). Changes in environmental pH have been shown to significantly affect the level of radiation-induced apoptosis and therefore the level of survival in mouse mammary adenocarcinoma cells (Lee *et al.* 1997).

These factors would influence the biological effectiveness of radiation and hence the net tissue response, although the complexity of tissue response is nonetheless often compounded by inter-patient variability. Radiobiological and cell biological studies which could elucidate the intricate mechanisms of cellular responses have become desirable. Indeed, such information would be very useful in the management or control of head and neck tumours, which remain very difficult to treat and which have defied all efforts in the clinic. The outcome of tumour therapy, by irradiation or drugs or a combination of the two approaches, greatly depends on a successful diagnosis and the choice of treatment.

## 1.2 Predictive Assays for Irradiation and Drug Toxicity

When deciding on the particular predictive assay to use prior to therapy, several factors come into play. An ideal predictive assay should be easy to perform, widely applicable, rapid, ethical, inexpensive, reproducible and reliable. In a review, Peters and co-workers categorised predictive assays into two broad groups: those assessing cellular radiosensitivity and drug toxicity, and those involving the assessment of factors that influence cellular response to drugs and radiation (Peters *et al.* 1986). Some of the techniques under these categories are briefly discussed in the following sections.

### 1.2.1 Assessment of Cellular Radiosensitivity and Drug Toxicity

Assays for establishing cellular radiosensitivity and response to drug treatment can be either direct or indirect (Peters *et al.* 1986). Direct methods include *in vitro* or *in situ* cell survival assays such as colony formation, vital dye staining and xenograft assays. Indirect indicators of cellular response to radiation or drugs are those that assess damage and damage repair. These indicators are based on the notion that a cell's ability to efficiently repair damage would greatly influence its overall survival. Examples of indirect assays are the micronucleus assay, assessment of chromosome aberrations, analysis of the suppression of DNA synthesis and cell proliferation, the apoptosis assay and the assessment of DNA strand breaks and repair.

#### 1.2.1.1 Cell Survival Assays

Cell viability determined by cell survival would measure whether a cell line or tissue would be sensitive or resistant to a particular cytotoxic treatment. When cells are subjected to damaging agents, the sustained damage may be repaired and the cells would then proceed in the cell cycle, and preserve their reproductive integrity. In the event of inadequate repair, the cells enter apoptotic pathways and are eliminated. The surviving cells can be detected by the dye staining or by the colony assay. More resistant cell types would show higher levels of survival than sensitive cells.

##### 1.2.1.1.1 Vital-Dye Staining Assay

Vital-dye staining assays such as the "crystal violet" assay work on the principle that cells that are viable after cytotoxic treatment would take up the dye or metabolise or interact with a dye precursor to produce positive staining. Ideally, the amount of dye picked up is directly proportional to the number of viable cells (Brock *et al.* 1990). It is therefore possible to determine the proportion of cells surviving the induced damage. This assay is an easy option for assessing cell survival in non-clonogenic cell lines.

This technique has a number of shortcomings. Cell debris or even components of the culture medium, if not adequately rinsed off, tend to pick up the dye. Besides, all living cells are detected irrespective of whether they are dividing or residing in $G_0$. For these reasons, vital-dye staining assays usually lead to an overestimation of reproductively viable cells (Brock *et al.* 1990). If cultures

are left to grow over too long periods, some cells float-off at confluence resulting in reduced dye uptake and low levels of survival. On the other hand, if a particular cell type does not float off at confluence, cells may stop proliferating and this would diminish the differential between treated and untreated samples. Cell types that grow in suspension or exhibit low anchorage in culture are not suitable for this assay.

#### 1.2.1.1.2 Colony Assay

This technique assesses reproductive integrity in response to cytotoxic agents or irradiation (Puck and Marcus 1956). The colony assay has become widely accepted as the gold standard for determining radiosensitivity and drug toxicity (Barranco *et al.* 1971, Rockwell and Kallman 1973, Pourreau-Schneider and Malaise 1981, Palcic and Skarsgard 1984, Chen *et al.* 1984, Dertinger *et al.* 1984, Stuschke *et al.* 1992, Warenius *et al.* 1994, Skarsgard *et al.* 1994, 1996, Budach *et al.* 1997, Tsuboi *et al.* 1998). This assay measures the cell's capacity to retain its reproductive integrity in response to toxins and to genotoxic stress. The assay requires that cells are dividing and that they pass through 5-10 post-treatment mitoses and continue to form viable colonies or clusters of at least 50 cells (visible or detectable microscopically). Colonies which consist of too few cells, at the termination of an investigation, are considered to have lost their reproductive integrity and are therefore not scored as survivors. This approach is therefore not convenient for primary cell cultures or fresh biopsies that are usually characterized by very low plating efficiencies and poor ability to form colonies (Rockwell 1985).

Non-adherent cell types or those that exhibit poor anchorage are also not suitable for this method, since mild physical disturbances can detach colonies during sample preparation and lead to low levels of survival. Cell types which tend to spread in culture instead of aggregating in clusters are not ideal for the conventional clonogenic assay, and a modified approach using thin layers of soft agar is used (Courtenay and Mills 1978, Stuschke *et al.* 1992, 1993). Another disadvantage of the colony assay is the relatively long incubation periods, which may require 1-2 weeks (Villa *et al.* 1994, Budach *et al.* 1997, Guo *et al.* 1998, Juckett *et al.* 1998, Coco Martin *et al.* 1999, Akudugu *et al.* 2000), or even longer (Stuschke *et al.* 1992, Villa *et al.* 1994), depending on the cell type.

#### 1.2.1.1.3 Xenograft Assay

Xenografts are human tumour biopsies transplanted in immune-deficient animals. The aim of this technique is to mimic the *in vivo* characteristics in the donor. Normally, genetically athymic or "nude" mice, or animals in which the immune response has been suppressed by drugs or whole-body irradiation, are used for xenografts (Rofstad and Brustad 1981, Selby and Courtenay 1982, Dertinger *et al.* 1984, Steel *et al.* 1983). The main strength of this assay is that human karyotypes are usually maintained.

The shortfalls of the procedure, however, are that the tumour may be rejected by the recipient or undergo kinetic changes and cell selection. These changes

can lead to significant differences between the responses of the xenografts and the original tumours. Furthermore, while the histological properties of the human tumour may be maintained by the xenograft, the stromal tissue is of mouse origin and this would affect any endpoint that is influenced by the vascular microenvironment (Mantyla *et al.* 1982, Zywietz 1990, Zywietz *et al.* 1995). Although this technique proves to be capable in ranking a variety of human tumour types in the order of clinical responsiveness, certain tumour types particularly breast and ovarian tumours have been difficult to graft.

These complexities and difficulties have been adequately addressed by an *in vitro* system in which cells are forced to grow in suspension. After each mitosis, the daughter cells stick to each other to form a spherical lump of cells, otherwise known as a spheroid (Sutherland *et al.* 1970, 1971, Yuhas *et al.* 1978, 1984). Depending on the cell type, a spheroid may mature, with a diameter of the order of 700 μm, after a fortnight. Spheroids are a suitable model tumour system since they contain a heterogeneous population of cells. These systems are simpler, more reproducible, cheaper and easier to manipulate than xenografts. A spheroid mimics the characteristics of a growing tumour like cell-to-cell contact and nutritional stress from diffusion limitations, and even forms central necrosis in the course of time (Sutherland *et al.* 1986). The main limitation in using this system is that not all cell types are capable of forming spheroids in suspension.

### 1.2.1.2 Micronucleus Assay

The micronucleus concept originated over 130 years ago when Neumann discovered small rounded structures in the cytoplasm of erythrocytes that stained like the nucleus (Neumann, 1869). The phenomena which are responsible for the production of micronuclei have been under investigation for a long time (Howell 1891, Jolly 1907, Discombe 1948, Brenneke 1937, Thoday 1951, Evans *et al.* 1959). Mouse and rat embryos (Brenneke, 1937) and *Vicia faba* (Thoday, 1951) were introduced into the micronucleus study more recently.

The idea that micronuclei may reflect cytogenetic damage caused by irradiation is not new (Boller and Schmid 1970, Heddle 1973). The suggestion that micronucleus formation may reflect chromosomal damage in lymphocytes was also introduced in 1976 (Countryman and Heddle 1976). At this time, the major shortfall of this assay was that it did not distinguish between proliferating and non-proliferating cells. The assay was revolutionized when cytochalasin B was introduced. This drug blocks cells in cytokinesis. Cells which have undergone mitosis can be identified from the appearance of two or more main nuclei within the same cytoplasm (Fenech and Morley, 1985). Since then, there has been enormous proliferation of papers on the use of the micronucleus test as a predictive assay for radiosensitivity and drug toxicity (Müller and Streffer 1984, 1986, 1991, Tofilon *et al.* 1989, Wandl *et al.* 1989,

Masunaga *et al.* 1990, Shibamoto and Streffer 1991, Ono *et al.* 1994, Khan *et al.* 1998).

Although there is considerable potential for the application of this assay, its use remains controversial (van Beuningen *et al.* 1981, Bush and McMillan 1993, Villa *et al.* 1994, Akudugu *et al.* 2000). The main strength of the micronucleus assay is that it is easy to perform, and that cells need not be clonogenic. It is much faster to perform than the cell survival assay and has been applied to assess the response of primary tumour cells to radiation and drugs.

#### 1.2.1.3 Apoptosis Assay

Apoptosis, also referred to as programmed cell death, has been known for many years (Kerr *et al.* 1972). The importance of this mode of cell death for cell survival has been widely illustrated (Radford and Murphy 1994, Radford *et al.* 1994, Abend *et al.* 1995, Mathieu *et al.* 1996, Guo *et al.* 1997,1998, Bache *et al.* 1997, Olive and Durand 1997). It is widely suggested that apoptotic propensity could be an indicator for radiosensitivity or drug toxicity. Apoptotic propensity therefore is of considerable importance. While some cells exhibit a high apoptotic propensity within hours after irradiation or drug treatment (Mirkovic *et al.* 1994, Weil *et al.* 1996), others express significant levels of apoptosis only after days (Abend *et al.* 1995, Guo *et al.* 1998, 1999). High apoptotic propensity also may reflect high sensitivity to cytotoxic treatment, but

a low apoptotic propensity does not necessarily imply high resistance to cytotoxins (Olive *et al.* 1996).

Apoptosis is a cellular response to damage which can be detected either by flow cytometric methods (Ormerod *et al.* 1993, Olive *et al.* 1996) or by microscopy (Falkvoll 1990, Stephens *et al.* 1991, Meyn *et al.* 1993, Guo *et al.* 1998). Gel electrophoresis of the fragmented nucleosome DNA has also been used to quantify apoptosis (Ramakrishnan *et al.* 1993). Flow cytometric and the terminal transferase (TUNEL) techniques tend to be elaborate and complicated. Assessment of apoptosis by fluorescence microscopy is simple, reliable and reproducible (Falkvoll 1990, Stephens *et al.* 1991, Meyn *et al.* 1993).

#### 1.2.1.4 Damage and Repair Assessment

Damage induced by irradiation or other cytotoxic agents may be classified into lethal, sublethal and potentially lethal damage. Lethal damage is irreparable and inevitably leads to cell death. Sublethal damage is reparable under normal conditions, but can interact with other sublethal lesions to form a lethal damage. A potentially lethal damage can be modified by changes in the post-irradiation or drug treatment environmental conditions into a reparable or irreparable lesion. Certain drugs or suboptimal growth conditions can modify potentially lethal lesions induced by a cytotoxic agent. Generally, these categories of damage would manifest as DNA single strand breaks (SSBs) or double strand breaks (DSBs) and chromosome damage. It has been widely

demonstrated that a strong correlation exists between chromosome damage and survival (Elkind and Sutton 1960, Carrana 1973, Scott and Zampetti-Bosseler 1980, Zampetti-Bosseler and Scott 1981, Fornace *et al.* 1980).

A variety of assays exist for determining the level of DNA and chromosomal damage and the subsequent repair. These include the alkaline elution filter technique which is SSB-specific (Kohn *et al.* 1981, Wlodek and Hittelman 1987) and neutral elution filter assay for DNA double strand breaks (Bradley and Kohn 1979). Other DNA damage assessment assays are the fluorometric analysis of DNA unwinding (FADU) (Birnboim and Jevcak 1981, Ogiu *et al.*1992, Dolling *et al.* 1998) and gel electrophoretic techniques (Smith *et al.* 1989, Ager *et al.* 1990, Theron *et al.* 2000). Damage assessment at the chromosome level is widely performed by use of premature chromosome condensation (PCC) (Wlodek and Hittelman 1988a, Durante *et al.* 1998, Greinert *et al.* 1999) and fluorescence *in situ* hybridization (FISH) (Schmid *et al.* 1992, Lucas *et al.* 1992, Lucas 1997, Durante *et al.* 1997).

The unifying feature of these techniques is that they quantify damaged and undamaged DNA. This is then used as an indirect signal for predicting survival. A cell's ability to retain reproductive integrity is not only related to the level of damage inflicted, but is also an expression of damage repair (Wlodek and Hittelman 1988a,b, Roos *et al.* 2000). The major limitation of repair assays is the distribution of cells in cell cycle phases. Variations in cell distribution can produce significant variations in expression of damage, and therefore, render

the prediction of survival unreliable in relation to the amount of residual damage (Wlodek and Hittelman 1988a,b).

### 1.2.2 Factors Influencing Cellular Sensitivity to Radiation and Drugs

Some of the factors influencing cellular radiosensitivity and drug sensitivity are intrinsic properties such as cell kinetics and ploidy, and environmental factors like bioenergetics, oxygenation, radiation sensitizers and radiation protectors.

Metabolic activity is one of the main factors which influence cellular responses to damage. Bioenergetic measurements have shown considerable potential in predicting tumour response (Vaupel *et al.* 1989, Koutcher *et al.* 1992).

The significance of oxygen to tumour radiosensitivity became apparent in 1936 (Mottram 1936). After several decades of research, it was concluded that the radiosensitizing effect of oxygen applies to all types of irradiation, but is strongly dependent on the radiation energy (Littbrand and Revesz 1969, Cullen *et al.* 1980, Whillans and Rauth 1980, Palcic and Skarsgard 1984, Palcic *et al.* 1984). More recent studies have demonstrated the crucial importance of oxygenation in the tumour response (Kallman and Dorie 1986, Lartigau *et al.* 1992, Vaupel *et al.* 1996). Low oxygen tension (hypoxia) decreases tumour control by irradiation and agents were discovered which would sensitize cells to irradiation (Parker *et al.* 1969, Stratford *et al.* 1984, Skarsgard *et al.* 1986, Taylor and Brown 1987, Shibamoto *et al.* 1987, 1989, 1991, 1992).

On the other hand, it is clear that normal tissue must be protected from radiation damage. This has been achieved by such agents like β-Mercaptoethylamine and WR2721 (Rasey *et al.* 1984, Utley *et al.* 1976, Washburn *et al.* 1974, Yuhas 1980).

Changes in the bioenergetics and oxygen tension or the presence of radiosensitizers or radioprotectors therefore would influence the cellular irradiation response. In the assessment of radiosensitivity or drug toxicity for any predictive purposes, it would be essential to keep these factors constant.

## 1.3 THESIS OBJECTIVE

The response of tumours to chemotherapy or radiotherapy is of prime concern in choosing a treatment modality. In this senario, non-invasive predictive assays, preferably *in vitro*, would play a central role. Ideally, such assays should be tumour and patient specific. This would improve the choice of treatment and hence improve tumour curability. Predictive assays presently in operation are based on the following responses: cell survival, DNA repair, apoptosis and micronucleus formation.

The clonogenic survival assay is generally accepted as the gold standard. Neither micronucleus formation, apoptosis nor repair assays are capable of reconstructing reproductive integrity as measured by the colony assay. It has also been noted that even the widely accepted clonogenic assay does not always predict clinical outcome (Bush and McMillan 1993, Villa *et al.* 1994, Akudugu *et al.* 2000). Micronucleation, apoptosis and repair are cellular responses to the induction of DNA damage. These processes ultimately affect clonogenicity. The interaction between these processes and their influence on overall cell survival remains largely unresolved. Micronucleus, apoptosis and repair assays alone cannot adequately reconstruct cell survival. Thus other unknown processes must play a role (Abend *et al.* 2000). In fact, no single predictive assay is universally applicable and great caution must be exercised in the application of these assays and the interpretation of results.

In view of these limitations, it was felt that the interaction between repair, micronucleation, apoptosis and survival needs to be examined. Such information may help to resolve the current limitations in the use of predictive assays. Repair assays may require irradiation doses of 10-100 Gy, which are not clinically relevant. The capacity to repair high dose damage thus may be irrelevant because radiotherapy operates at a low dose per fraction, typically 2 Gy. Micronucleation and apoptosis assays also have their shortfalls. The micronucleus assay does not successfully rank cell types according their sensitivity to drugs and radiation, and its applicability is still a matter of controversy (van Beuningen *et al.* 1981, Bush and McMillan 1993, Villa *et al.* 1994, Akudugu *et al.* 2000). An understanding of the interrelationship between micronucleus formation, apoptosis and DNA repair on one hand and cell survival on the other would lead to a better understanding of the mechanisms underlying the cellular responses to radiotherapy or chemotherapy. Such comparative studies could help to explain variations of sensitivities between patients and cell types. An understanding of the relationship between damage processing and cell survival would benefit not only radiotherapy and chemotherapy, but also biodosimetry i.e. radiation accidents and toxicology. There is thus a critical need of reliably assessing radiosensitivity and relating repair capacity, apoptosis and chromosome damage (micronucleation) to radiosensitivity.

I have used seven neuroblastoma cell lines and six neuroepithelial cell lines to test a number of hypotheses on how cell survival, micronucleation, apoptosis

and repair are interrelated in response to treatment with irradiation and drugs. This choice of cell lines was motivated by the difficulties in treating head and neck tumours with radiation, and thus the need to elucidate possible reasons for the apparent radioresistance using cell lines of glial and neuronal origin. The hypotheses under consideration are:

a) Micronuclei formation represents the induction of lethal damage and should directly indicate the net cellular response as given by the proportion of surviving cells.

b) High linear energy transfer (LET) irradiation is more damaging than low LET irradiation. Neutrons therefore should induce more micronuclei than $^{60}$Co $\gamma$-rays, and micronucleus induction with neutrons should be independent of cell type and origin.

c) Apoptosis is a major route of cell death upon treatment with cytotoxic agents. It can be expected that cell types which are more susceptible to micronucleus formation (which is an early signal of damage) express a higher proportion of apoptosis.

d) If micronuclei formation and apoptosis are the only pathways which lead to cell death, it should be possible to reconstruct cell survival measured by the clonogenic assay.

e) Micronucleus formation is a reflection of non-reparable damage. A low MNF thus represents efficient repair.

f) Apart from assessing radiation damage, the micronucleus assay should be able to detect damage caused by other cytotoxic agents e.g. drug toxicity.

# CHAPTER 2

# MATERIALS AND METHODS

## 2.1 Chemicals, Drugs and Culture Media

### *2.1.1 Fixative for Colony Assay*

The fixative for the clonogenic assay consists of a mixture of glacial acetic acid, methanol and water in the ratio of 1:1:8 (v/v/v). When colonies were of sufficient size for counting, the medium was replaced with fixative after cultures were washed with 1% phosphate buffered saline (PBS). The cells were fixed for 30 minutes at room temperature (~22°C).

### *2.1.2 Staining Solution for Colony Assay*

The colony stain consisted of 0.01% Amido Black, also known as Naphthol Blue Black, ($C_{22}H_{14}N_6O_9S_2Na_2$; FW = 616.5) in fixative, i.e. a final concentration of 0.062 g/l. The fixed cells were stained for 30 minutes at room temperature (~22°C). The staining solution was then removed and the colonies washed with PBS and air-dried for counting.

### *2.1.3 Fixative for Micronucleus and Apoptosis Assays*

Micronucleus and apoptosis cultures were fixed in a mixture of methanol and glacial acetic acid in the ratio of 3:1 (v/v). Samples were fixed for 5 minutes at room temperature (~22°C) and air-dried for staining.

### *2.1.4 Staining Solution for Micronucleus and Apoptosis Assays*

Micronucleation and apoptosis were observed by means of fluorescence microscopy. The dye used in this study is acridine orange ($C_{17}H_{20}N_3Cl$, FW = 301.8; Sigma, South Africa; structural formula in figure 2.1). Acridine orange is a fluorochrome which specifically stains nucleic acids showing DNA as green fluorescence and RNA as red fluorescence.

A stock staining solution consisting of 1.0 mg acridine orange per ml phosphate buffer (pH = 6.8) can be stored in the dark at 4°C for several months. The actual staining solution consists of 0.4 ml of stock solution in 40 ml to final concentration is 10 μg acridine orange per ml of buffer. Pre-warming the stain to 37°C enhances the interchelation of the fluorochrome and therefore improves image quality during microscopy. The effective staining time was in the order of 2 minutes. Stained samples were immediately washed in buffer and mounted on slides for microscopy.

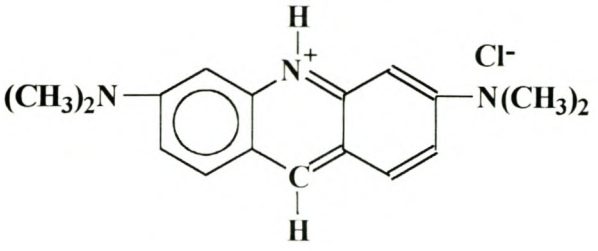

ACRIDINE ORANGE

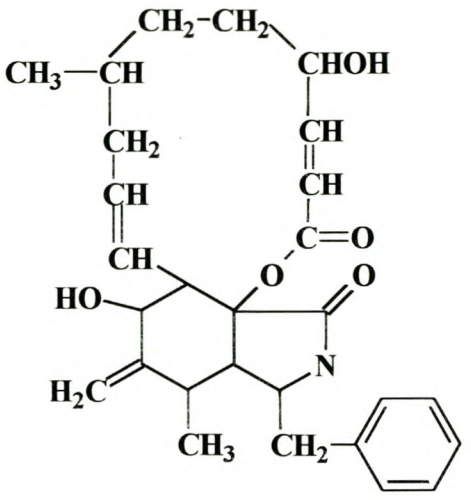

CYTOCHALASIN B

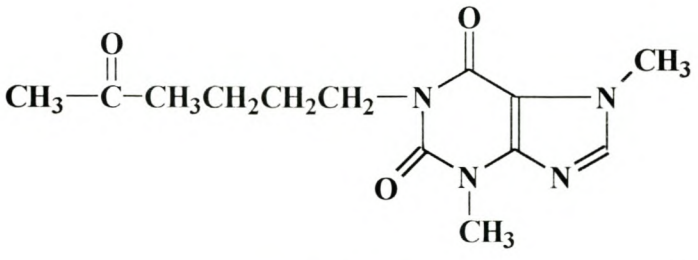

PENTOXIFYLLINE

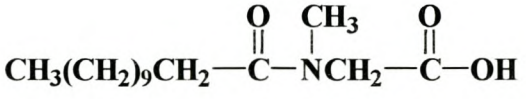

N-LAUROYL-SARCOSINE

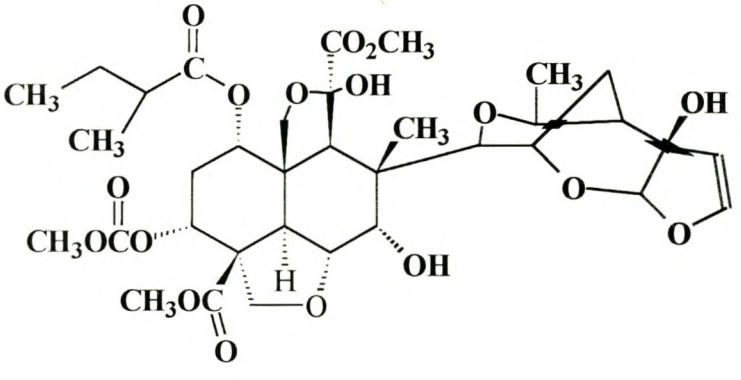

AZADIRACHTIN A

**FIGURE 2.1** Molecular structures of acridine orange, cytochalasin B, pentoxifylline, N-lauroyl-sarcosine and azadirachtin A.

### *2.1.5 Fixative and Staining Solution for DNA Analysis*

Cells were fixed overnight in ice-cold (4°C) 70% ethanol, and stained in 1.0% PBS containing 0.1% glucose, 50 μg/ml propidium iodide (PI) and 100 μg/ml RNase. The fixed cells were centrifuged at 2000 rpm, resuspended in the staining solution, covered with tin foil and incubated for 30 minutes at 37°C. Stock solutions of RNase (1 mg per ml 1.0% PBS) and PI (1 mg per ml 1.0% PBS) can be stored in the dark at 4°C for several weeks.

### *2.1.6 Lysing and Washing Solutions for DNA Repair Assay*

Agarose plugs containing cells were submersed in an ice-cold lysing solution containing 50 mM EDTA, 1% N-Lauroylsarcosine ($C_{15}H_{29}NO_3$; FW = 271.4; Sigma, South Africa; structure in figure 2.1) and 1 mg/ml proteinase K, and incubation for 1 hour at 4°C, followed by lysing at 37°C for 20 hours. The plugs were then washed five times and stored in 2 ml of 50 mM EDTA solution.

### *2.1.7 Cytochalasin B*

Cytochalasin B ($C_{29}H_{37}NO_5$; FW = 479.6; Sigma, South Africa; structure in figure 2.1) is a cell permeable fungal toxin, which inhibits cell division by blocking the formation of contractile microfilaments (Fenech and Morley 1985). It also inhibits glucose transport.

The stock solution consisting of 2 mg of cytochalasin B per ml of dimethylsulphoxide (DMSO) was stored in liquid nitrogen (-196°C). An aliquot

of the stock was dissolved in culture medium and added to cultures at a final concentration of 2 μg of cytochalasin B per ml of medium.

*2.1.8 Pentoxifylline (PENT)*

Pentoxifylline ($C_{13}H_{18}N_4O_3$, FW = 278.3; Sigma, South Africa; structure in figure 2.1) inhibits the synthesis of tumour necrosis factor α (Semmler *et al.* 1993), and abrogates the $G_2$/M block (Russell *et al.* 1995, Li *et al.* 1998). The drug also inhibits repair and sensitizes cells when present at the time of irradiation (Theron *et al.* 2000). The stock solution of pentoxifylline, 20 mg/ml, is stable at 4°C for several weeks.

*2.1.9 Azadirachtin A*

Azadirachtin A ($C_{35}H_{44}O_{16}$; FW = 720.7; Sigma, South Africa; structure in figure 2.1) is an isomer of a series of limonoids. It is derived from the seed kernels of the tropical neem tree, *azadirachta indica* A. Azadirachtin A is known to affect growth, reproduction and metamorphosis in insects, and is generally used as an insecticide (Rembold and Annadurai 1993). The compound was dissolved in 30% ethanol/water. Azadirachtin A in solution can be stored in the dark at 4°C for several weeks.

*2.1.10 Culture Media*

Culture media were supplemented with 10% fetal calf serum, 100 μg/ml streptomycin and 100 U/ml penicillin. All media were buffered with sodium

hydrogen carbonate ($NaHCO_3$) and the pH adjusted with drops of hydrochloric acid (HCl) to about 7.02 before sterile filtration. For the glioblastoma cell lines, the medium was also supplemented with 2.2 μg/ml sodium pyruvate. Media were purchased from Sigma (South Africa) and contained L-glutamine.

*2.1.10.1 Eagle's Modified Minimum Essential Medium (EMEM)*

This culture medium was obtained by dissolving 9.58 g of EMEM containing non-essential amino acids and 2 g of $NaHCO_3$ in a litre of millipore-filtered water.

*2.1.10.2 Dulbecco's Modified Minimum Essential Medium (DMEM)*

13.53 g of DMEM and 3.7 g of $NaHCO_3$ were dissolved in a litre of millipore-filtered water. The medium was then supplemented with 4.50 μg/ml glucose, 2.2 μg/ml sodium pyruvate and 0.58 μg/ml L-glutamine.

*2.1.10.3 RPMI-1640 Medium*

This medium was obtained by dissolving 10.44 g of RPMI-1640 and 2 g of $NaHCO_3$ in a litre of millipore-filtered water.

## 2.2 Cell Lines

*2.2.1 SK-N-BE(2C) (Passages 2-17)*

SK-N-BE(2C) is a human bone marrow neuroblastoma derived from SK-N-BE(2). SK-N-BE(2) originates from a 22 months old Caucasian male. SK-N-

BE(2C) grows in continuous culture as monolayer. It exhibits neuroblast-like and epithelial-like morphology and forms loosely adherent aggregates at confluence. The cells are pluri-potential with regard to neuronal enzyme expression and display a high capacity to convert tyrosine to dopamine (Biedler and Spengler 1976).

*2.2.2 SK-N-SH (Passages 2-13)*

The SK-N-SH neuroblastoma cell line originates from the bone marrow of a 4 years old Caucasian female and grows in monoclonal continuous culture as monolayer. It has neuroblast-like or epithelial-like morphology. SK-N-SH is tumourigenic in nude mice. Special features include biochemical markers, receptors, chemotherapeutic agents, nucleic acids, neural tissue and cytotoxicity (Biedler *et al.* 1973).

*2.2.3 SH-SY5Y (Passages 2-15)*

SH-SY5Y is derived from SK-N-SH and exhibits mainly epithelial-like morphology. It also grows as monolayer. Other properties include tumour markers, chemotherapeutic agents, nucleic acids, neurotransmitter studies, converts glutamate to GABA and exhibits dopamine-beta-hydroxylase activity (Biedler *et al.* 1973, Jalava *et al.* 1990).

*2.2.4 KELLY (Passages 2-19)*

KELLY is a human neuroblastoma with neuroblast-like morphology and grows in continuous culture as monolayer. The cells possess a genomic amplification

of the N-*myc* gene. Special features are protein secretion and N-myc RNA production (Schwab *et al.* 1983).

### *2.2.5 N2α (Passages 20-35)*

N2α is a human neuroblastoma cell line, with a neuron-like or amoeboid-like morphology. The cells grow in continuous culture as monolayer. It is derived from sympathetic cells in the peripheral nervous system. Cells are tumourigenic in syngeneic animals and produce a microtubular protein believed to play a role in the contractile system giving axoplasmic flow in nerve cells. The cell line was purchased from the Highveld Biological Association (South Africa).

### *2.2.6 OP-6 (Passages 4-19) and OP-27(Passages 14-27)*

OP-6 and OP-27 are mouse neuroblastoma cell lines, and were a gift from Professor N. Illing of the University of Cape Town, South Africa. The cells grow in continuous culture as monolayer under the influence of a temperature sensitive SV40 large T antigen which, when inactivated at 39°C, renders the cells non-proliferating.

### *2.2.7 Glioblastoma Cell Lines*

The neuroepithelial or glioblastoma cell lines are of human origin and were kindly donated by Dr. A. Giese of University Klinikum Eppendorf (Hamburg, Germany). The tumour promoter gene (TP53) status of these cell lines is as follows: G-60 (TP53mt), G-28 (TP53mt), G-44 (TP53wt),

G-120 (TP53wt), G-112 (TP53mt) and G-62 (TP53wt). G-28 is a gliosarcoma derived from a 67-year-old male (Westphal *et al.* 1988)

## 2.3 Culture Maintenance and Cell Storage

Except for the OP-6 and OP-27 cell lines which grow at 33°C, all the other cell lines were kept at 37°C. N2α, SH-SY5Y and SK-N-BE(2C) were maintained in RPMI-1640 medium. The KELLY, SK-N-SH and glioblastoma cell lines were cultured in Eagle's modified minimum essential medium (EMEM). The OP-6 and OP-27 cell lines were cultured in Dulbecco's modified minimum essential medium (DMEM). All cell lines were incubated in a 5% carbon dioxide humidified atmosphere in air.

For cryogenic storage, cells were trypsinised, centrifuged and resuspended in 10% dimethylsulphoxide (DMSO) in fetal bovine serum (FBS). The cell suspension was transferred into clearly marked plastic vials and immediately quenched in liquid nitrogen (-196°C). Each vial was marked with the name of the cell line, growth medium, passage number and date of storage. To put cells back into culture, the frozen cell suspension was resuspended in growth medium incubated.

## 2.4 Irradiation and Drug Treatment

### *2.4.1 $^{60}Co$ γ Irradiation*

Cultures were exposed to $^{60}Co$ γ-rays at room temperature (~22°C) to graded doses of 0-10 Gy for the clonogenic assay. Doses of 0-6 Gy were used for the micronucleus and apoptosis assays. The mean dose rate was 1.21 Gy/min (1.18-1.29 Gy/min). The field size was 30 × 30 $cm^2$ and a vertical beam of SSD = 80 cm was used. Samples were placed on a 4 cm thick backscatter block consisting of perspex. The build-up material consisted of 20 mm polyethylene.

For the repair experiments, samples were irradiated (with a 35 × 30 $cm^2$ field, SSD << 45 cm) without build-up in ice-cold minimum essential medium (MEM) containing 2% HEPES buffer. Samples were exposed to doses ranging from 0-100 Gy at a dose rate of 2.92 Gy/min (2.35-3.18 Gy/min).

### *2.4.2 p(66/$Be^+$) Neutron Irradiation*

Neutron irradiation was from a vertical beam directed downwards. Cell cultures were placed in a 29 × 29 $cm^2$ field (SSD = 150 cm) on a 15 cm backscatter block of perspex. Cultures were irradiated at a dose rate of 0.5 Gy/min to doses of 0.5 - 2.5 Gy and 0.5 - 5.0 Gy for micronucleus and colony assays, respectively. The build-up material consisted of 20 mm polyethylene.

### *2.4.3 Azadirachtin A Treatment*

3-4 hours after plating and when the plated cells had attached, azadirachtin A was added to cultures at a concentration of 20 μg per ml of medium. After 24 hours incubation, the medium was changed. For the micronucleus assay, the fresh medium was treated with cytochalasin B.

### *2.4.4 Pentoxifylline Treatment*

The effect of pentoxifylline on clonogenicity was investigated. 18 hours after 4 Gy $^{60}$Co γ-irradiation, cultures were treated with pentoxifylline to a final concentration of 556 μg per ml of medium. The drug was removed by a change of medium 24 hours later. For micronucleation, a change of medium was not necessary since the cultures were terminated 40 hours after irradiation.

## 2.5 Cell Survival Assay

Cell survival was determined by the colony assay in response to p(66/Be$^{+}$) neutron and $^{60}$Co γ-irradiation and upon treatment with azadirachtin (glioma cell lines). Single-cell suspensions (1-20x10$^{3}$ cells per flask, adjusted for dose level) were plated into 25 cm$^{2}$ culture flasks, incubated for 4 hours and irradiated or treated with azadirachtin. After growing for 8-12 days, colonies were fixed, stained, air-dried and counted. A minimum of three independent experiments were performed for each cell line. The mean surviving fractions were fitted to the linear-quadratic (L-Q) model to generate the survival curves.

Data for azadirachtin and pentoxifylline experiments were presented as histograms.

## 2.6 Micronucleus Assay

Cell lines were prepared for nuclear observation as described elsewhere (Ono *et al.* 1994). Exponentially growing cells were trypsinised into single-cell suspensions and plated (1-3x$10^4$ cells per plate) into 35 mm plastic petri dishes (Corning, New York) each containing a 22 mm glass coverslip (Chance Propper, England) to a final medium volume of 2 ml.

After cells were attached, the samples were irradiated with $^{60}$Co $\gamma$-rays or p(66/$Be^+$) neutrons or treated with azadirachtin. Of the 13 cell lines, G-120, G60, G-28, G-44, G-62, G-112, SK-N-SH and KELLY cell lines were irradiated with neutrons. Only the glioblastoma cell lines were treated with azadirachtin A. Immediately after the irradiation or drug treatment, and not later than 30 minutes, cultures were treated with cytochalasin B.

To determine the incubation period for the expression of the highest yield of binucleated cells (proportion of observed cells containing two main nuclei), cultures were were terminated at 8-hour intervals, fixed, air-dried, stained and the coverslips mounted on glass microscope slides for fluorescence microscopy. Maximum binucleation occurred after 1 day in OP-6 and OP-27

and 2 days in the human cell lines. Subsequent experiments were stopped after 24 hours for OP-6 and OP-27 and 40 hours for the human cell lines.

At least 200 binucleated cells were evaluated per dose point and experiment and a minimum of three independent experiments were performed for each cell line. Micronuclei were scored according to the criteria of Ono *et al* (1994). See also figure 2.2. The susceptibility of a cell line to the induction of micronuclei was expressed by the micronuclei frequency (MNF) or the micronucleation index. MNF was expressed as the mean (± SD) number of micronuclei (MN) per binucleated cell (BNC). Micronucleation index was defined as the proportion of binucleated cells containing at least a micronucleus.

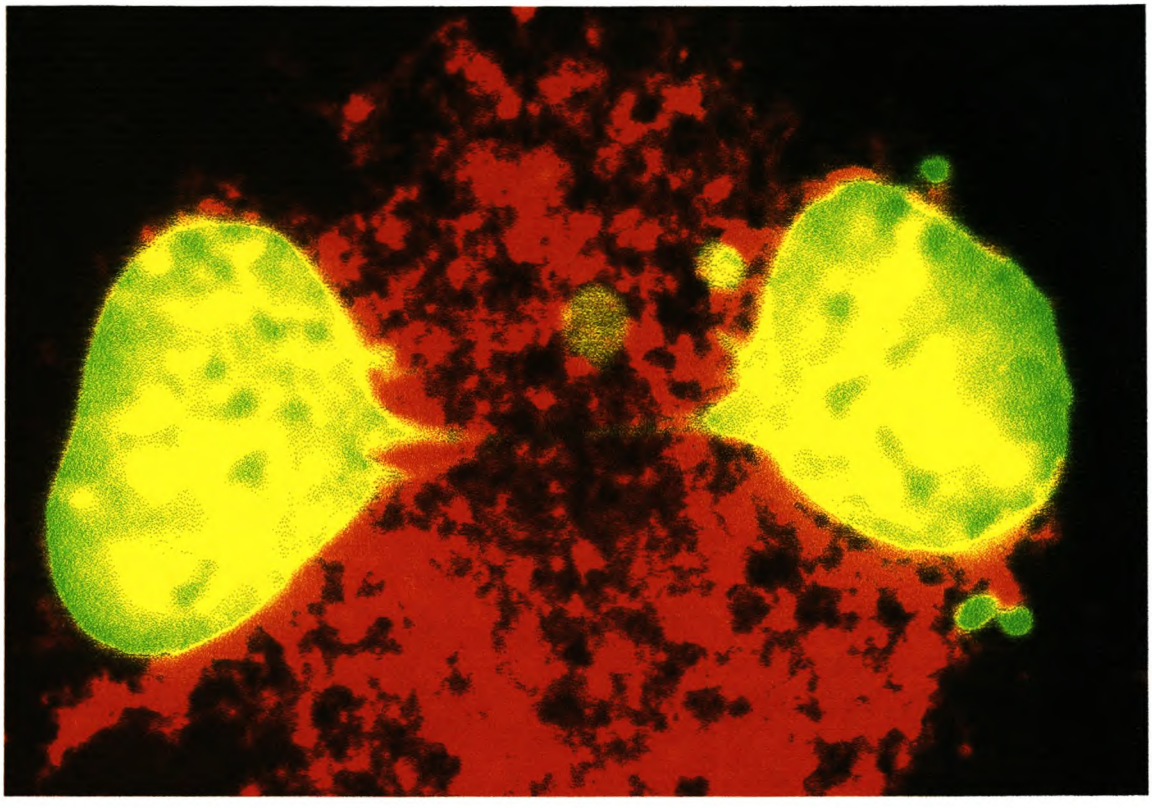

**Figure 2.2** A binucleated cell of the N2α line with five micronuclei following a 4 Gy $^{60}$Co γ irradiation.

## 2.7 Determination of the Normal Nuclear Division Fraction (NNDF) and the Mitotic Index (MI)

The normal nuclear division fraction (NNDF) represents the fraction of cytokinesis-block binucleated cells that do not contain micronuclei can be considered as representative of the mitotic fraction (Ono *et al.* 1994). In fact, the NNDF decreases exponentially with increasing radiation dose. The similarity in dose-response of NNDF and clonogenic survival suggests that NNDF may be a suitable indication of radiosensitivity.

The number of mononucleated and binucleated cells were scored concurrently with the assessment for the expression of micronuclei in each cell line in the neutron/cobalt, pentoxifylline and azadirachtin experiments. Binucleation indices (fractions of binucleated cells) in unirradiated cultures were established for each cell line. Dose-response curves for the NNDF were generated for the neutron/cobalt experiments. Since an insignificant proportion of cells contained more than two main nuclei, the mitotic index (MI) was expressed as the fraction of binucleated cells observed for the pentoxifylline and azadirachtin experiments. The data were presented as histograms. The mitotic suppression factor (MSF), the degree to which irradiation or toxins decrease the mitotic index, was then calculated as the ratio of binucleation in treated to non-treated samples.

## 2.8 Relative Biological Effectiveness (RBE)

For each of the cell lines used in the neutron/cobalt experiments, the RBEs were calculated from the cell inactivation parameters as follows: a) the ratio of the surviving fraction at 2 Gy, $RBE_{SF2} = SF2_\gamma/SF2_n$; b) the ratio of the $\alpha$-coefficients, $RBE_\alpha = \alpha_n/\alpha_\gamma$; c) the ratio of the $\alpha/\beta$-ratios, $RBE_{\alpha/\beta} = (\alpha/\beta)_\gamma/(\alpha/\beta)_n$; d) the ratio of the mean inactivation doses, $RBE_{\overline{D}} = \overline{D}_\gamma/\overline{D}_n$; and e) the ratio of the areas under the NNDF-dose response curves, $RBE_{\overline{NDF}} = (\overline{NDF}_\gamma)/(\overline{NDF}_n)$. $\gamma$ and *n* denote $^{60}$Co $\gamma$- and p(66/Be$^+$) neutron-irradiation, respectively.

## 2.9 Apoptosis Assay

The culturing procedure was as described for the micronucleus assay, except that cultures were not incubated with cytochalasin B after $^{60}$Co $\gamma$-irradiation, and then prepared for fluorescence microscopy. The cell lines used in this assay were SK-N-SH, KELLY, G-120, G-60, G-28, G-44 and G-62. Apoptotic cells were scored according to criteria described elsewhere (Mirkovic *et al.* 1994, Hu and Hill 1996, Weil *et al.* 1996). These included either cells with picnotic, fragmented or crescent-shaped nuclei, overall shrinkage or membrane-bound bodies containing picnotic nuclei that were smaller than the normal surrounding nuclei.

Three independent experiments were performed for each data point, and at least 500 cells were counted per experiment. The frequency of apoptotic events

($Fa_D$) was expressed as the mean (±SD) ratio of apoptotic cells to the total number of cells scored.

## 2.10 Determination of Cell Death via Other Pathways from Micronucleus and Apoptotic Data

The fraction of apoptotic cells increases rapidly with dose and reaches a plateau at higher doses (Mirkovic *et al.* 1994, Ling *et al.* 1994, Weil *et al.* 1996). However, in this study and for doses up to 6 Gy, the apoptotic propensity, $Fa_D$, varied linearly with irradiation dose and is given by the expression:

$$Fa_D = \xi D \qquad (1)$$

where $D$ is the dose and $\xi$ is the coefficient for cell inactivation via apoptosis. It was also found that micronucleation varied with dose as follows:

$$Fm_D = Fm[1 - \exp(-\mu D)] \qquad (2)$$

where $\mu$ is the coefficient for induction of micronuclei in binucleated cells and $Fm$ is the maximum achievable fraction of micronucleated cells. The apoptotic and micronucleation data were corrected for background and fitted to equation 1 and 2, respectively, to derive the values of $Fm$, $\mu$ and $\xi$ for each cell line.

$Fa_D$ and $Fm_D$ represent the probability of cell inactivation via apoptosis and micronucleus formation, respectively. If apoptosis and micronucleation were the only modes of lethal damage, the corresponding survival probability ($SF_{MA}$) of a cell population would be:

$$SF_{MA} = 1 - P_{MA} \qquad (3).$$

$P_{MA}$ is the probability of inactivation through micronucleation or apoptosis ($P_{MA}$ = $Fa_D$ + $Fm_D$). Here, the two events are considered as independent events since the assessment of micronucleation is made after only one post irradiation division whereas apoptosis is scored at a much later time point. $SF_{COL}$ is defined as the survival probability determined by the colony assay. $SF_{MA}/SF_{COL}$ ratios were found to be dose-dependent and differ significantly from 1.0 (Table 3.3). The disparity between $SF_{MA}$ and $SF_{COL}$ is thought to be due to cell death via other events like small deletions, misrepair, chromosome aberrations and late apoptosis. Therefore, the clonogenic survival can be represented by the expression:

$$SF_{COL} = 1 - (P_{MA} + P_{oe}) \qquad (4)$$

where $P_{oe}$ is the probability of cell death via other event that are undetectable at the 40-hour time point. The probability of reproductive failure in this time frame would be given by:

$$P_{oe} = 1 - SF_{COL} - P_{MA} \quad (5).$$

## 2.11 Determination of DNA Index

The distribution of the DNA content was determined by flow cytometry, as described elsewhere (Hu and Hill 1996, Lee *et al.* 1997). Exponentially growing unirradiated cells were washed in PBS, trypsinised, centrifuged at 2000 rpm and resuspended in fixative.

For DNA analysis, the cells previously fixed in a mixture of PBS and 70% ethanol in the ratio of 1:10 (v/v) were centrifuged, washed with PBS and resuspended in staining solution. The final cell density was about 2 x $10^6$ per ml. Stained cells were analysed within four hours in a Becton Dickinson FACScan flow cytometer.

The distribution of the DNA content in each cell cycle phase was scored in samples of 10,000 cells per aliquot and was quantified using the CELLFIT software program. The DNA content of all cell lines was expressed in terms of the DNA index (DI), defined as the ratio of the $G_1$ peak to that of peripheral blood lymphocytes (PBL) which were stained and analysed concurrently. Murine and human PBL were used as internal standards for the murine and human cell lines, respectively.

## 2.12 DNA Repair Assay

The quantity of DNA double strand break damage was determined by constant-field gel electrophoresis (CFGE) as described elsewhere (Theron *et al.* 2000). Briefly, G-28, G-120 and G-60 cells were trypsinised from confluent cultures and resuspended in a 0.5% low melting agarose solution. Aliquots of 30 μl, containing ~0.5 x $10^5$ cells, were placed into each well of a disposable plug mold (BioRad), and allowed to solidify at 4°C for 45 minutes. The plugs were irradiated and samples for the determination of initial damage were immediately submitted to subsequent lysing and washing steps. Samples for determining residual damage were incubated at 37°C in growth medium for periods of 2 and 20 hours prior to lysing and washing. The rationale for using cell lines of the same origin is to eliminate cell-type specificity so that differences in repair capacity would be mainly due to cellular differences in radiosensitivity.

The washed plugs were then loaded into a 20 × 20 $cm^2$ 0.6% agarose gel and run in 0.5 × TBE buffer for 30 hours at a constant field strength of 1.2 V/cm. Gels were stained with ethidium bromide (0.5 μg/ml in 0.5 × TBE buffer) and subjected to fluorometric analysis with a GeneSnap (VacuTec) image analysis system. Three independent experiments were performed for each cell line. The fraction of DNA released from the plug ($F_{rel}$) was obtained from the equation: $F_{rel} = fl_{rel}/(fl_{plug}+fl_{rel})$, where $fl_{rel}$ and $fl_{plug}$ are the fluorescence measured in the lane and in the plug, respectively. Unirradiated samples were used as sample

subsets to subtract background fluorescence caused by non-specific DNA degradation.

Dose response curves were obtained by plotting $F_{rel}$ as a function of dose, representing initial damage (0 hour), residual damage (2 hours) and residual damage (20 hours). Since data could not be fitted by linear regression, data points were connected and the area under the curve (AUC) was calculated for each curve in GraphPad Prism (GraphPad Software, San Diego, USA) computer program.

# CHAPTER 3

# RESULTS

## 3.1 THE MICRONUCLEUS ASSAY AS A PREDICTIVE TOOL FOR CELLULAR RADIOSENSITIVITY

### 3.1.1 Interrelationship between Clonogenic Survival and Radiation-Induced Micronuclei Yield

The cellular radiosensitivity expressed in terms of the surviving fraction at 2 Gy of $^{60}$Co $\gamma$-irradiation ($SF2_\gamma$) was determined by clonogenic survival. The survival curves for the 7 neuroblastoma and 6 neuroepithelial cell lines are shown in figure 3.1. $SF2_\gamma$ values were obtained from the mean survival data fitted to the linear-quadratic (L-Q) model. The $SF2_\gamma$ values varied from 0.20 to 0.75. The cell inactivation parameters are summarised in table 3.1. The cell lines G-44, G-112, G-120, G-62, G-28 and N2$\alpha$ are deemed radioresistant because the $SF2_\gamma$ exceeded 0.60. OP-27, SK-N-SH, SH-SY5Y and KELLY cells display an $SF2_\gamma$ smaller than 0.35 and are deemed radiosensitive. The $SF2_\gamma$ values for the OP-6, SK-N-BE(2C) and G-60 cells were found to be 0.57, 0.54 and 0.43 respectively, and fall into an intermediate category of radiosensitivity.

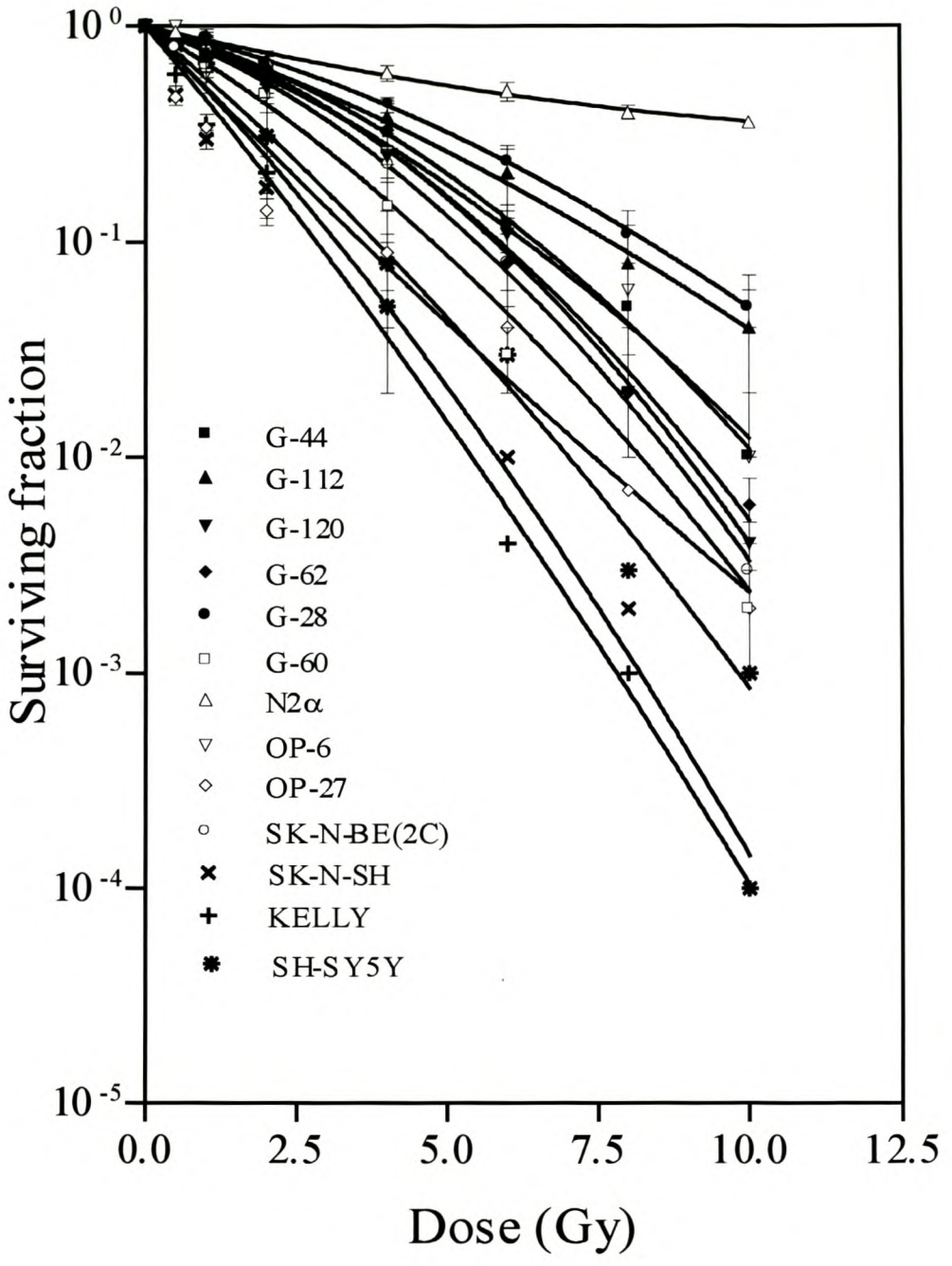


**FIGURE 3.1** Clonogenic survival curves for 7 neuroblastoma and 6 neuroepithelial (G-) cell lines after $^{60}Co$ γ-irradiation. Symbols represent the mean (± SD) surviving fraction from three separate experiments. Standard deviations are not transformed into a logarithmic scale. Survival curves were obtained by fitting experimental data to the L-Q model.

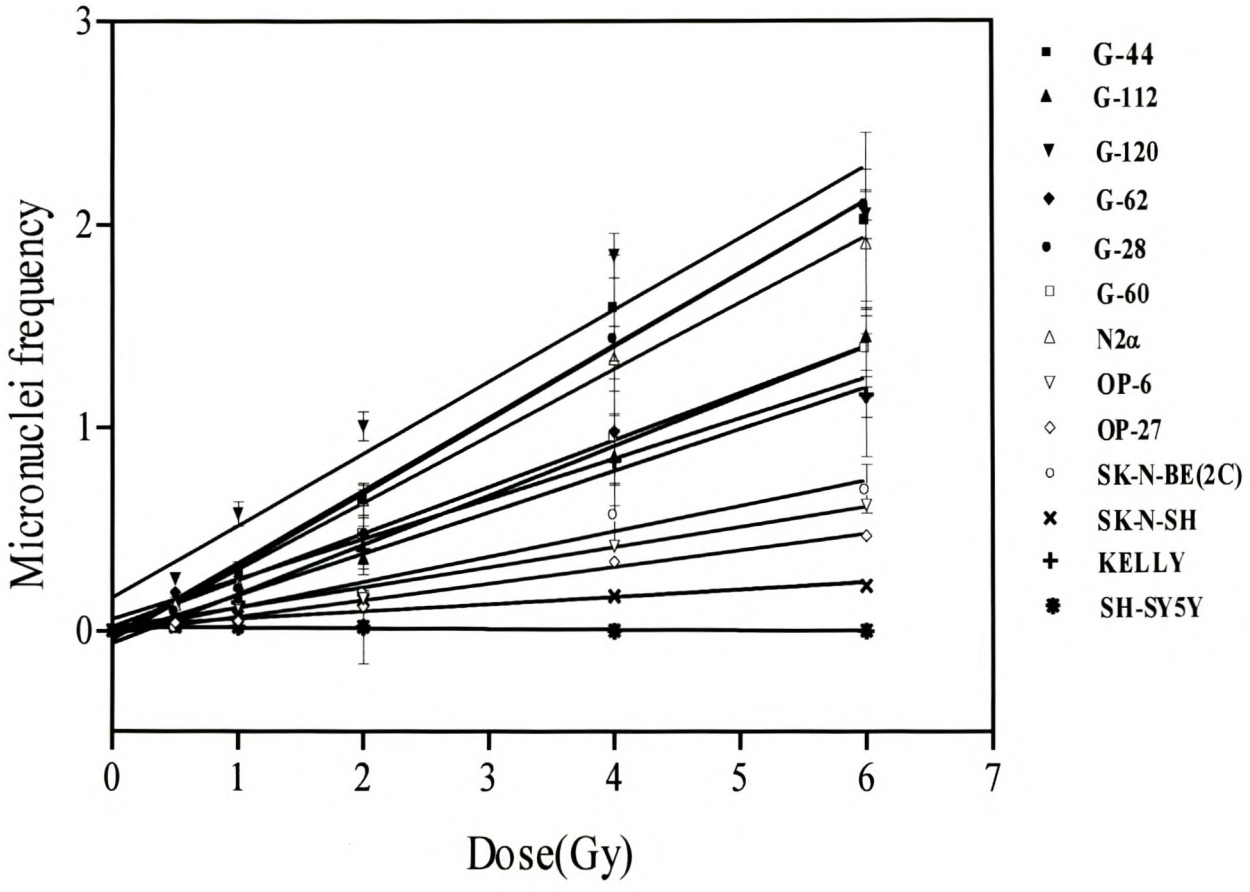


**FIGURE 3.2** The micronuclei frequency (number of micronuclei per binucleated cell) as a function of irradiation dose ($^{60}$Co γ-irradiation) in 7 neuroblastoma and 6 neuroepithelial (G-) cell lines. Symbols represent the mean (± SD) micronuclei frequency from three independent experiments, after subtraction of MN frequency at 0 Gy.

With the exception of the SH-SY5Y cell line, which does not respond to radiation-induced micronuclei formation, all cell lines show a linear relationship between radiation dose and micronuclei frequency (Figure 3.2). The MN frequency was expressed as the number of micronuclei per binucleated cell after subtraction of the MN frequency at 0 Gy. The slopes of the regression lines range from 0.04 to 0.36 MNF per Gy (Table 3.1). The regression coefficients vary between 0.94 to 1.00 ($P \leq 0.005$) and emerge as highly significant. Four of the six radioresistant cell lines (G-44, G-120, G-28 and N2$\alpha$) show steep regressions with slope exceeding 0.30 MNF per Gy. Two of the radiosensitive cell lines (OP-27 and SK-N-SH) produce shallow regressions with a slope smaller than 0.10 MNF per Gy.

It was therefore suspected that the response to micronuclei formation may be related to the number of lethal lesions which, for any given dose, would be higher in radiosensitive cells than in radioresistant cells. The number of lethal lesions induced by $^{60}$Co $\gamma$-irradiation ($-$ ln $SF_\gamma$) can be calculated from the surviving fraction, derived from the L-Q fit as described elsewhere (Bush and McMillan 1993, Villa *et al.* 1994). When the MN frequency for each dose point is plotted as a function of the number of lethal lesions, a strong linear correlation emerges in all the twelve cell lines (Figure 3.3). The slopes vary from 0.05 to 2.79 and the correlation coefficients range from 0.91 to 0.99 ($P < 0.05$). Although the slopes of the regressions do not rank the cell lines

according to radiosensitivity, most of the more radioresistant cell lines show a greater susceptibility to MN formation than the radiosensitive cell lines (Table 3.1). In the radiosensitive KELLY, OP-27 and SK-N-SH cell lines a single lethal lesion requires between 0.05 and 0.23 micronuclei. A lethal lesion in the radioresistant G-44, G-112, G-120, G-62, G-28 and N2$\alpha$ cell lines, however, equates to between 0.43 and 2.79 micronuclei.

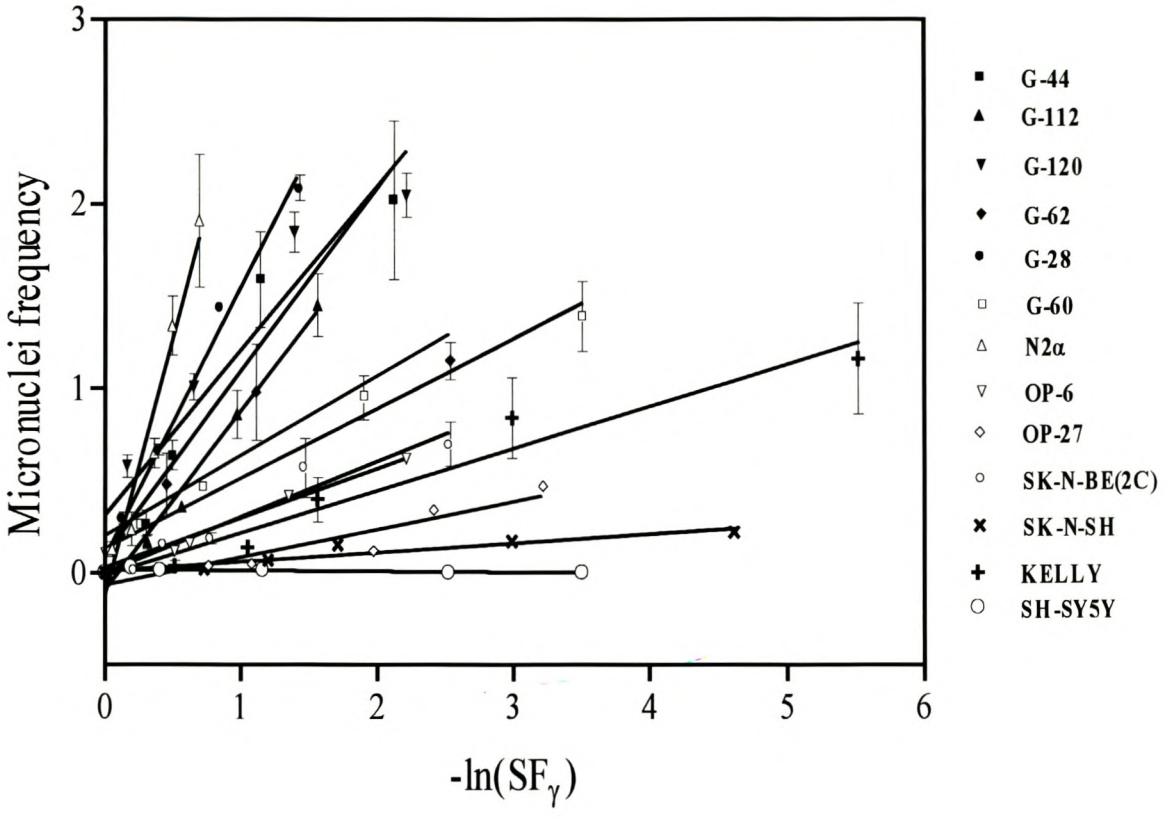


**FIFURE 3.3** Correlation between MN frequency (number of micronuclei per binucleated cell) and the number of lethal lesions (-ln $SF_\gamma$) in for 7 neuroblastoma and 6 neuroepithelial (G-) cell lines. The number of lethal lesions were calculated from the mean surviving fraction upon $^{60}Co$ γ-irradiation (data points from figure 3.1).

Since each cell line shows a good linear correlation between MN frequency and dose, it was thought that a reasonable correlation might exist between the surviving fraction at 2 Gy ($SF2_\gamma$) or the mean inactivation dose ($\overline{D}_\gamma$) and the MN frequency at 2 Gy ($MNF2_\gamma$). The $\overline{D}_\gamma$ values represent the areas under the survival curves in figure 3.4 (SF plotted on a linear scale). When the $SF2_\gamma$ values, derived from the L-Q fit, were plotted as a function of $MNF2_\gamma$ calculated from the MN frequency-dose regression in figure 3.5, it was found that in two groups of cell lines (i.e. OP-6, SK-N-BE(2C), G-112, G-62, N2$\alpha$ and G-28 and in G-120, G-60, OP-27, KELLY and SK-N-SH) the $MNF2_\gamma$ increased with irradiation resistance. Restricting this analysis to another group of cell lines (i.e. OP-6, SK-N-BE(2C), G-112, G-62, G-44 and G-120) produced no meaningful correlation between MN formation and radiosensivity. A plot of $\overline{D}_\gamma$ as a function of $MNF2_\gamma$ produces a week correlation with $r^2 = 0.39$ and $P = 0.02$ (Figure 3.6). The correlation between the expression of micronuclei and radiosensitivity was also investigated by plotting the $(\alpha/\beta)_\gamma$ ratio as a function of MNF per Gy (the slope of the micronuclei frequency-dose response curve) for each cell line (Figure 3.7). No significant correlation was found to exist between cellular susceptibility to micronuclei formation and radiosensitivity as determined by the $(\alpha/\beta)_\gamma$ ratio ($r^2 = 0.16$, $P = 0.17$).

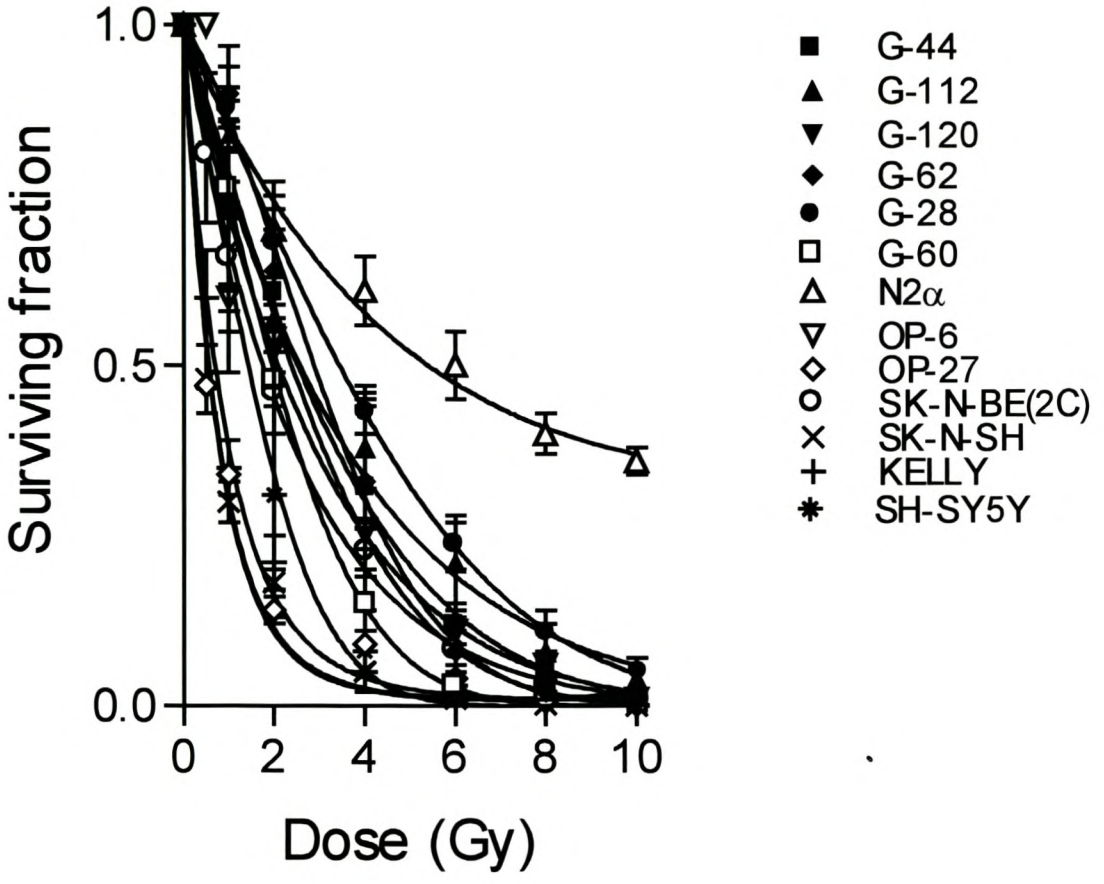


**FIGURE 3.4** Clonogenic survival curves for for 7 neuroblastoma and 6 neuroepithelial (G-) cell lines after $^{60}Co$ $\gamma$ irradiation. Symbols represent the mean ($\pm$ SD) surviving fraction from three separate experiments. Survival curves were plotted on a linear-linear scale. The area under each curve represents the mean inactivation dose ($\overline{D}_{\gamma}$).

**TABLE 3.1**

Summary of cell inactivation parameters for for 7 neuroblastoma and 6 neuroepithelial (G-) cell lines determined by the clonogenic and micronucleus assays. Parameters were derived after cells were exposed to $^{60}$Co $\gamma$-irradiation.

| Cell line | $SF2_\gamma$ | $MNF2_\gamma$ | $\alpha_\gamma$ ($Gy^{-1}$) | $\beta_\gamma$ ($Gy^{-2}$) | $\overline{D}_\gamma$ (Gy) | MNF per Gy | MNF per $-\ln SF_\gamma$ |
|---|---|---|---|---|---|---|---|
| G-44 | 0.63 | 0.69 | 0.18 | 0.03 | 3.15 | 0.36 | 0.99 |
| G-112 | 0.63 | 0.42 | 0.21 | 0.01 | 3.47 | 0.24 | 0.96 |
| G-120 | 0.60 | 0.87 | 0.18 | 0.04 | 2.89 | 0.35 | 0.89 |
| G-62 | 0.59 | 0.45 | 0.20 | 0.03 | 3.23 | 0.20 | 0.43 |
| G-28 | 0.69 | 0.68 | 0.15 | 0.02 | 4.01 | 0.36 | 1.46 |
| G-60 | 0.43 | 0.48 | 0.37 | 0.02 | 2.38 | 0.23 | 0.38 |
| N2$\alpha$ | 0.75 | 0.63 | 0.15 | 0.01 | 5.78 | 0.33 | 2.79 |
| OP-6 | 0.57 | 0.21 | 0.24 | 0.02 | 2.88 | 0.10 | 0.27 |
| OP-27 | 0.27 | 0.15 | 0.66 | 0.01 | 1.23 | 0.08 | 0.15 |
| SK-N-BE(2C) | 0.54 | 0.24 | 0.24 | 0.03 | 2.5 | 0.13 | 0.30 |
| SK-N-SH | 0.25 | 0.10 | 0.66 | 0.02 | 1.11 | 0.04 | 0.05 |
| KELLY | 0.20 | 0.38 | 0.77 | 0.01 | 1.24 | 0.20 | 0.23 |
| SH-SY5Y | 0.32 | 0.01 | 0.54 | 0.02 | 1.85 | 0.00 | 0.00 |

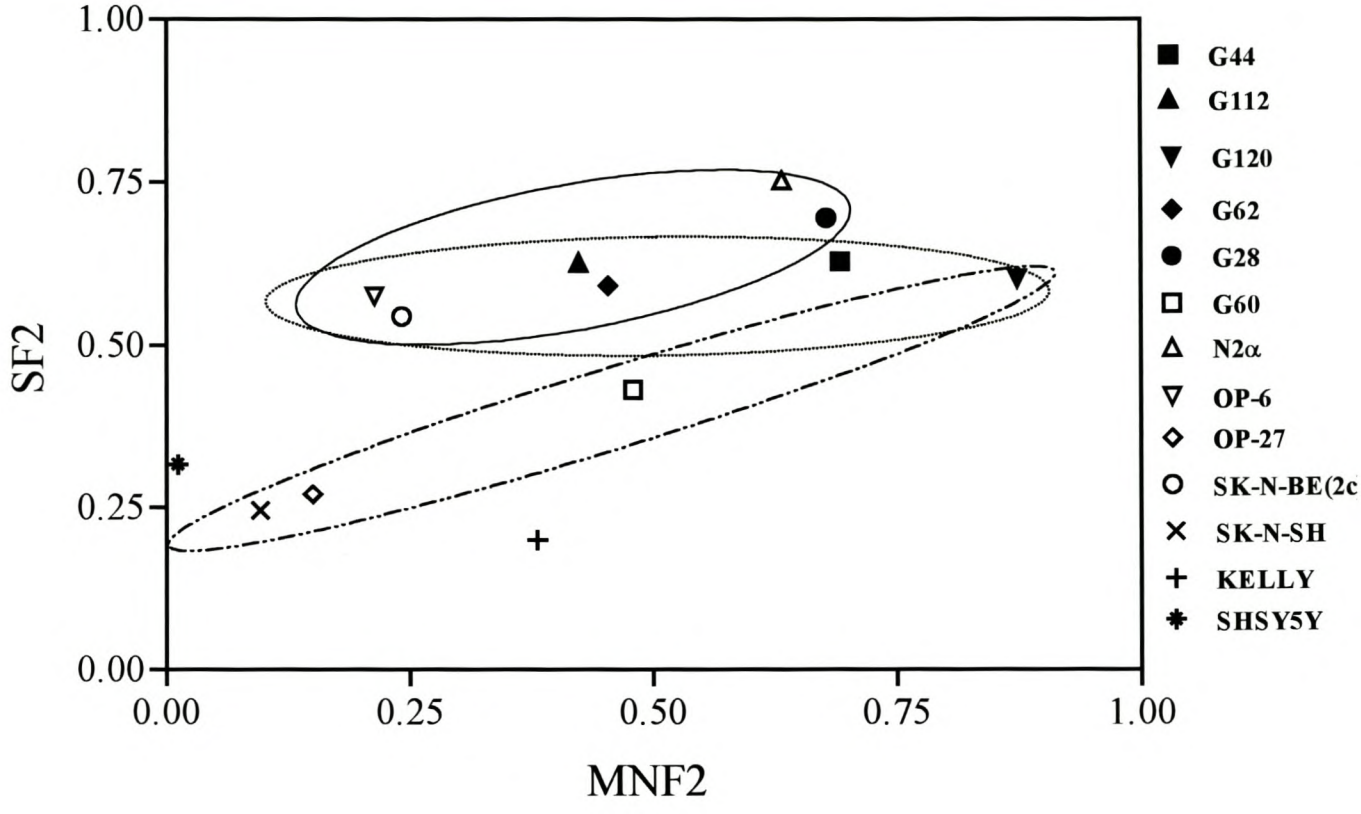


**FIGURE 3.5** Relationship between $^{60}Co$ γ-irradiation induced micronuclei frequency at 2 Gy ($MNF2_\gamma$) and surviving fraction at 2 Gy ($SF2_\gamma$) derived from data in figure 3.1 and figure 3.2, respectively. In the groups (G-44, G-120, G-60, OP-27, KELLY, SK-N-SH) and (G-112, G-62, G-28, N2α, OP-6) MN formation increases linearly with radiosensitivity, while no significant correlation exists between MN frequency and radiosensitivity in the group consisting of G-44, G-112, G-120, G-62, G-28, SK-N-BE(2C) and OP-6 cell lines.

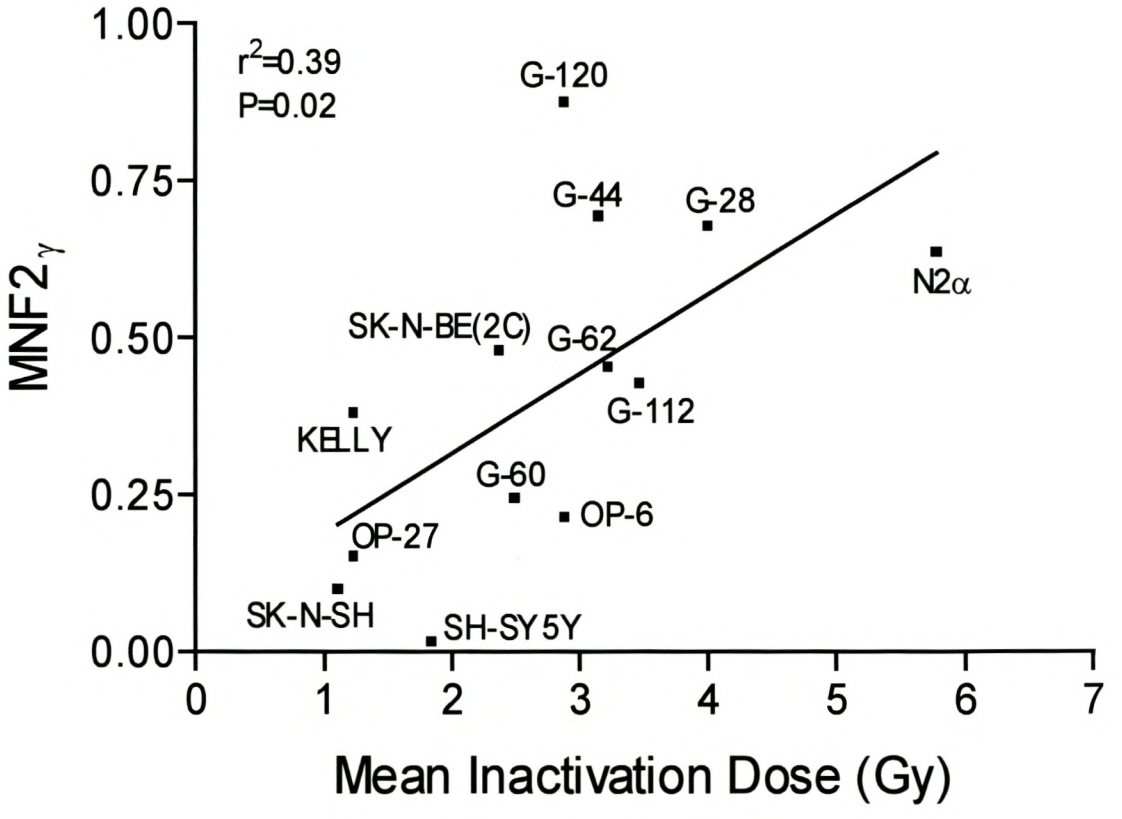


**FIGURE 3.6** Plot of micronuclei frequency at 2 Gy of $^{60}Co$ γ-irradiation as a function of mean inactivation dose in for 7 neuroblastoma and 6 neuroepithelial (G-) cell lines. $MNF2_\gamma$ and the mean inactivation dose were calculated from figures 3.2 and 3.4, respectively.

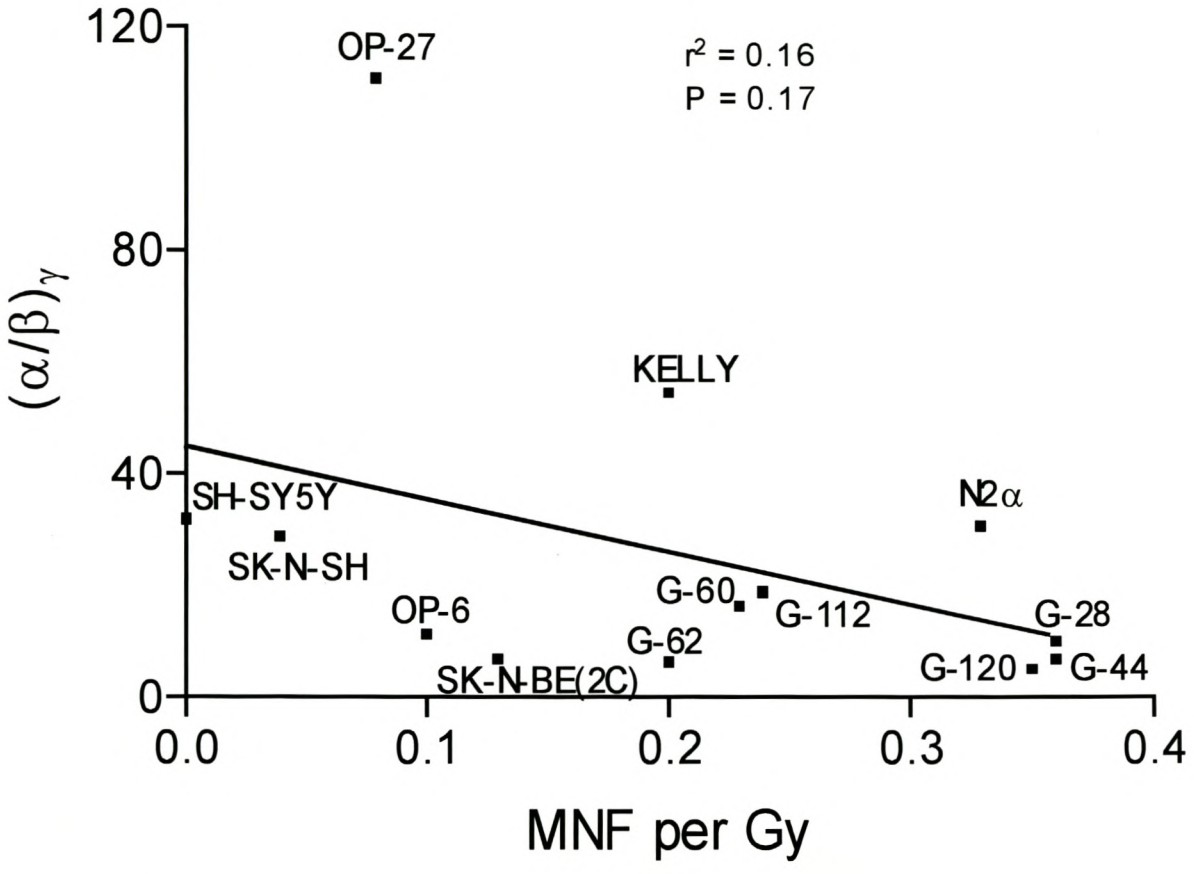


**FIGURE 3.7** Plot of $\alpha/\beta$ ratios as a function of micronuclei frequency per Gy of $^{60}Co$ $\gamma$-irradiation in for 7 neuroblastoma and 6 neuroepithelial (G-) cell lines. The $\alpha/\beta$ ratios were derived from figure 3.1. The micronuclei frequency per Gy represents the slopes of the micronuclei frequency-dose response regressions in figure 3.2.

The cellular DNA content was derived from the histograms in figure 3.8 by comparing the $G_1$-peaks of cell lines with the $G_1$-peaks of mouse and human lymphocytes. Figure 3.9 shows that the DNA index is poorly correlated with $SF2_\gamma$ and $MNF2_\gamma$. The correlation coefficient for DNA index and $SF2_\gamma$ was found to be 0.36 ($P$ = 0.25). The correlation coefficient for DNA index and $MNF2_\gamma$ was 0.33 ($P$ = 0.30). Figure 3.10 shows an even poorer correlation between DNA index and the mean inactivation dose ($r^2$ = 0.01, $P$ = 0.74). Similarly, no significant correlation exists ($r^2$ = 0.19, $P$ = 0.15) between DNA content and the $\alpha$-coefficient of cell inactivation (Figure 3.11). Figure 3.12 shows the variation of the $(\alpha/\beta)_\gamma$ ratio with DNA content. A very weak correlation ($r^2$ = 0.01, $P$ = 0.78) exists when 12 cell lines are considered (Figure 3.12A). Interestingly, a significant correlation is apparent when the data for KELLY and OP-27 are omitted showing that increase of DNA index correlates with decrease of $(\alpha/\beta)_\gamma$ ratio ($r^2$ = 0.78, $P$ = 0.0008, Figure 3.12B).

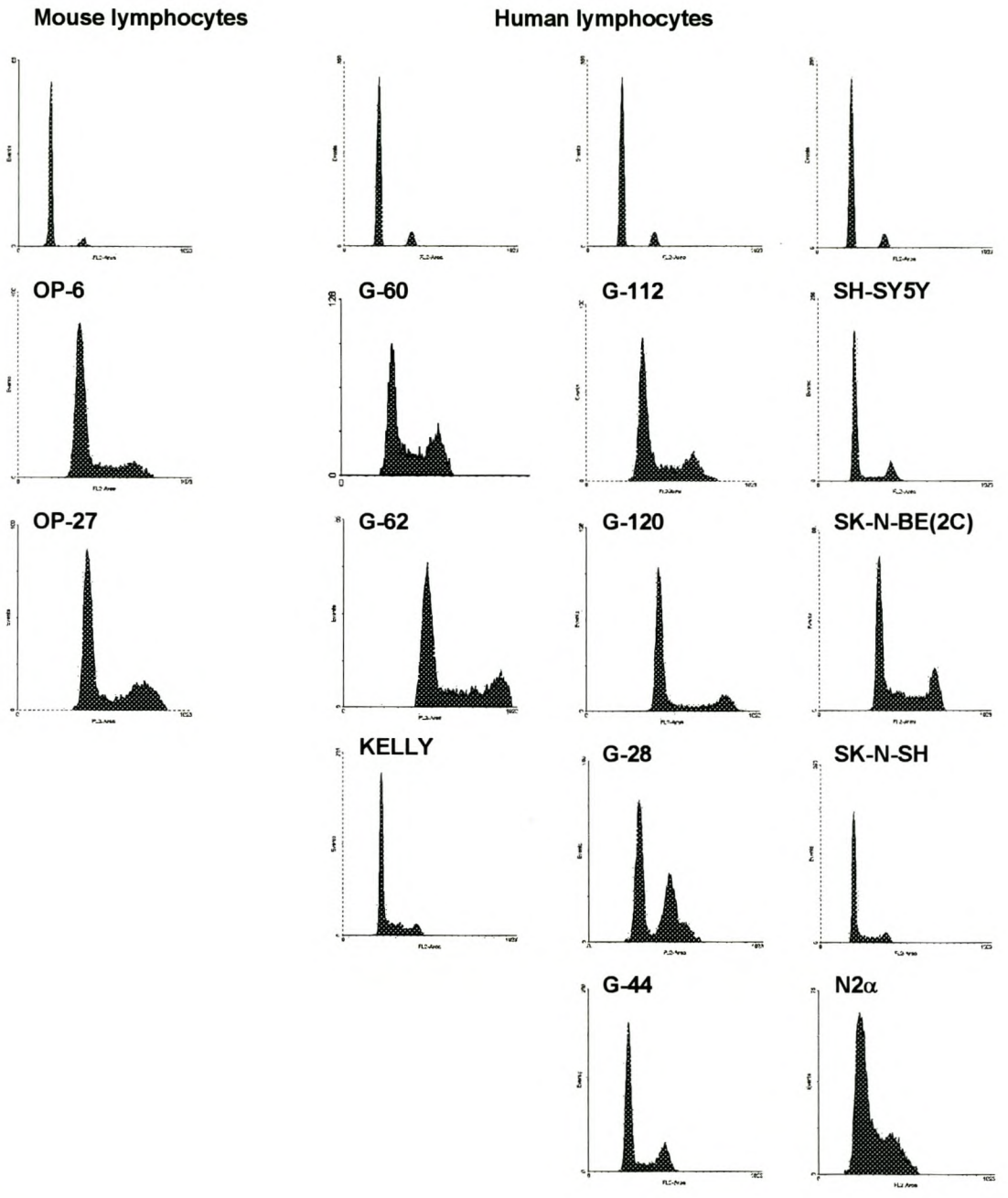


**FIGURE 3.8** DNA profiles for for 7 neuroblastoma and 6 neuroepithelial (G-) cell lines. Ploidy is determined by comparing the position of the $G_1$ peak of each cell line to that of lymphocytes (mouse lymphocytes versus OP-6 and OP-27; human lymphocytes versus G-28, G-44, G-62, G-120, G-112, G-60, SH-SY5Y, SK-N-SH, SK-N-BE(2C), N2α and KELLY.

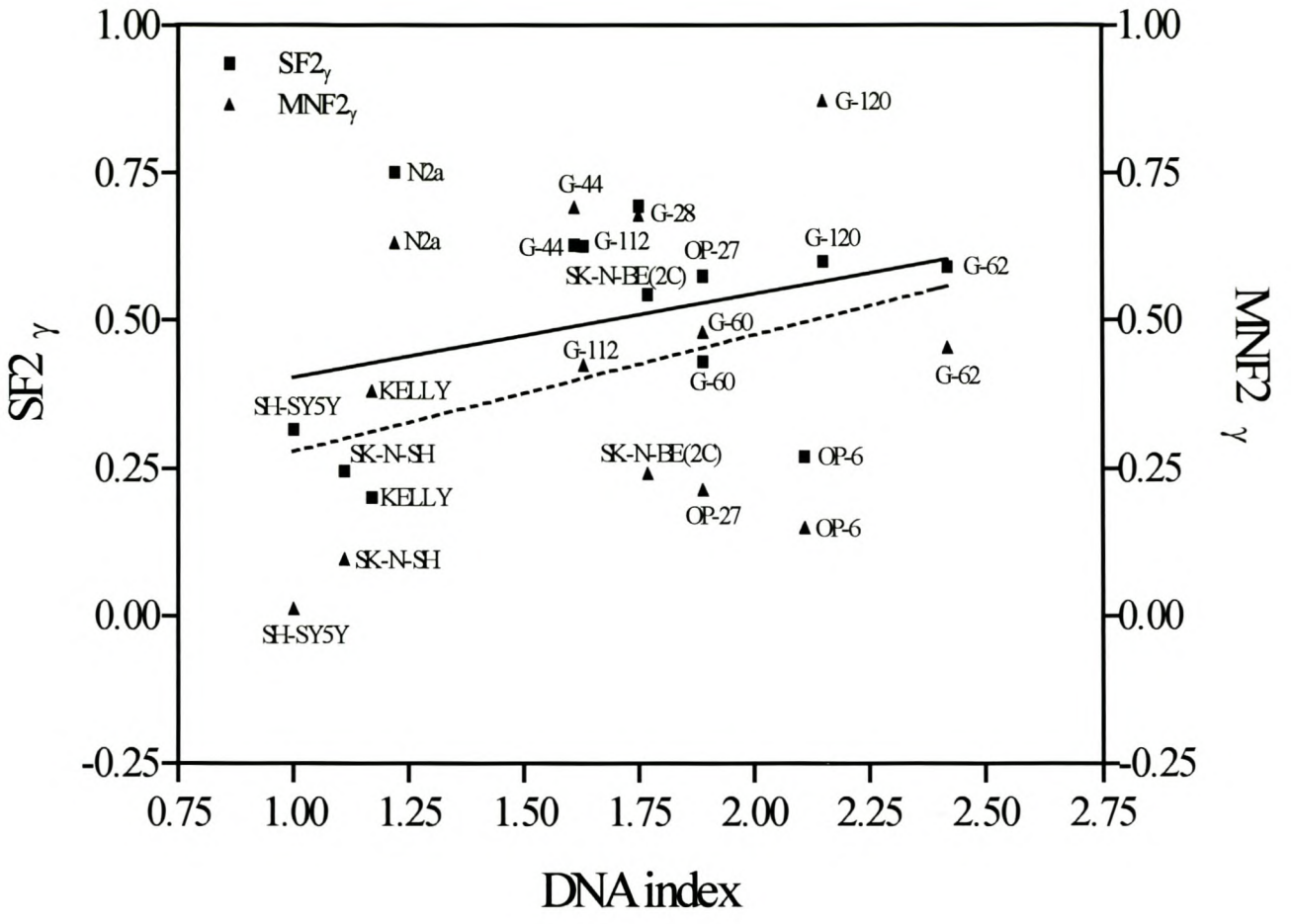


**FIGURE 3.9** Correlation between DNA index and radiosensitivity ($SF2_\gamma$) and between DNA index and micronuclei frequency ($MNF2_\gamma$) for for 7 neuroblastoma and 6 neuroepithelial (G-) cell lines. ▲------▲: DNA index versus $MNF2_\gamma$ ($r^2$ = 0.11, $P$ = 0.30), ■——■: DNA index versus $SF2_\gamma$ ($r^2$ = 0.13, $P$ = 0.25).

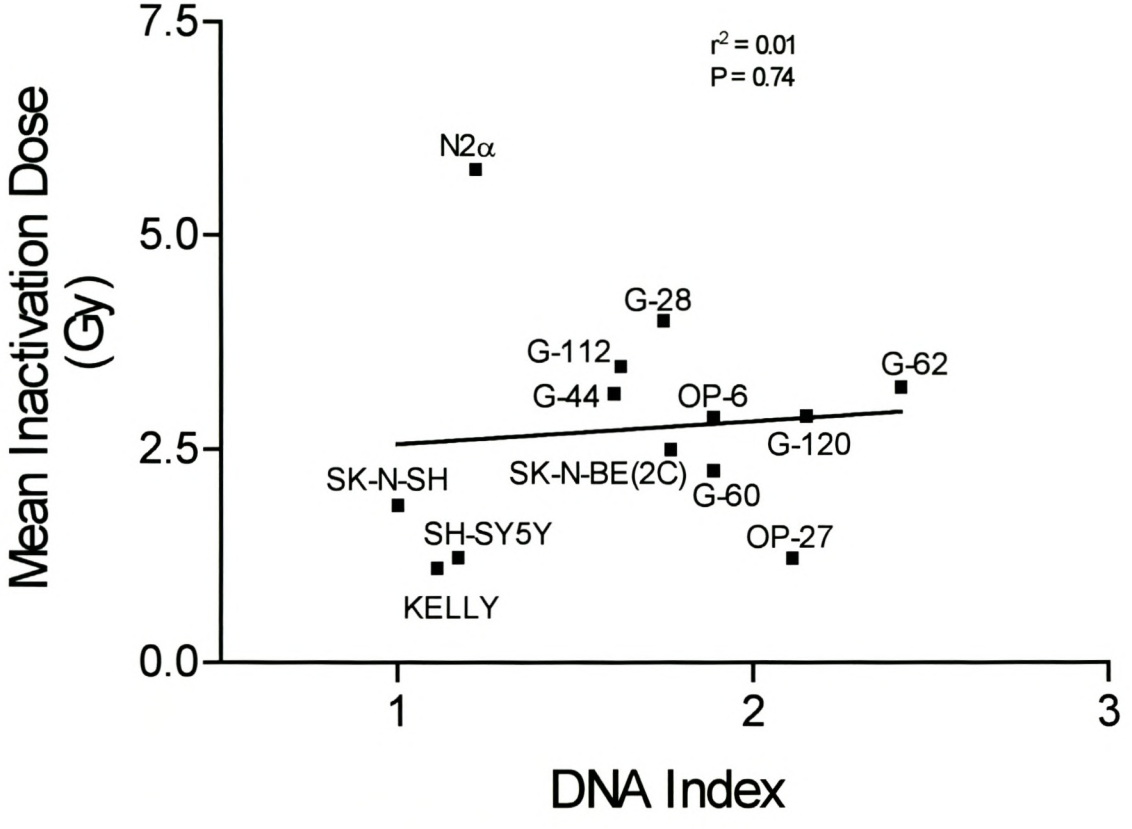


**FIGURE 3.10** A plot of the mean inactivation dose ($\overline{D}_\gamma$) upon $^{60}Co$ γ-irradiation as a function of cellular DNA content in for 7 neuroblastoma and 6 neuroepithelial (G-) cell lines. The $\overline{D}_\gamma$ values were derived from figure 3.4, while the DNA index was determined from the histograms in figure 3.8.

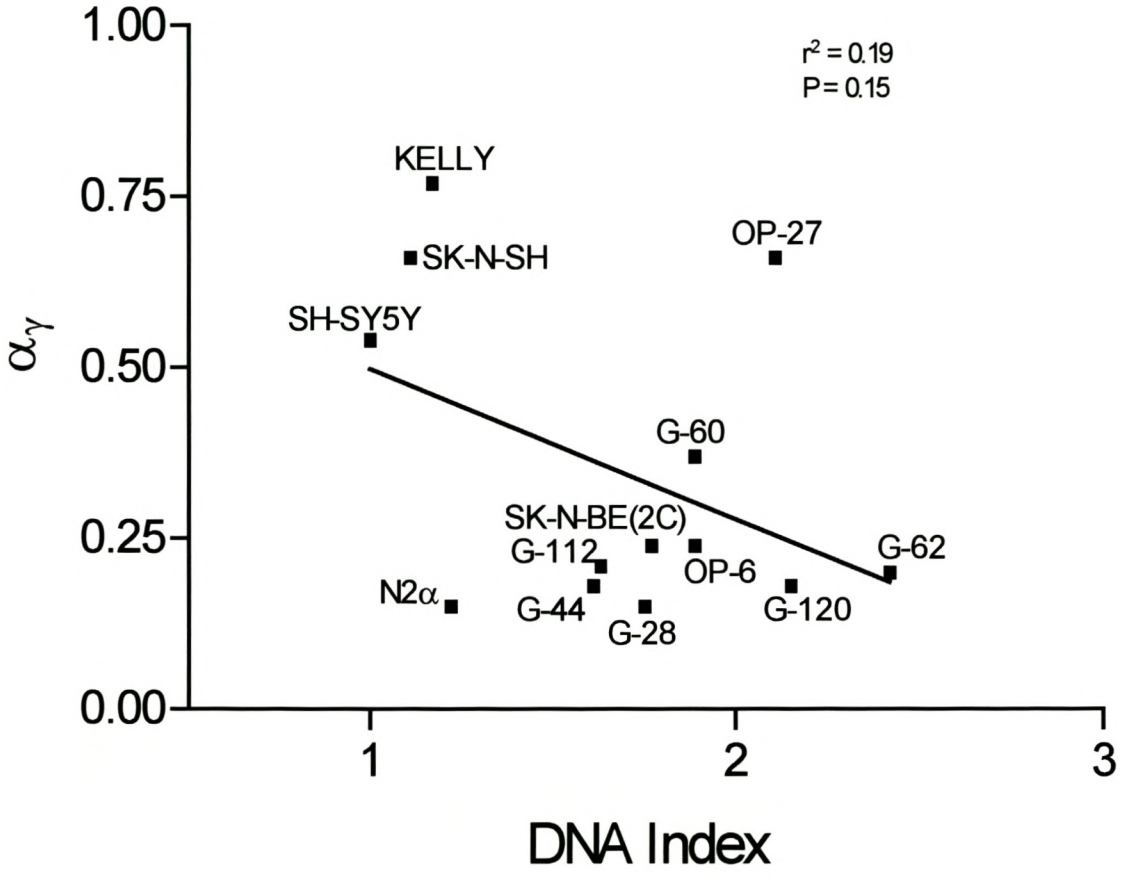


**FIGURE 3.11** A plot of the α-coefficient of cell inactivation ($\alpha_\gamma$) upon $^{60}Co$ γ-irradiation as a function of cellular DNA content in 7 neuroblastoma and 6 neuroepithelial (G-) cell lines. The DNA index was determined from the histograms in figure 3.8. The $\alpha_\gamma$ values were calculated from survival curves fitted to the L-Q model.

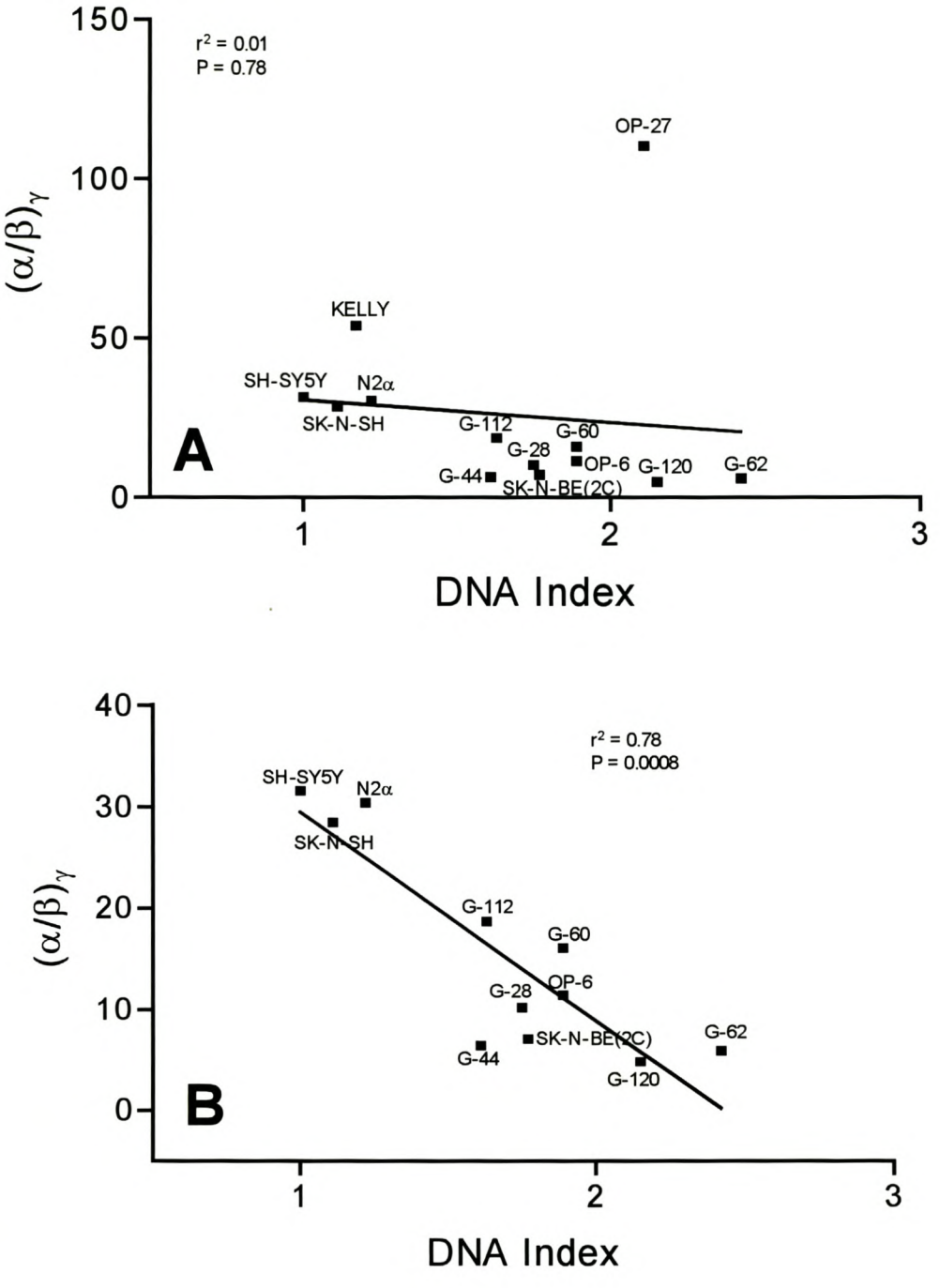


**FIGURE 3.12** The relationship between the $^{60}Co$ γ-irradiation inactivation parameter $(\alpha/\beta)_\gamma$ ratio as a function of cellular DNA content in: A) 13 cell lines and B) 11 cell lines. The DNA index was determined from the histograms in figure 3.8. The α/β-values were calculated from the survival curves fitted to the L-Q model in figure 3.1.

### 3.1.2 The Effect of Linear Energy Transfer (LET) on the Relationship Between Micronucleation and Cell Survival

High linear energy transfer (LET) p(66/$Be^{+}$) neutrons are expected to be more potent in the induction of chromosomal damage than low LET γ-rays. Figure 3.13 demonstrates that there is indeed a steeper micronuclei frequency-dose response for neutron irradiation than for $^{60}Co$ γ-irradiation. The efficiency of γ-rays and neutrons to induce micronuclei in these cell lines range from 0.04-0.36 micronuclei per Gy and 0.18-1.59 micronuclei per Gy, respectively. Neutrons are therefore found to be 3.8 (1.8 to 5.5)-fold more potent than γ-rays in inducting micronuclei. Micronuclei formation induced by neutron irradiation varied widely between cell lines. A wide range of the neutron response between cell lines demonstrates that no correlation exists between micronucleation and radiosensitivity. Figure 3.14 also shows that the photon and neutron responses were not correlated ($r^2$ = 0.19, *P* = 0.40). The eight cell lines fell into three different groups. The SK-N-SH cell line (SF = 0.25) shows a very weak tendency to form micronuclei after neutron and gamma irradiation. In the G-60 (SF2 = 0.43), G-62 (SF2 = 0.59), KELLY (SF2 = 0.20) and G-112 (SF2 = 0.63) cell lines where micronucleation is low and in a narrow range, the neutron induced micronucleation varies widely from 0.50 - 1.31 MN per Gy. Within this group of cell lines, increase of the photon induced MNF was associated with a linear increase of the neutron induced micronucleation (r = 0.90, *P* = 0.05). In the moderately photon-resistant cell lines (G-44, SF2 = 0.63; G-28, SF2 = 0.69; G-120, SF2 = 0.60), there was an even wider spread

of the neutron micronuclei frequency of 0.63 - 1.59 MN per Gy, giving a correlation coefficient of 0.74 ($P$ = 0.47). The micronuclei frequency response of these 3 cell lines to γ-irradiation was essentially similar.

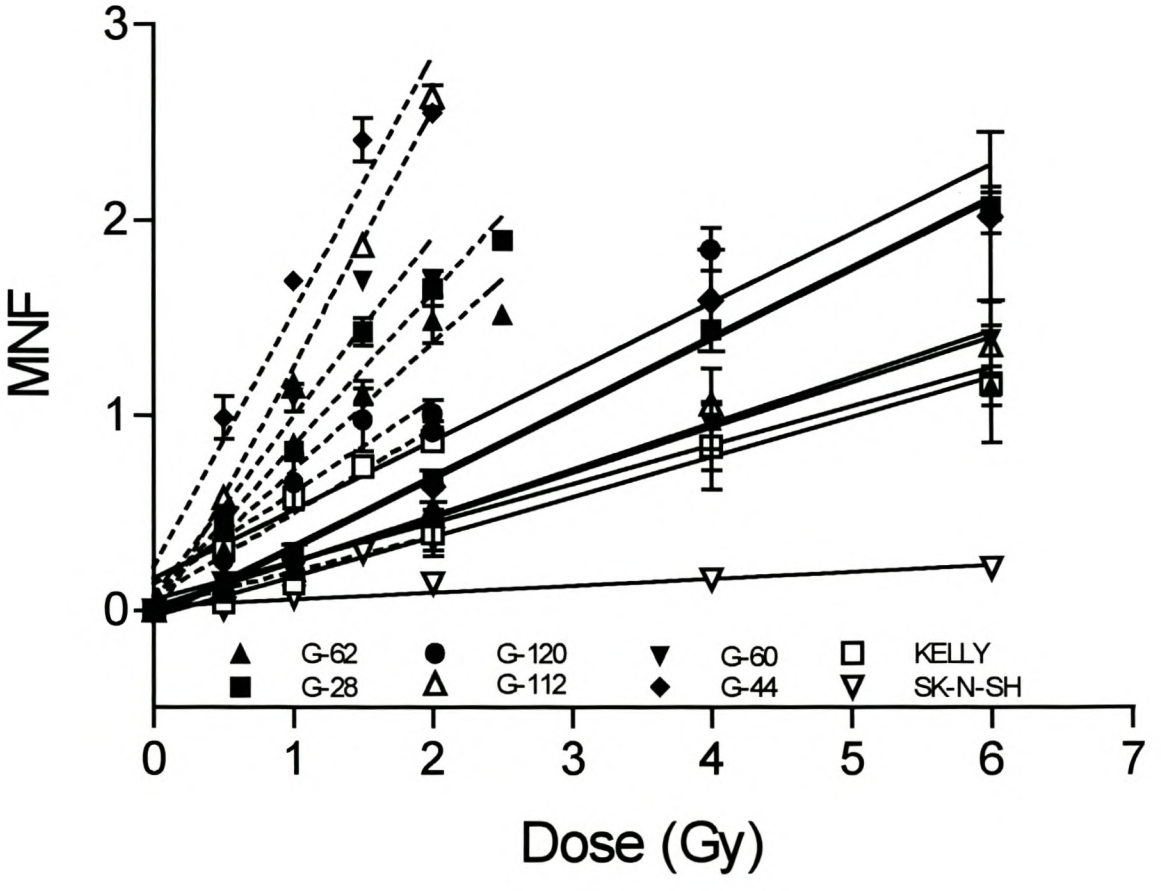


**FIGURE 3.13** Micronuclei frequency-dose response in 2 neuroblastoma (KELLY and SK-N-SH) and 6 neuroepithelial (G-) cell lines upon $^{60}Co$ γ-irradiation (——) and p(66/$Be^{+}$) neutron irradiation (……). Symbols represent the mean (± SD) of three independent experiments.

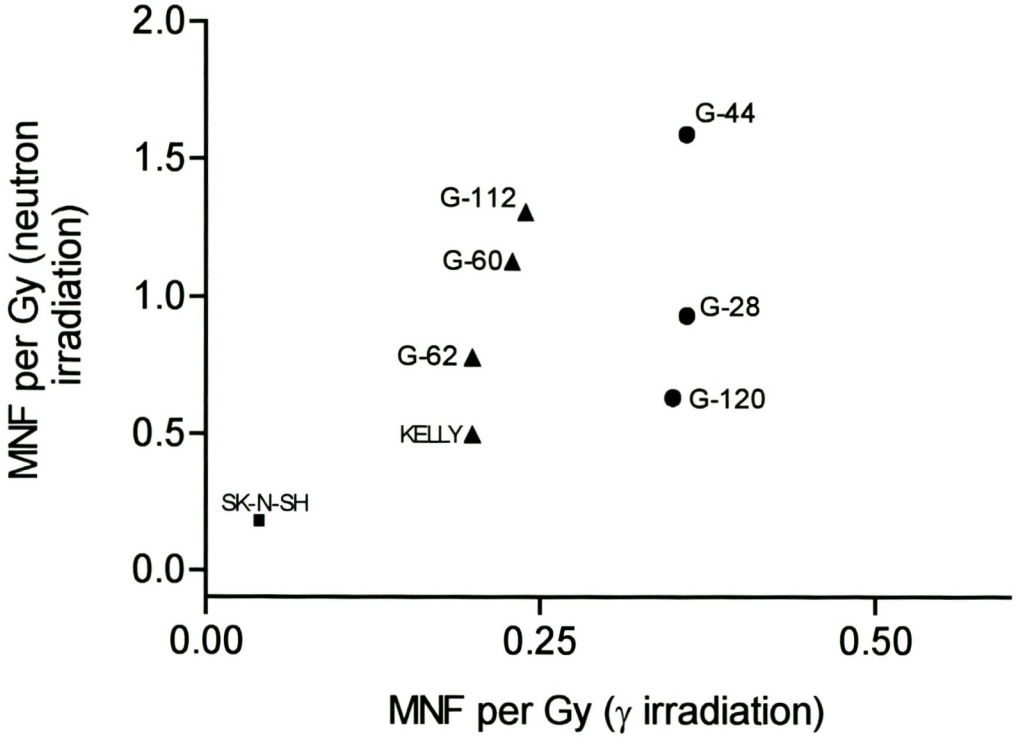


**FIGURE 3.14** Correlation between p(66/Be$^{+}$) neutron and $^{60}$Co γ-induced micronuclei formation in 2 neuroblastoma (KELLY and SK-N-SH) and 6 neuroepithelial (G-) cell lines. Symbols represent the slope of the micronuclei frequency-dose response regressions in figure 3.13.

### 3.1.3 Determination of Relative Biological Effectiveness (RBE) by the Micronucleus Assay.

Figure 3.15 shows the cell survival curves following neutron and γ-irradiation from which the mean inactivation doses are calculated. The mean inactivation dose is calculated for doses ranging from 0-5 Gy. A summary of the cell survival parameters is presented in table 3.2.

The dose dependence of the normal nuclear division fraction (NNDF) for neutron and γ-irradiation is shown in figure 3.16. Neutron irradiation induces more chromosomal damage and, therefore, produces lower numbers of cells without micronuclei as indicated by the rapid fall of NNDF with irradiation dose. In analogy to the mean inactivation dose, $\overline{D}$, the areas under the NNDF-dose response curves were represented by $\overline{NDF}$ and are presented in table 3.2 for the dose range 0-2 Gy.

The relative biological effectiveness, calculated from cell survival and micronucleation parameters, are plotted as functions of radiosensitivity expressed in terms of the photon mean inactivation dose is shown in figure 3.17. A moderate correlation exists between $RBE_{SF2}$ ($r^2$ = 0.61, $P$ = 0.07) and $RBE_{\alpha}$ ($r^2$ = 0.55, $P$ = 0.09) and $\overline{D}$. Relative biological effectiveness derived from $\overline{NDF}$ shows a very poor correlation with $\overline{D}$ ($r^2$ = 0.01, $P$ = 0.84). RBEs

obtained from $\alpha/\beta$-ratios and $\overline{D}$-values show significant correlations with $\overline{D}$, with $r^2 = 0.85$ ($P = 0.009$) and $r^2 = 0.84$ ($P = 0.01$), respectively. In the G-28, G-112, SK-N-SH and G-120 cell lines, RBEs derived from all five inactivation parameters show a wide variability. RBEs calculated from SF2, $\alpha$-coefficients, $\overline{D}$ and $\overline{NDF}$ are not significantly different in the KELLY cell line. In the G-44 cell line, RBEs from $\overline{D}$ and $\overline{NDF}$ are similar. No significant difference exists between RBEs derived from SF2, $\overline{D}$ and $\overline{NDF}$ for G-60. In the G-62 cell line, there is no significant difference in RBE values obtained from all five inactivation parameters.

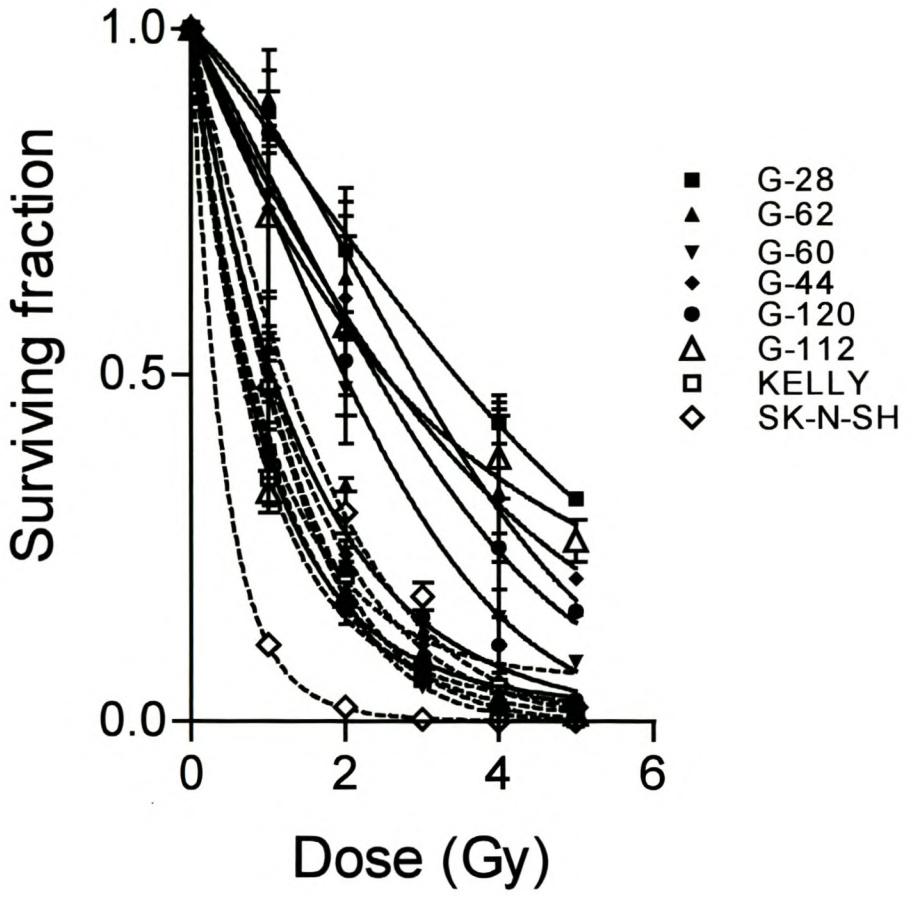


**FIGURE 3.15** Linear plot of cell survival in response to p(66/$Be^{+}$) neutron (-----) and $^{60}Co$ $\gamma$ (——) irradiation in 2 neuroblastoma (KELLY and SK-N-SH) and 6 neuroepithelial (G-) cell lines. Symbols represent the mean (± SD) surviving fraction for three independent experiments. The area under each curve represents the mean inactivation dose, $\overline{D}$.

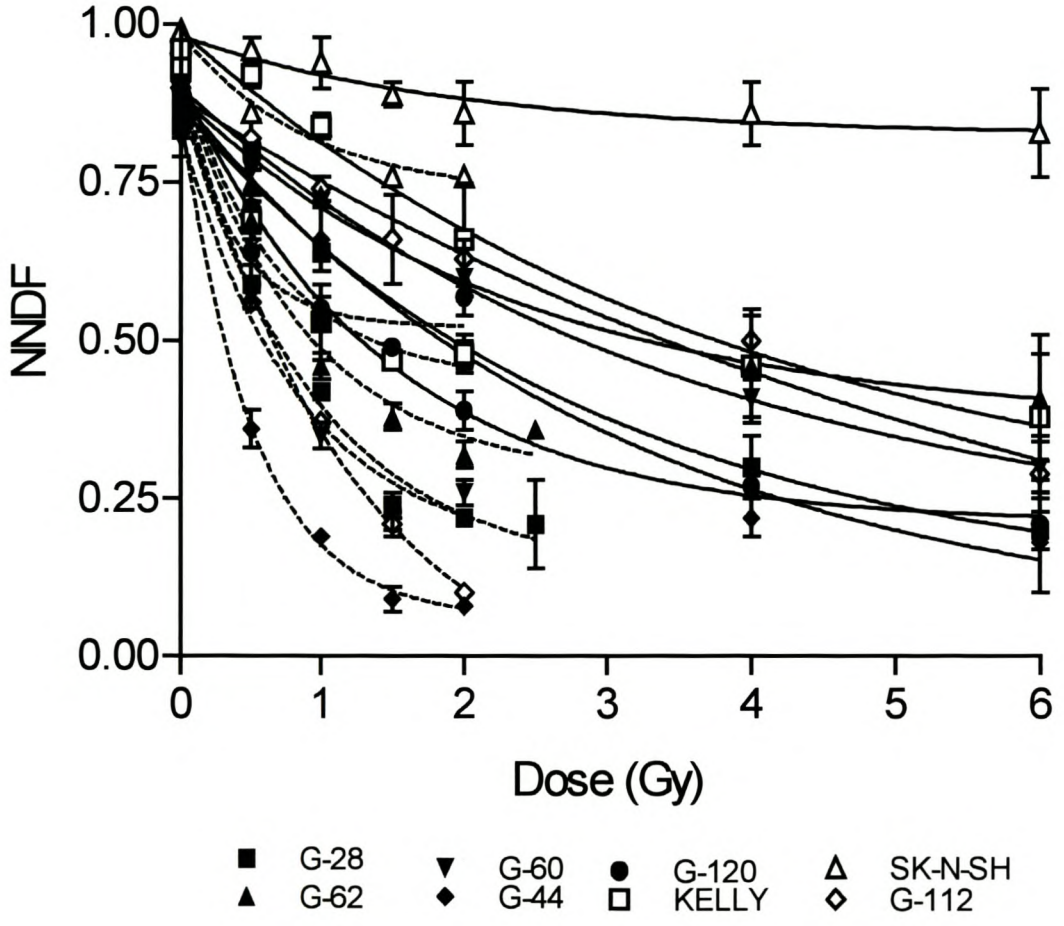


**FIGURE 3.16** Dependence of the normal nuclear division fraction (NNDF) upon p(66/$Be^{+}$) neutron (-----) and $^{60}Co$ $\gamma$ (——) irradiation in 2 neuroblastoma (KELLY and SK-N-SH) and 6 neuroepithelial (G-) cell lines. Symbols represent the mean (± SD) NNDF from three independent experiments. $\overline{NDF}$ represents the area under each curve.

**TABLE 3.2**

Cell inactivation parameters for 2 neuroblastoma (KELLY and SK-N-SH) and 6 neuroepithelial (G-) cell lines. SF2, $\alpha$, $\alpha/\beta$ and $\overline{D}$ are derived from clonogenic survival data. $\overline{NDF}$ represents the area under the normal nuclear division fraction-dose response curves. $\gamma$ and n denote $^{60}Co$ $\gamma$- and p(66/$Be^{+}$) neutron-irradiation, respectively.

| Cell line | $SF2_\gamma$ | $SF2_n$ | $\alpha_\gamma$ ($Gy^{-2}$) | $\alpha_n$ ($Gy^{-2}$) | $(\alpha/\beta)_\gamma$ ($Gy^{-1}$) | $(\alpha/\beta)_n$ ($Gy^{-1}$) | $\overline{D}_\gamma$ (Gy) | $\overline{D}_n$ (Gy) | $\overline{NDF}_\gamma$ (Gy) | $\overline{NDF}_n$ (Gy) |
|---|---|---|---|---|---|---|---|---|---|---|
| G-28 | 0.69 | 0.16 | 0.15 | 0.90 | 10.20 | 107.93 | 3.21 | 1.16 | 1.33 | 0.90 |
| G-62 | 0.59 | 0.30 | 0.20 | 0.38 | 5.90 | 3.36 | 2.94 | 1.55 | 1.45 | 1.07 |
| G-120 | 0.60 | 0.26 | 0.18 | 0.68 | 4.81 | 101.23 | 2.59 | 1.38 | 1.19 | 1.20 |
| G-44 | 0.63 | 0.26 | 0.18 | 0.53 | 6.43 | 6.98 | 2.74 | 1.40 | 1.34 | 0.56 |
| G-60 | 0.43 | 0.21 | 0.37 | 0.41 | 16.31 | 2.13 | 2.25 | 1.25 | 1.46 | 0.85 |
| KELLY | 0.20 | 0.18 | 0.77 | 0.59 | 54.10 | 4.53 | 1.25 | 1.22 | 1.66 | 1.20 |
| G-112 | 0.63 | 0.13 | 0.27 | 0.81 | 9.00 | 40.50 | 2.79 | 1.14 | 1.49 | 0.82 |
| SK-N-SH | 0.25 | 0.02 | 0.46 | 2.11 | 7.67 | 42.20 | 1.52 | 0.63 | 1.85 | 1.67 |

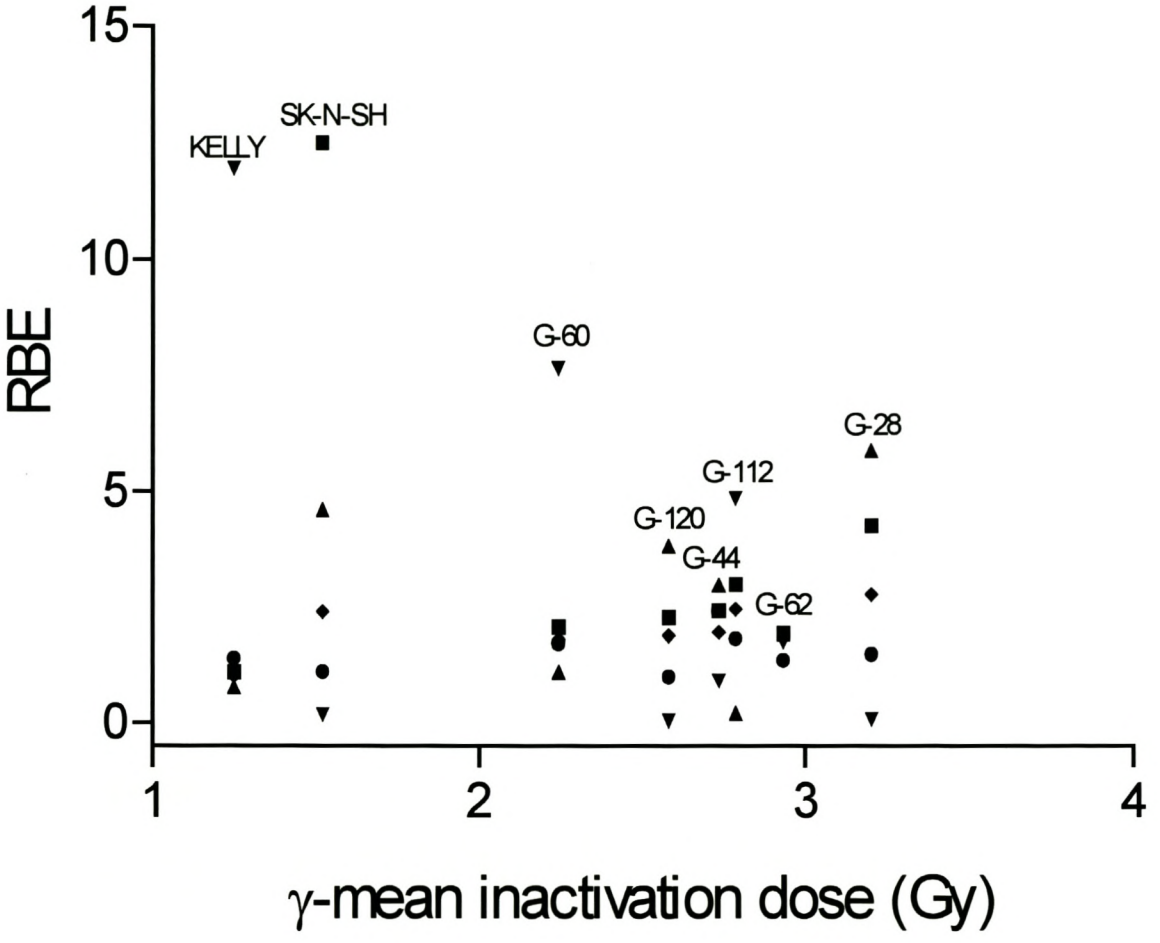


**FIGURE 3.17** Interrelationship between the relative biological effectiveness (RBE) calculated from the following cell inactivation parameters: SF2 (■), α-coefficient (▲), α/β ratio (▼), $\overline{D}$ (◆) and $\overline{NDF}$ (●) and the photon mean inactivation dose $\overline{D}_\gamma$ for 2 neuroblastoma (KELLY and SK-N-SH) and 6 neuroepithelial (G-)cell lines.

## 3.2 RADIATION-INDUCED CELL SURVIVAL, MICRONUCLEATION AND APOPTOSIS

### 3.2.1 Micronucleation and Apoptosis

Figure 3.18 shows the dose-response of the fraction of binucleated cells containing micronuclei and the apoptotic fraction in 2 neuroblastoma and 5 neuroepithelial cell lines. For doses from 0-6 Gy, micronucleation is adequately defined by an exponential function of dose ($0.93 \leq R^2 \leq 0.99$). Figure 3.18 also shows that in the same dose range, the apoptotic propensity in the seven cell lines is linearly related to dose ($0.90 \leq r^2 \leq 0.99$; $0.0001 \leq P \leq 0.014$). The *P*-values were obtained from two-sided tests.

The interrelationship between micronucleation and apoptosis was tested by plotting the fraction of micronucleated BNC as a function of apoptotic propensity (Figure 3.19). In the dose range 0-6 Gy, micronucleation varies as an exponential function of apoptosis ($0.95 \leq R^2 \leq 0.99$). Micronucleation increases rapidly with apoptosis and reaches a maximum value as the irradiation dose increases.

### 3.2.2 Radiosensitivity and Apoptosis

The coefficient for inactivation via apoptosis after $^{60}Co$ $\gamma$-irradiation $\xi$, represented by the regression slopes in figure 3.17, varies from 0.01 to 0.03

(0.02 ± 0.01) per Gy (Table 3.3). With the exception of G-62 and G-60 cell lines, all the other cell lines exhibit the same ξ-value. In the seven cell lines, no meaningful correlation exists between cellular susceptibility to radiation-induced apoptosis and radiosensitivity.

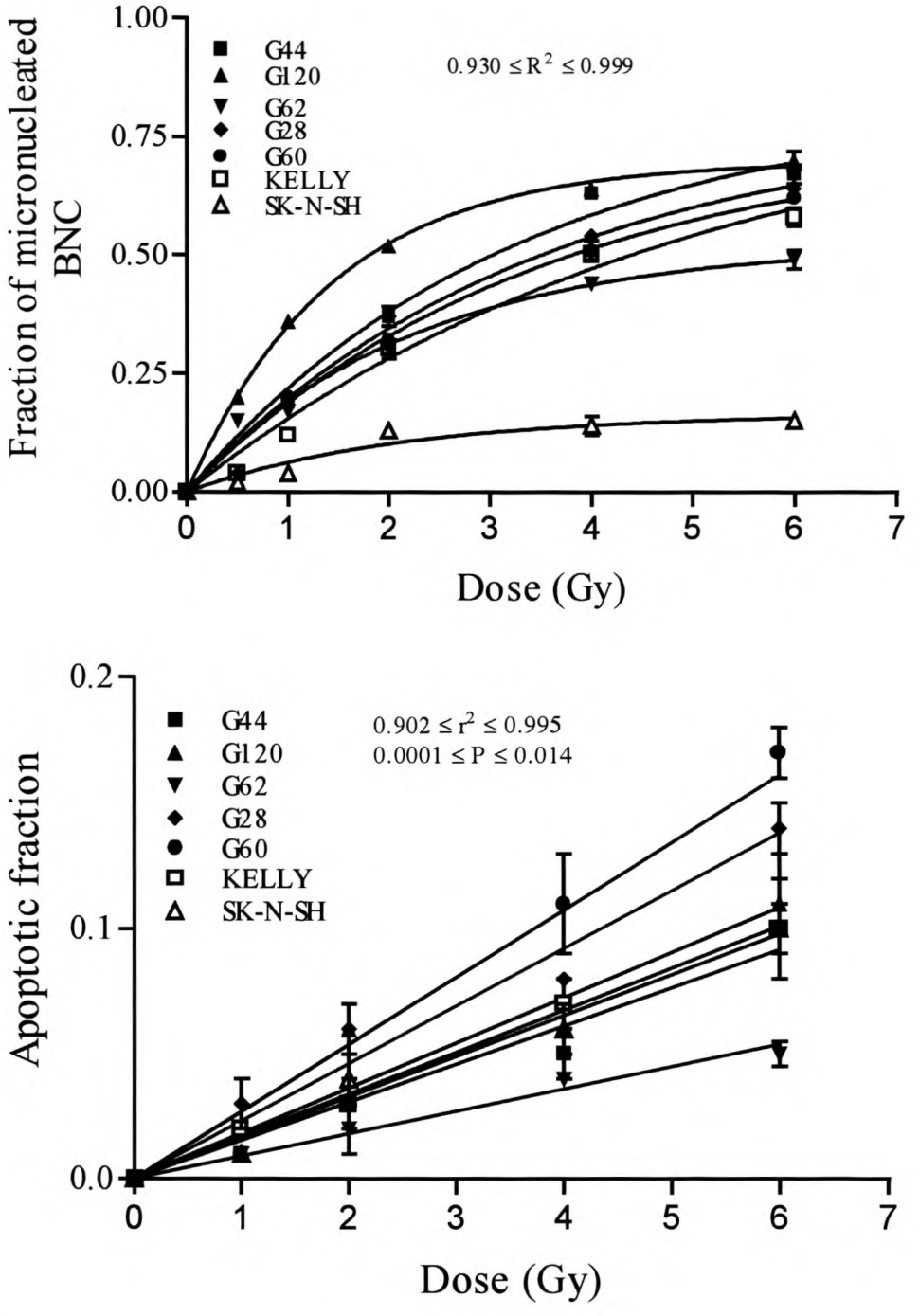


**FIGURE 3.18** Proportion of micronucleated binucleated cells plotted as a function of $^{60}$Co γ-irradiation dose (Upper panel). Measured data (mean ± SD), corrected for background micronucleation, were fitted to the function, $Fm_D = Fm[1 - \exp(-\mu_\gamma D)]$. Fraction of apoptotic cells plotted as a function of $^{60}$Co γ-irradiation dose (Lower panel). Pooled experimental data (mean ± SD), corrected for background apoptosis were fitted to the regression, $Fa_D = \alpha D$.

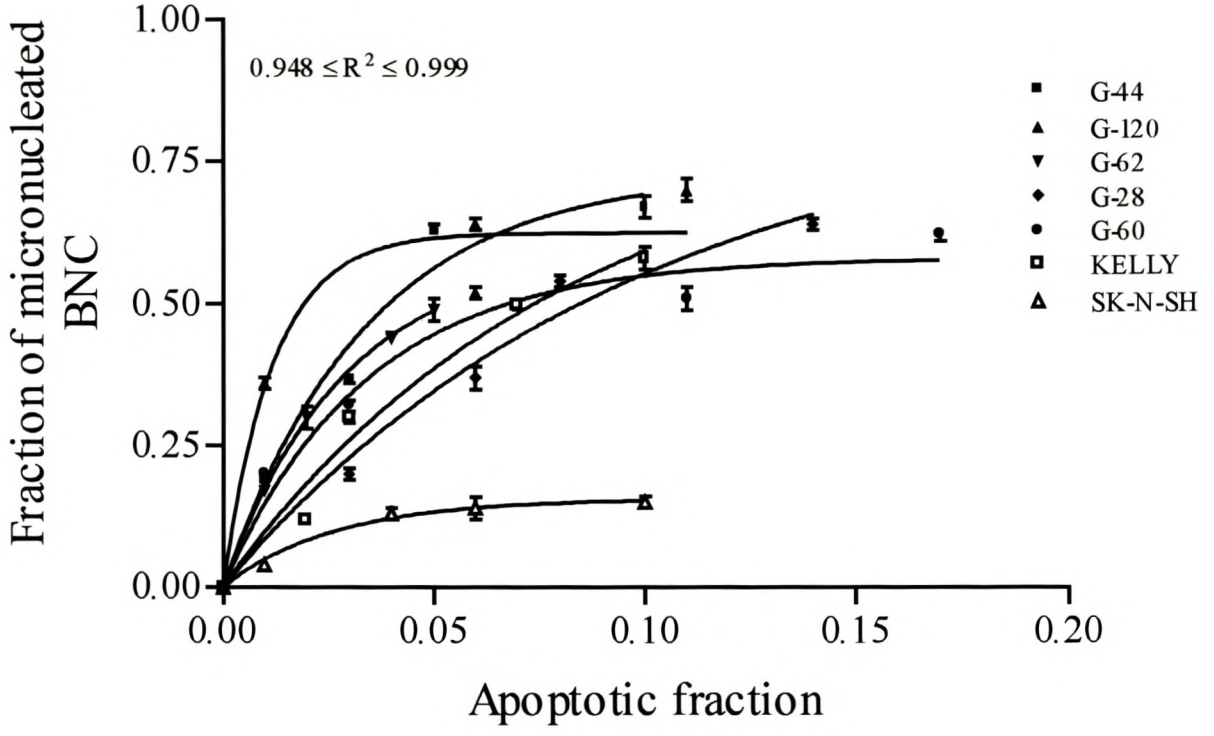


**FIGURE 3.19** Fraction of micronucleated binucleated cells plotted as a function of apoptotic propensity in 2 neuroblastoma (KELLY and SK-N-SH) and 5 neuroepithelial (G-) cell lines. Each data point represents the relationship between induction of micronuclei and apoptosis for doses of $^{60}Co$ $\gamma$-irradiation ranging from 0-6 Gy.

**TABLE 3.3**

The ratio of cell survival derived from micronucleation and apoptosis ($SF_{MA}$) to cell survival by colony formation ($SF_{COL}$) as a function of $^{60}Co$ $\gamma$-irradiation dose in 2 neuroblastoma (KELLY and SK-N-SH) and 5 neuroepithelial (G-) cell lines. The coefficients for induction of micronuclei and apoptosis are represented by $\mu_\gamma$ and $\xi$, respectively. The maximum binucleation indices for unirradiated (0 Gy) and irradiated (4 Gy) samples, after 40 hours of incubation with cytochalasin B, are denoted with $\beta_0$ and $\beta_4$, respectively.

$(SF_{MA})/SF_{COL}$

| | G-44 | G-120 | G-62 | G-28 | G-60 | KELLY | SK-N-SH |
|---|---|---|---|---|---|---|---|
| Dose | $\beta_0$=0.84±0.01 | $\beta_0$=0.49±0.01 | $\beta_0$=0.35±0.02 | $\beta_0$=0.76±0.02 | $\beta_0$=0.70±0.07 | $\beta_0$=0.41±0.05 | $\beta_0$=0.28±0.07 |
| (Gy) | $\beta_4$=0.71±0.02 | $\beta_4$=0.14±0.01 | $\beta_4$=0.12±0.03 | $\beta_4$=0.74±0.01 | $\beta_4$=0.28±0.02 | $\beta_4$=0.13±0.08 | $\beta_4$=0.12±0.02 |
| | $\mu_\gamma$=0.31±0.07 | $\mu_\gamma$=0.69±0.03 | $\mu_\gamma$=0.45±0.07 | $\mu_\gamma$=0.29±0.07 | $\mu_\gamma$=0.29±0.02 | $\mu_\gamma$=0.20±0.07 | $\mu_\gamma$=0.47±0.19 |
| | $\xi$=0.016±0.002 | $\xi$=0.018±0.003 | $\xi$=0.009±0.001 | $\xi$=0.022±0.002 | $\xi$=0.030±0.003 | $\xi$=0.017±0.001 | $\xi$=0.017±0.001 |
| | $SF2_\gamma$=0.63 | $SF2_\gamma$=0.60 | $SF2_\gamma$=0.59 | $SF2_\gamma$=0.69 | $SF2_\gamma$=0.43 | $SF2_\gamma$=0.20 | $SF2_\gamma$=0.25 |
| 0.0 | 1.00 | 1.00 | 1.00 | 1.00 | 1.00 | 1.00 | 1.00 |
| 0.5 | 0.96 | 0.87 | 0.99 | 0.95 | 1.07 | 1.35 | 1.34 |
| 1.0 | 0.93 | 0.78 | 1.01 | 0.92 | 1.16 | 1.83 | 1.82 |
| 2.0 | 0.94 | 0.73 | 1.13 | 0.89 | 1.42 | 3.45 | 3.39 |
| 4.0 | 1.11 | 1.05 | 1.95 | 0.89 | 2.40 | 12.78 | 14.60 |
| 6.0 | 1.54 | 2.22 | 4.89 | 0.93 | 4.26 | 50.00 | 71.11 |

### 3.2.3 Radiosensitivity and Micronucleation

Figure 3.20 shows that micronucleation does not rank the cell lines according to radiosensitivity. The coefficient of cell inactivation via micronucleation, $\mu_\gamma$, varies significantly from 0.20 ± 0.07 to 0.69 ± 0.03 per Gy. The interrelationship between the micronucleus formation and radiosensitivity was tested using cell survival at 2 Gy ($SF2_\gamma$), mean inactivation dose ($\overline{D}_\gamma$), $\alpha$-coefficient and $(\alpha/\beta)_\gamma$ ratio.

As illustrated in figures 3.20 and 3.21, there is no significant correlation between the coefficient of micronucleus formation, $\mu_\gamma$, and any of the parameters of cellular radiosensitivity. For $SF2_\gamma$, $\overline{D}_\gamma$, and $(\alpha/\beta)_\gamma$ the regression characteristics are $r^2 = 0.07$; $P = 0.58$, $r^2 = 0.04$; $P = 0.68$ and $r^2 = 0.26$; $P = 0.25$, respectively. Since micronuclei are an expression of DNA damage, it was suspected that a correlation may be apparent between DNA content and micronucleation. The relationship between micronucleation and cellular DNA content was examined in figure 3.20. No significant correlation exists between DNA index and micronucleus formation ($r^2 = 0.21$; $P = 0.31$). Figure 3.22 represents the variation of the coefficient for micronucleation with the $\alpha$-coefficient. No meaningful correlation exists between $\alpha_\gamma$ and $\mu_\gamma$ ($r^2 = 0.11$, $P = 0.47$).

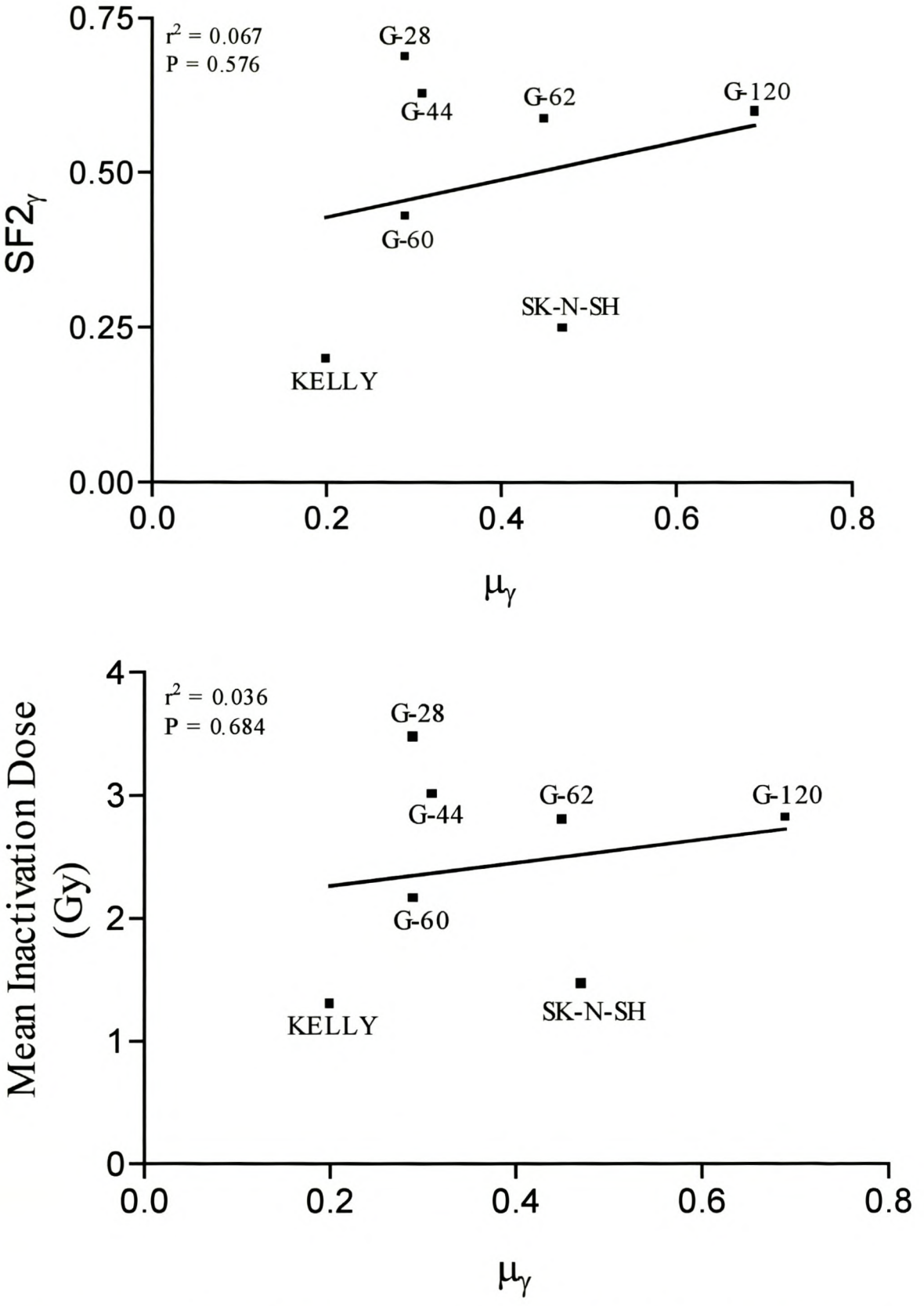


**FIGURE 3.20** Plots of the surviving fraction at 2 Gy ($SF2_\gamma$) and the mean inactivation dose ($\overline{D}_\gamma$) as functions of the coefficient for the formation of micronuclei ($\mu_\gamma$) upon $^{60}Co$ $\gamma$-irradiation for 2 neuroblastoma (KELLY and SK-N-SH) and 5 neuroepithelial (G-) cell lines.

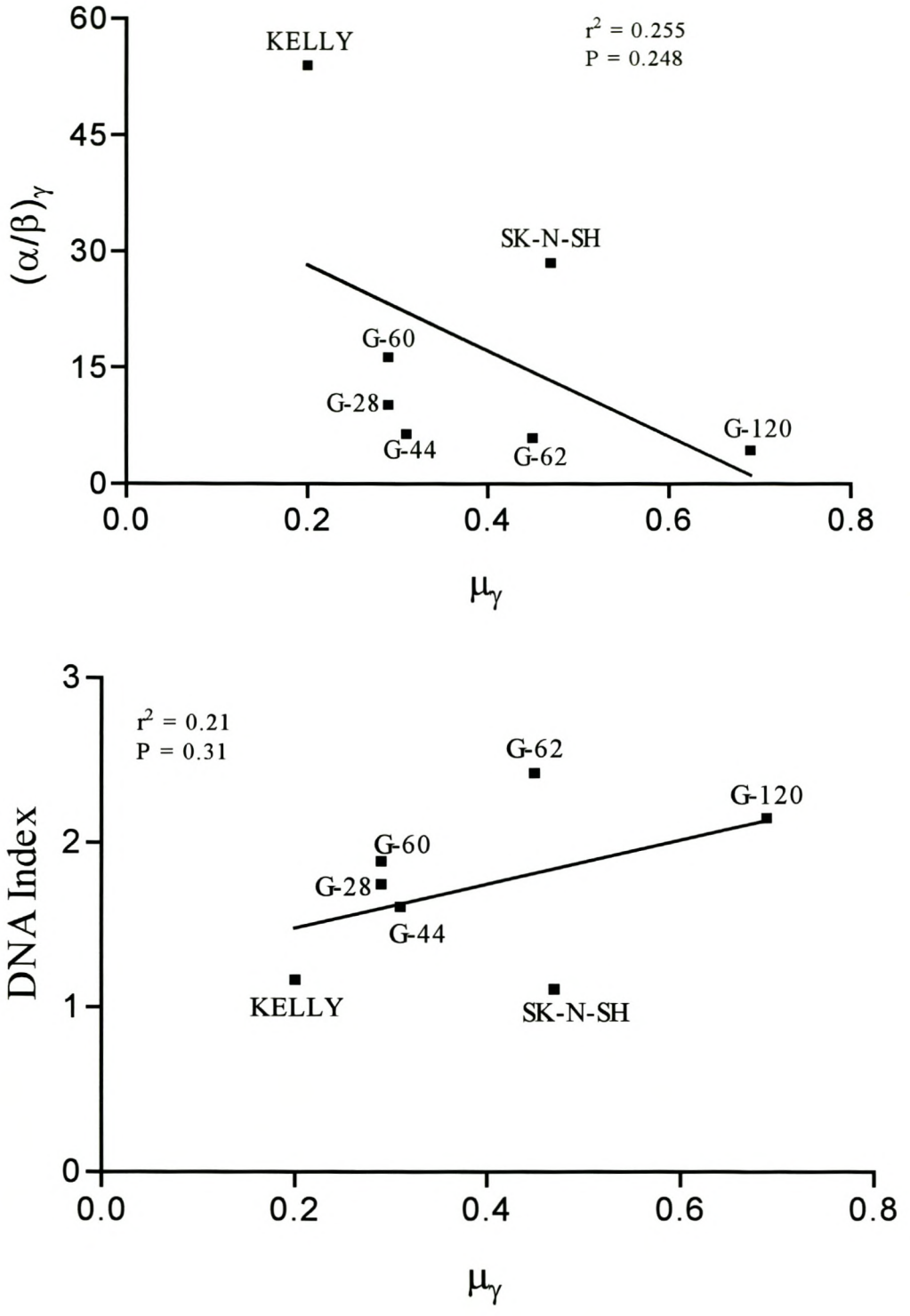


**FIGURE 3.21** Plots of the $(\alpha/\beta)_\gamma$ ratio and DNA index as functions of the coefficient for the formation of micronuclei ($\mu_\gamma$) upon $^{60}$Co $\gamma$-irradiation for 2 neuroblastoma (KELLY and SK-N-SH) and 5 neuroepithelial (G-) cell lines.

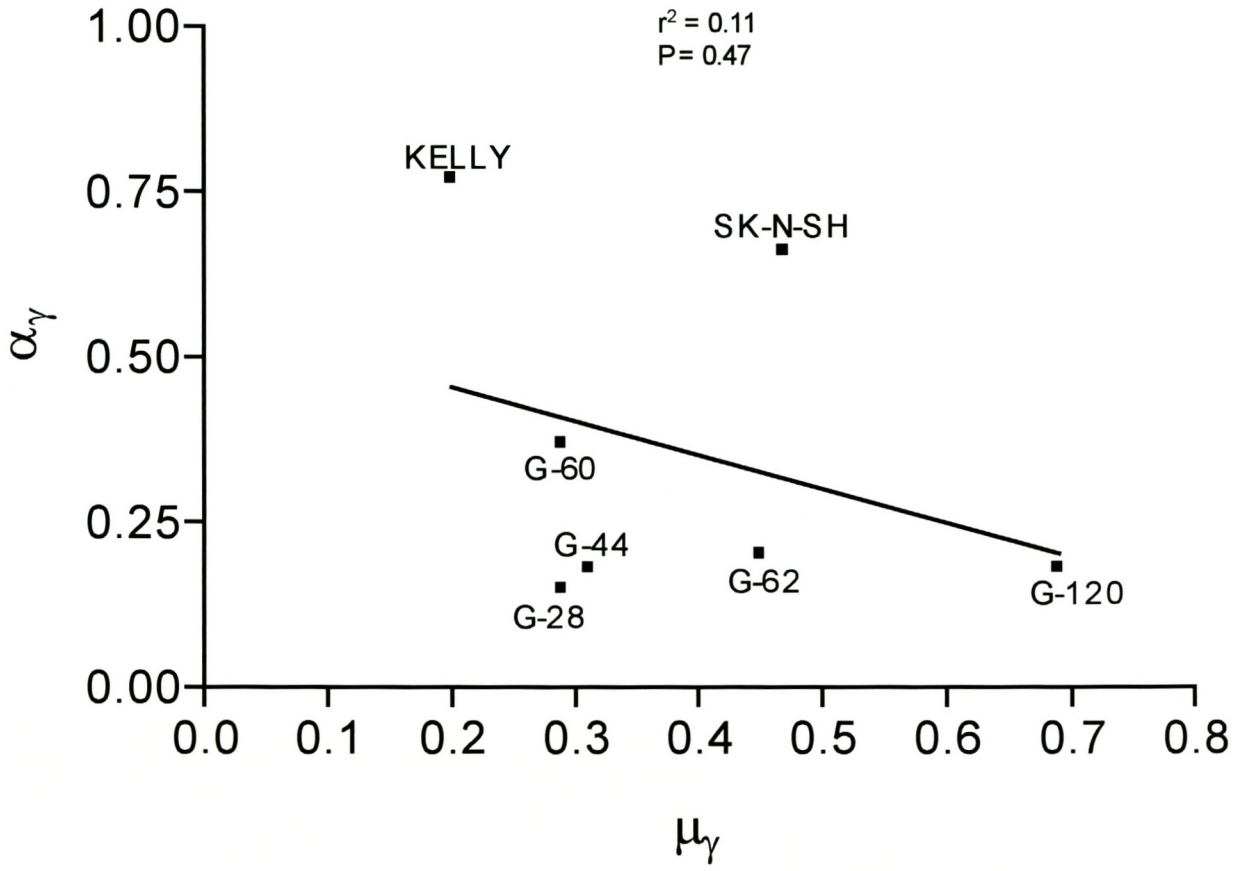


**FIGURE 3.22** Relationship between the α-coefficient of inactivation and the coefficient for the formation of micronuclei ($\mu_\gamma$) in 2 neuroblastoma (KELLY and SK-N-SH) and 5 neuroepithelial (G-) cell lines upon $^{60}$Co γ-irradiation.

### 3.2.4 Dependence of Cell Death Due to Non-Micronucleation and Non-Apoptotic Events on Irradiation Dose

The probability of radiation inactivation via events other than apoptosis and micronuclei formation, $P_{oe}$, was deduced from figure 3.18 using equation 5, and is plotted in figure 3.23. In the more sensitive cell lines (KELLY, SK-N-SH and G-60) $P_{oe}$ increases with dose, reaches a maximum and then declines at higher doses. For the resistant cell lines, a threshold dose is required for the onset of cell inactivation due to events other than apoptosis and micronucleation. The minimum dose at which this mode of cell death occurs in the resistant G-62, G-44 and G-120 cell lines is 0.87, 3.04, and 3.85 Gy, respectively (Figure 3.23). Doses up to 6 Gy seem to fall short of inducing cell death via small deletions, chromosome aberrations and misrepair in the G-28 cell line.

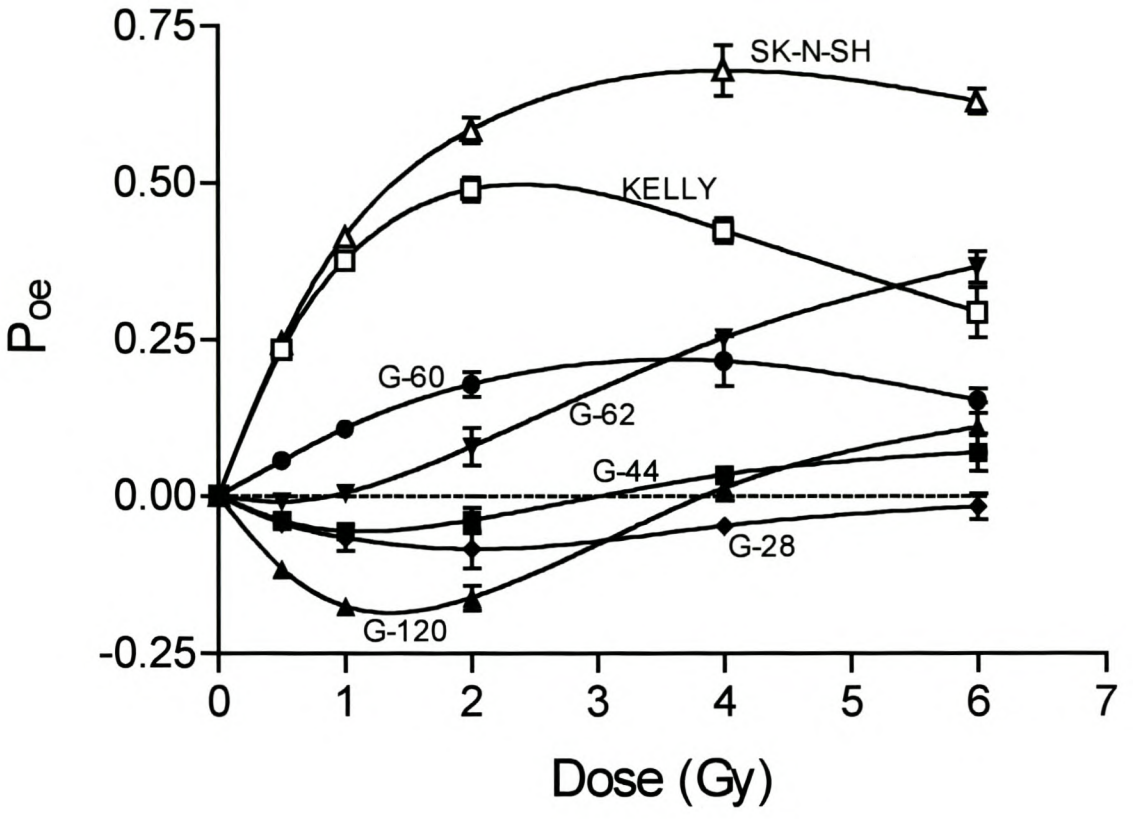


**FIGURE 3.23** Probability of cell death due to non-apoptotic events and micronucleation, $P_{oe}$, as a function of $^{60}Co$ γ-irradiation dose in 2 neuroblastoma (KELLY and SK-N-SH) and 5 neuroepithelial (G-) cell lines. Each curve is represented by the equation, $P_{oe} = 1 - (SF_{COL} + P_{MA})$, where $SF_{COL}$ is the clonogenic surviving fraction and $P_{MA}$ is the probability of inducing either micronuclei or apoptosis.

## 3.3 INTERRELATIONSHIP BETWEEN CELL SURVIVAL, MICRONUCLEATION, APOPTOSIS AND REPAIR.

The fractions of DNA released in CFGE experiments, $F_{rel}$, were plotted as functions of irradiation dose to give the dose response curves for initial DNA dsb damage and residual damage in three glioblastoma cell lines after 2 and 20 hours repair for the dose range 0-100 Gy (Figure 3.24). The area under the initial damage curve ($AUC_0$) was then compared to the area under each of the residual damage curves ($AUC_2$ or $AUC_{20}$). Figure 3.24 shows that the three cell lines show very similar levels of initial DNA damage. The $AUC_0$ for the G-28, G-120 and G-60 cell lines are 47.92, 48.95 and 44.36, respectively. The ratios of $AUC_0/AUC_2$ and $AUC_0/AUC_{20}$ therefore represent the extent to which DNA dsb damage is repaired. The cell survival, micronucleation, apoptotic and repair parameters are summarised in table 3.4.

The three cell lines show very similar levels of initial damage. There is no significant correlation between the extent of repair after 2 hours and radiosensitivity. In the first 2 hours, the G-28 and G-120 cell lines (with SF2 values of 0.69 and 0.60, respectively) exhibit similar repair proficiencies. After 20 hours of repair, however, strong correlations are apparent between radiosensitivity measured by SF2s, $\alpha$-coefficients and mean inactivation doses and it is shown that the more radioresistant cells repair more damage than the more radiosensitive cells.

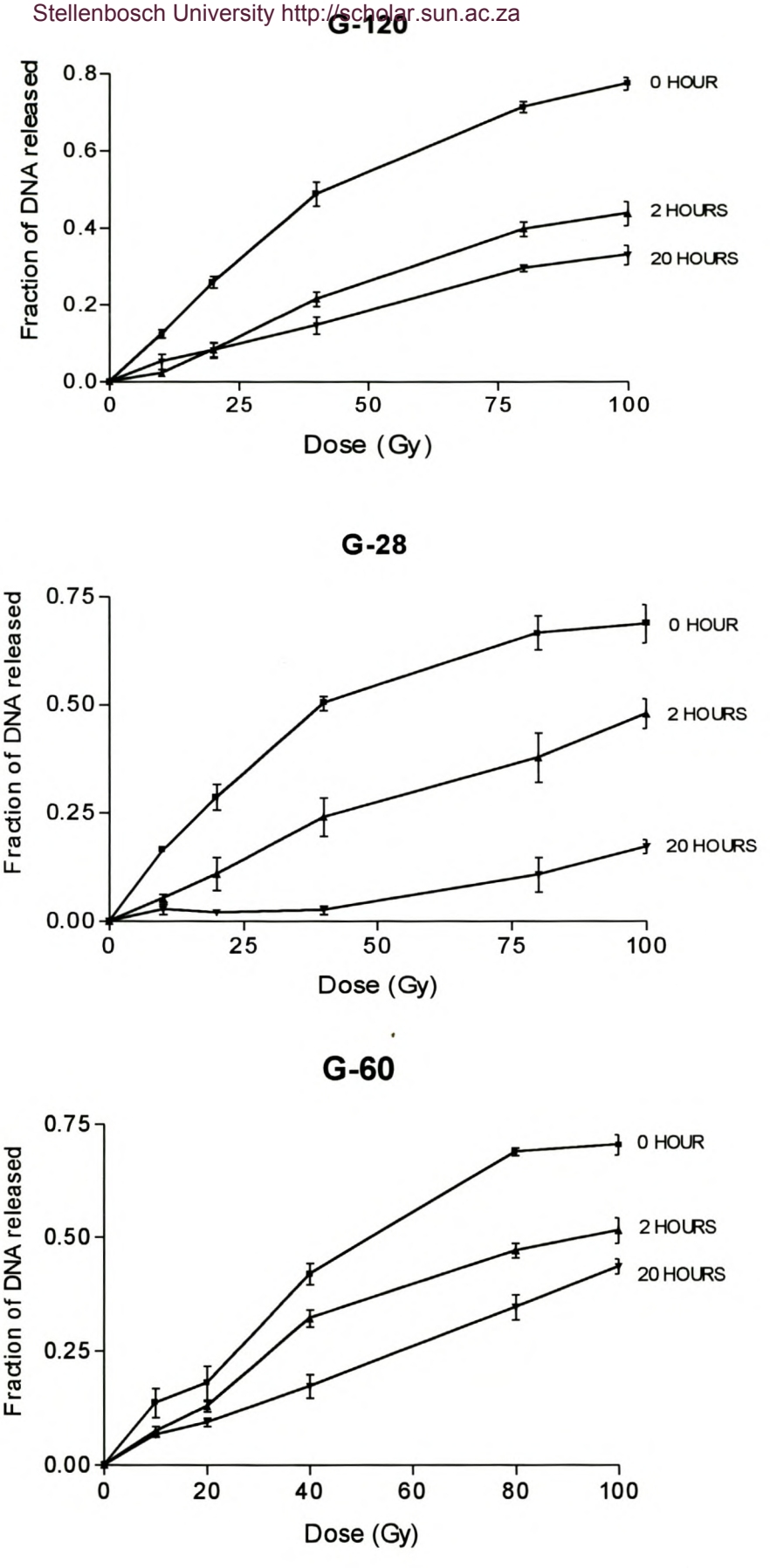


**FIGURE 3.24** Dose response curves for initial and residual DNA dsb damage in 3 glioblastoma cell lines after high dose $^{60}Co$ $\gamma$ irradiation.

Figure 3.25 represents plots of the cell inactivation parameters as functions of cellular DNA repair capacity. As SF2 and $\overline{D}$ values decrease, the 20 hours DNA damage repair capacity also diminishes giving correlation coefficients of 0.83 ($P$ = 0.38) and 0.97 ($P$ = 0.16), respectively. Increases in the $\alpha$-coefficient, which imply increased sensitivity to irradiation, correspond to low repair proficiency. This correlation was more significant for the 2 hour repair (r = 0.94, $P$ = 0.36).

The proportion of cells expressing micronuclei and the number of micronuclei per cell per unit dose correlate more strongly with repair after 2 hours (r = 0.68, $P$ = 0.53 and r = 0.96, $P$ = 0.18, respectively) than after 20 hours (r = 0.40, $P$ = 0.74 and r = 0.65, $P$ = 0.55, respectively). The coefficient for cell inactivation via apoptosis also shows a significant correlation with the 2 hours repair (r = 0.99, $P$ = 0.07), but no meaningful relationship with the 20 hour repair (r = 0.30, $P$ = 0.81). For 2 hours of repair, a higher susceptibility to apoptosis implies poorer repair proficiency (Figure 3.25).

**TABLE 3.4**

A summary of the cell survival, micronuclei formation, apoptosis and repair parameters. SF2, $\alpha$ and $\beta$ are derived from figure 3.1. $\overline{D}$ represents the area under the curves in figure 3.4. MNF/Gy represents the slope of the regressions in figure 3.2. The inactivation coefficients via micronucleation ($\mu$) and via apoptosis ($\xi$) are obtained from figure 3.18. DNA index is determined from the histograms in figure 3.8. The repair coefficients $AUC_0/AUC_2$ and $AUC_0/AUC_{20}$ are calculated from the areas of the dose response curves in figure 3.24.

| | **G-28** | **G-120** | **G-60** |
|---|---|---|---|
| SF2 | 0.69 | 0.60 | 0.43 |
| $\alpha$ ($Gy^{-1}$) | 0.15 | 0.18 | 0.37 |
| $\beta$ ($Gy^{-2}$) | 0.015 | 0.037 | 0.023 |
| $\alpha/\beta$ ($Gy^{-1}$) | 10.0 | 4.86 | 16.09 |
| $\overline{D}$ (Gy) | 3.21 | 2.59 | 2.25 |
| MNF/Gy ($Gy^{-1}$) | 0.36 | 0.35 | 0.23 |
| $\mu$ ($Gy^{-1}$) | 0.29 | 0.69 | 0.29 |
| $\xi$ ($Gy^{-1}$) | 0.022 | 0.018 | 0.030 |
| DNA Index | 1.75 | 2.15 | 1.89 |
| $AUC_0/AUC_2$ | 1.88 | 2.02 | 1.40 |
| $AUC_0/AUC_{20}$ | 7.62 | 2.68 | 2.01 |

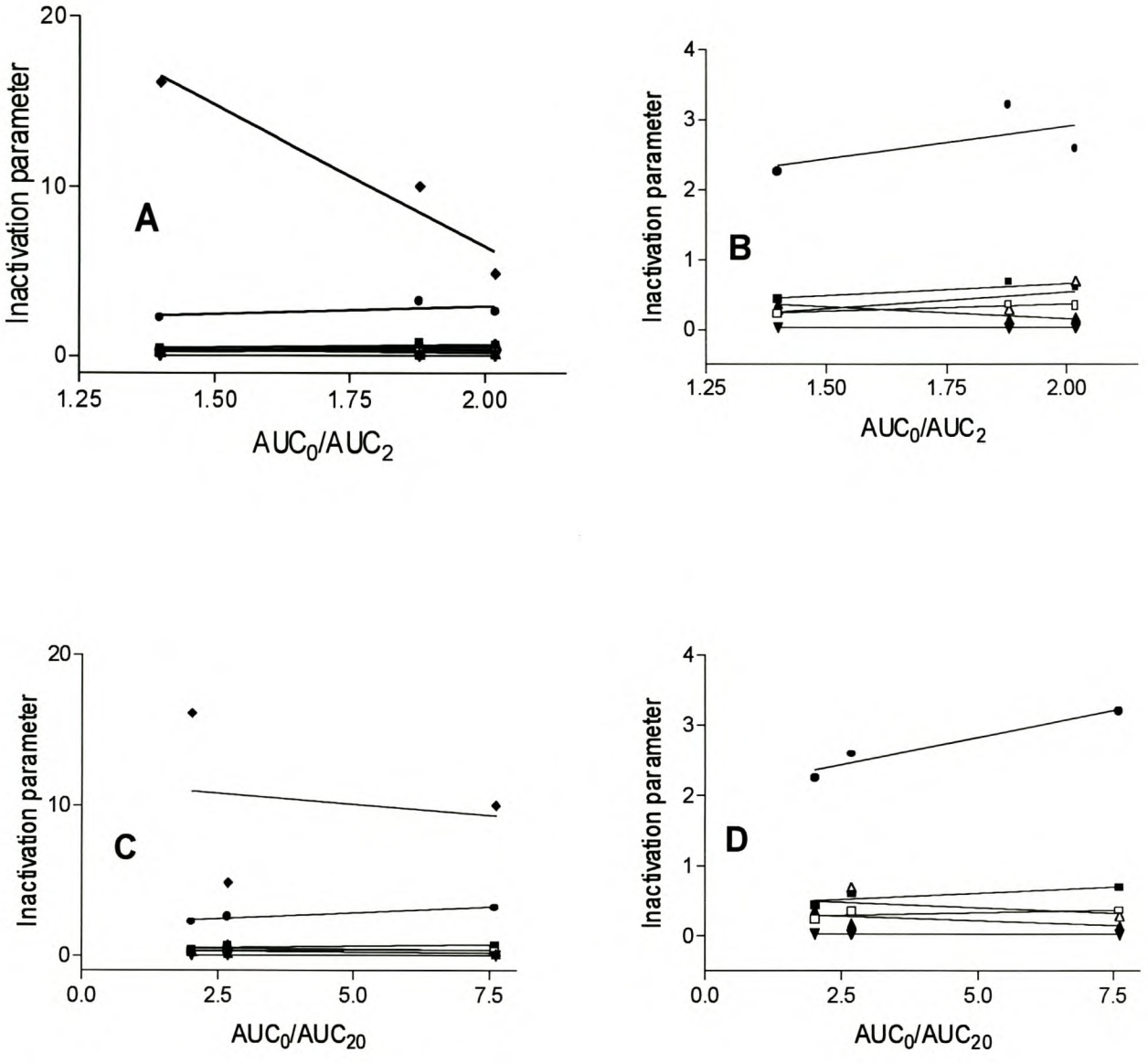


**FIGURE 3.25** Correlation between various cell inactivation parameters and DNA dsb damage repair 2 hours and 20 hours after $^{60}Co$ γ-irradiation to doses ranging from 0 to 100 Gy. Repair proficiency was expressed as the ratio of the areas under the damage-dose response curves for 0 hour versus 2 hours ($AUC_0/AUC_2$) and 20 hours ($AUC_0/AUC_{20}$). The inactivation parameters were: SF2 (■), α-coefficient (▲), β-coefficient (▼), α/β ratio (◆), mean inactivation dose (●), micronuclei frequency per Gy (□), coefficient of inactivation via micronucleation (Δ) and coefficient of inactivation via apoptosis (∇).

## 3.4 THE MICRONUCLEUS ASSAY FOR ASSESSING RADIATION-INDUCED MITOTIC DELAY AND DRUG TOXICITY

### 3.4.1 *In Vitro* Cytotoxic Effects of Azadirachtin A on Human Glioblastoma Cells

The availability of a DNA damage assay (micronucleus assay) prompted me to examine the curious observation that the neem toxin azadirachtin A should be insect specific and that much larger quantities of the toxin are required to inactivate mammalian cells (Cohen *et al.* 1996), and in particular human tumour cell lines. The questions under investigation were: Does azadirachtin A induce any DNA damage in human cells and is the toxic dose indeed much higher than in insect cells? Preliminary studies on azadirachtin A in human glioblastoma cells using the vital dye staining method (Brock *et al.* 1990), established a dose-response for TP53 wild-type and TP53 mutants (Figure 3.26). Presence of 28 $\mu$M azadirachtin A for 24 hours in the medium suppresses the surviving fraction from 1.00 (control) to between 0.45 and 0.75, depending upon the cell line.

Figures 3.26 and 3.27 demonstrate the cytotoxic effect in cell cultures exposed to 28 $\mu$M of azadirachtin A on cell proliferation (binucleation) and DNA damage as indicated by micronuclei frequency (MNF) in TP53 wild-type and in TP53 mutants.

Figure 3.27 shows that azadirachtin suppresses the binucleation index by 11, 8, and 24% in G-28, G-112 and G-60, respectively. In the TP53 wild-type G-120 and G-62, binucleation is unchanged, while the TP53 wild-type G-44 cell line shows a 14% reduction in binucleation (Figure 3.28 and Table 3.5).

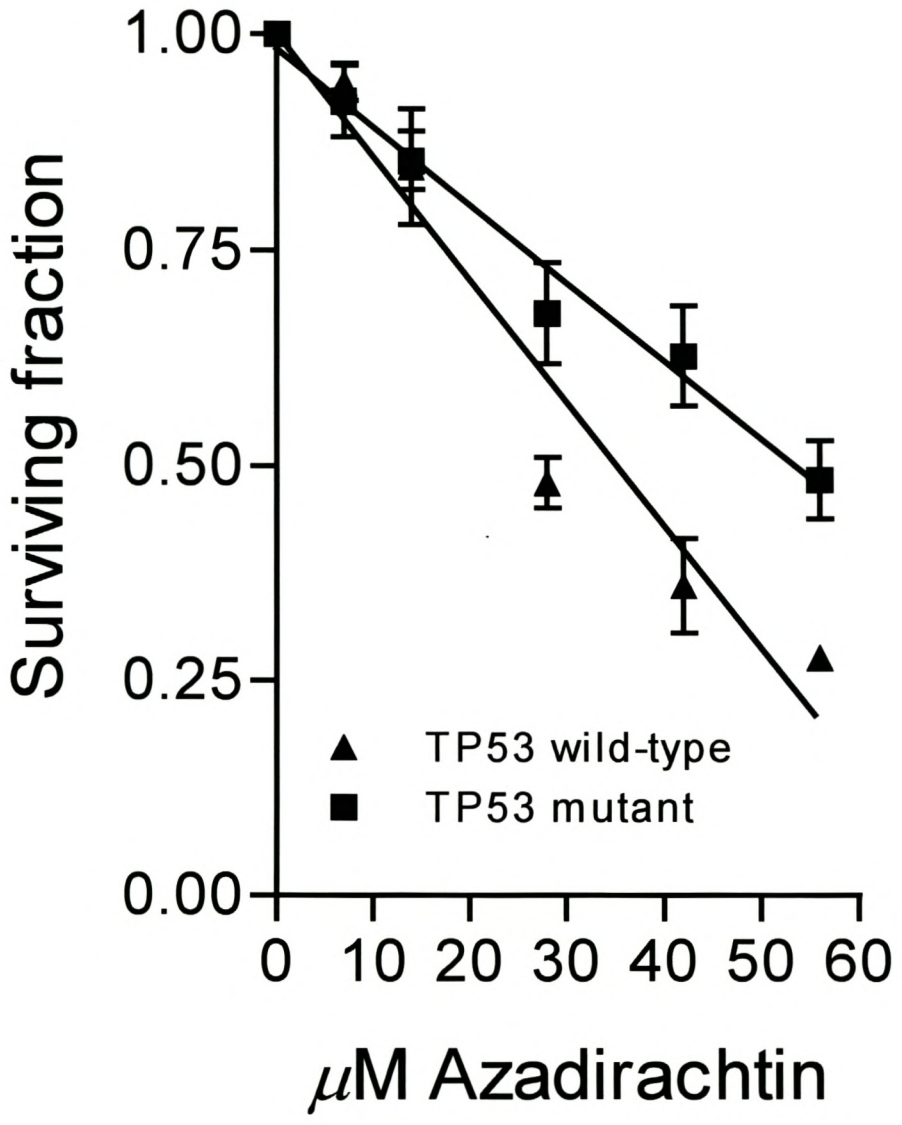


**FIGURE 3.26** Toxicity of azadirachtin A in TP53 mutant (G-28, G-112, G-60) and in TP53 wild-type (G-120, G-44, G-62) human glioblastoma cell lines. Surviving fractions were determined by the vital dye staining method.

While azadirachtin consistently induces high levels of micronucleation and micronuclei frequency in the TP53 mutant cell lines, its influence in the TP53 wild-type cells lines is more varied. G-120 cells show no change in MNF, but an 8% reduction in micronucleation. In G-44 cells, both micronucleation and MNF are significantly reduced. In G-62 cell line, the exposure to azadirachtin significantly increases micronucleation and micronuclei frequency by 9% and 23%, respectively.

The influence of azadirachtin on cell survival is shown in figure 3.29. At 28 $\mu$M concentration, the toxin was found to significantly reduce cell survival to the level of 0.31-0.75 depending upon the cell line. The TP53 mutant cell lines are generally toxin resistant ($0.53 \leq SF \leq 0.75$), while the TP53 wild-type cells tend to be more sensitive to azadirachtin than the TP53 mutant cell lines ($0.31 \leq SF \leq 0.49$).

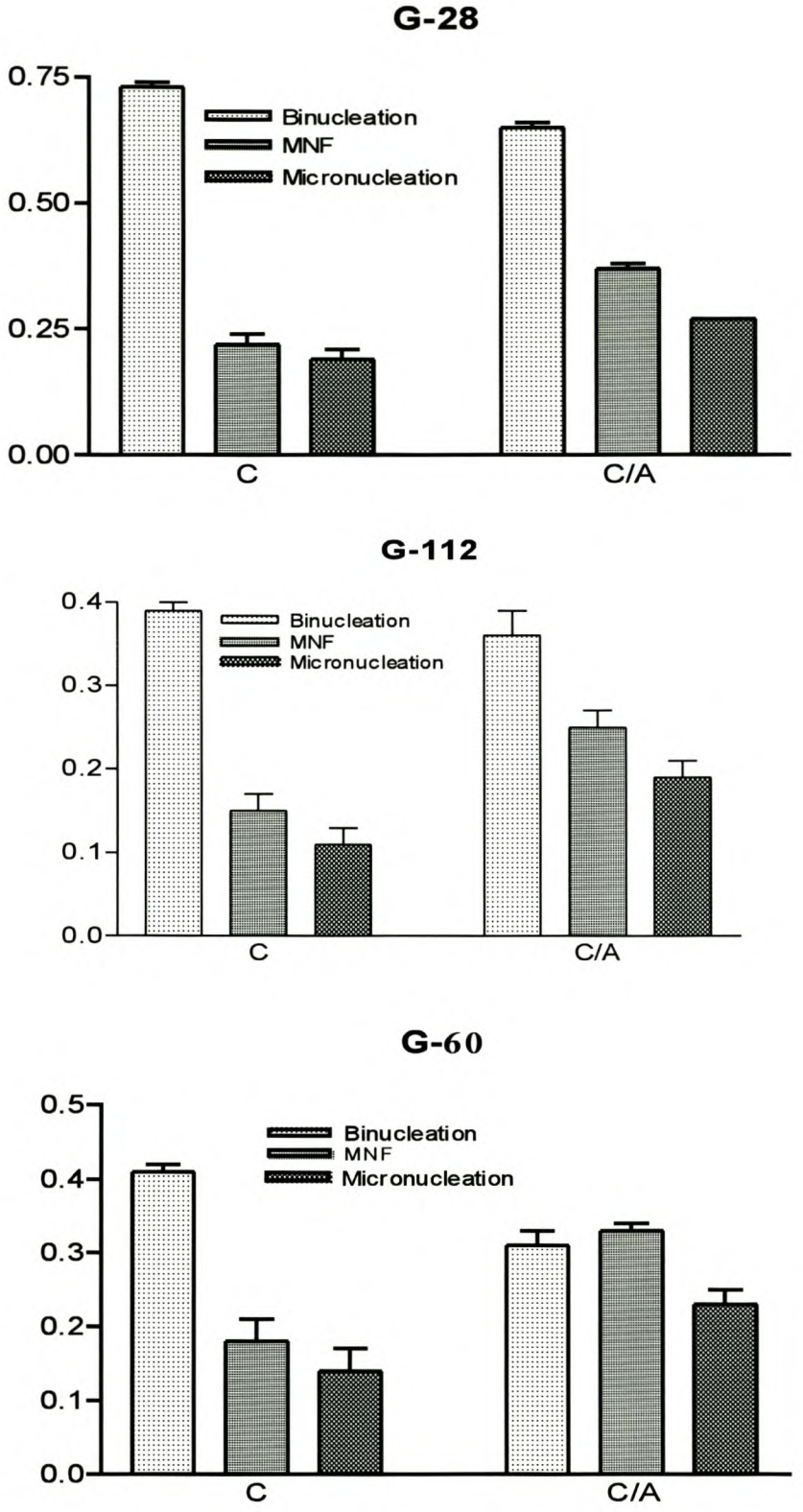


**FIGURE 3.27** Effect of the insecticide azadirachtin A on binucleation, micronuclei frequency (MNF) and the proportion of cells containing micronuclei (micronucleation) in TP53 mutant human glioblastoma cell lines (C/A). Control samples were treated with only cytochalasin B (C).

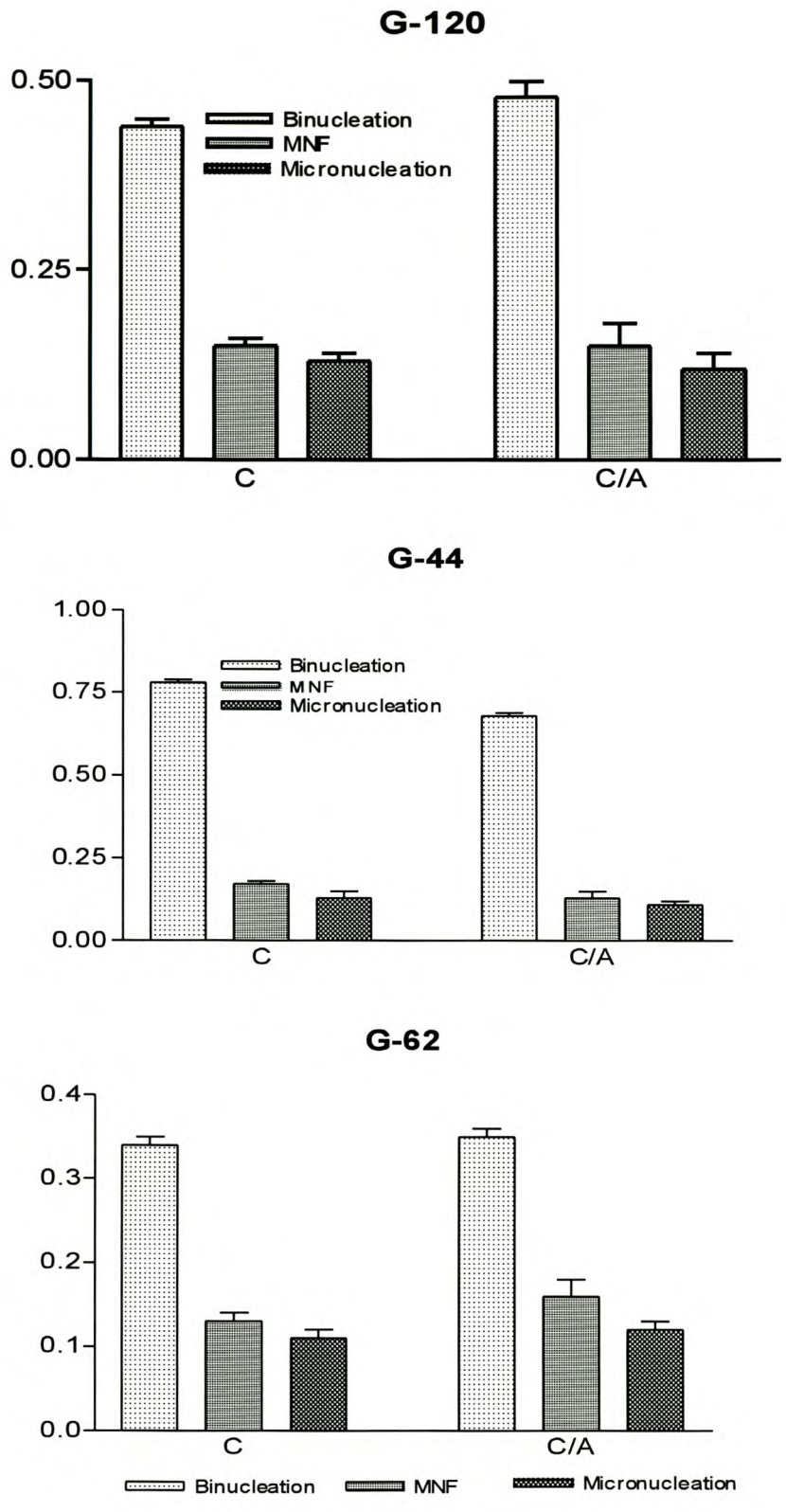


**FIGURE 3.28** Effect of the insecticide azadirachtin A on binucleation, micronuclei frequency (MNF) and the proportion of cells containing micronuclei (micronucleation) in TP53 wild-type human glioblastoma cell lines (C/A). Control samples were treated with only cytochalasin B (C).

**TABLE 3.5**

Effect of azadirachtin on proliferation, micronuclei expression and cell survival in TP53 mutant (G-28, G-112, G-60) and in TP53 wild-type (G-120, G-44, G-62) human glioblastoma cell lines. These data are derived from figures 3.27 and 3.28, and represent the ratio of the mean value for the treated to the control for each parameter.

| Cell Line | Binucleation | MNF | MN |
|---|---|---|---|
| G-28 | 0.89 | 1.70 | 1.42 |
| G-112 | 0.92 | 1.67 | 1.73 |
| G-60 | 0.76 | 1.82 | 1.62 |
| G-120 | 1.09 | 1.00 | 0.92 |
| G-44 | 0.86 | 0.77 | 0.85 |
| G-62 | 1.03 | 1.23 | 1.09 |

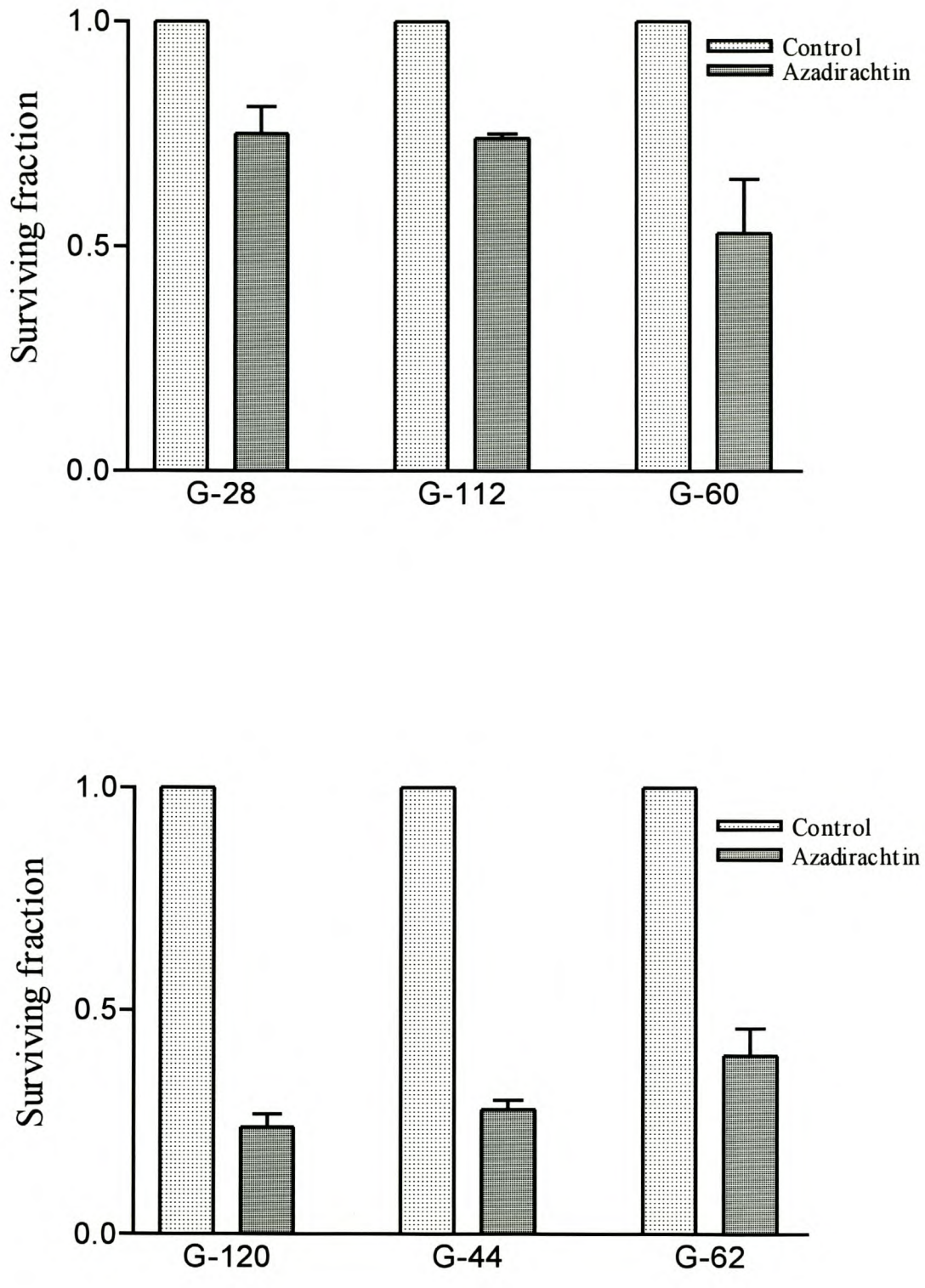


**FIGURE 3.29** Effect of azadirachtin A on cell survival in TP53 mutant (Upper panel) and in TP53 wild-type (Lower panel) human glioblastoma cell lines. Cell survival is determined by the colony assay.

### 3.4.2 Effect of Pentoxifylline on Radiation-Induced Binucleation and Micronucleation

The effect of pentoxifylline on irradiated cells is shown in figure 3.30. Figures 3.31 and 3.32 represent the influence of PENT on binucleation and the expression of micronuclei in TP53 mutant and in TP53 wild-type glioblastoma cell lines, respectively. Table 3.6 summarises the data on the effect of PENT on radiation-induced binucleation, micronucleus formation and cell survival.

In the G-28 and G-60 cell lines, PENT alone decreases binucleation by 13%, but produces a 19% increase of binucleation in the G-112 cells. For the proportion of micronucleated cells and micronuclei frequency, G-28 and G-112 show an increase, but G-60 exhibits a decrease (Table 3.6). When PENT is added 18 hours after 4 Gy irradiation, there is a reduction in binucleation in G-28 and G-112, but a significant increase in G-60. G-28 and G-60 show an increase while G-112 shows a decrease in micronucleation and micronuclei frequency. In G-28, G-112 and G-60 cells, no correlation was apparent between the TP53 status and the mode of action of PENT on the basis binucleation, micronucleation and micronucleus frequency. All TP53 mutant cell lines show a reduction of cell survival by 30-58% when PENT was added 18 hours after irradiation.

PENT has no significant effect on binucleation in unirradiated G-44 cultures, but causes a suppression of 50% and 26% in G-120 and G-62, respectively

(Table 3.6). The proportion of cells containing micronuclei is also decreased in G-120 and G-62, but MNF is unaffected in G-62. MNF decreased by 31% in the G-120 cell line. In the G-44 cells, PENT increases both micronucleation and MNF. When PENT is added to irradiated cells, G-120 and G-44 show a significant increase in binucleation while the proportion of binucleated cells in G-62 remains unaffected. On average, PENT has no measurable effect on micronucleation and MNF in all TP53 wild-type cell lines. The TP53 wild-type cell lines show a greater reduction (65-74%) in survival than the TP53 mutant cell lines when treated with PENT after irradiation.

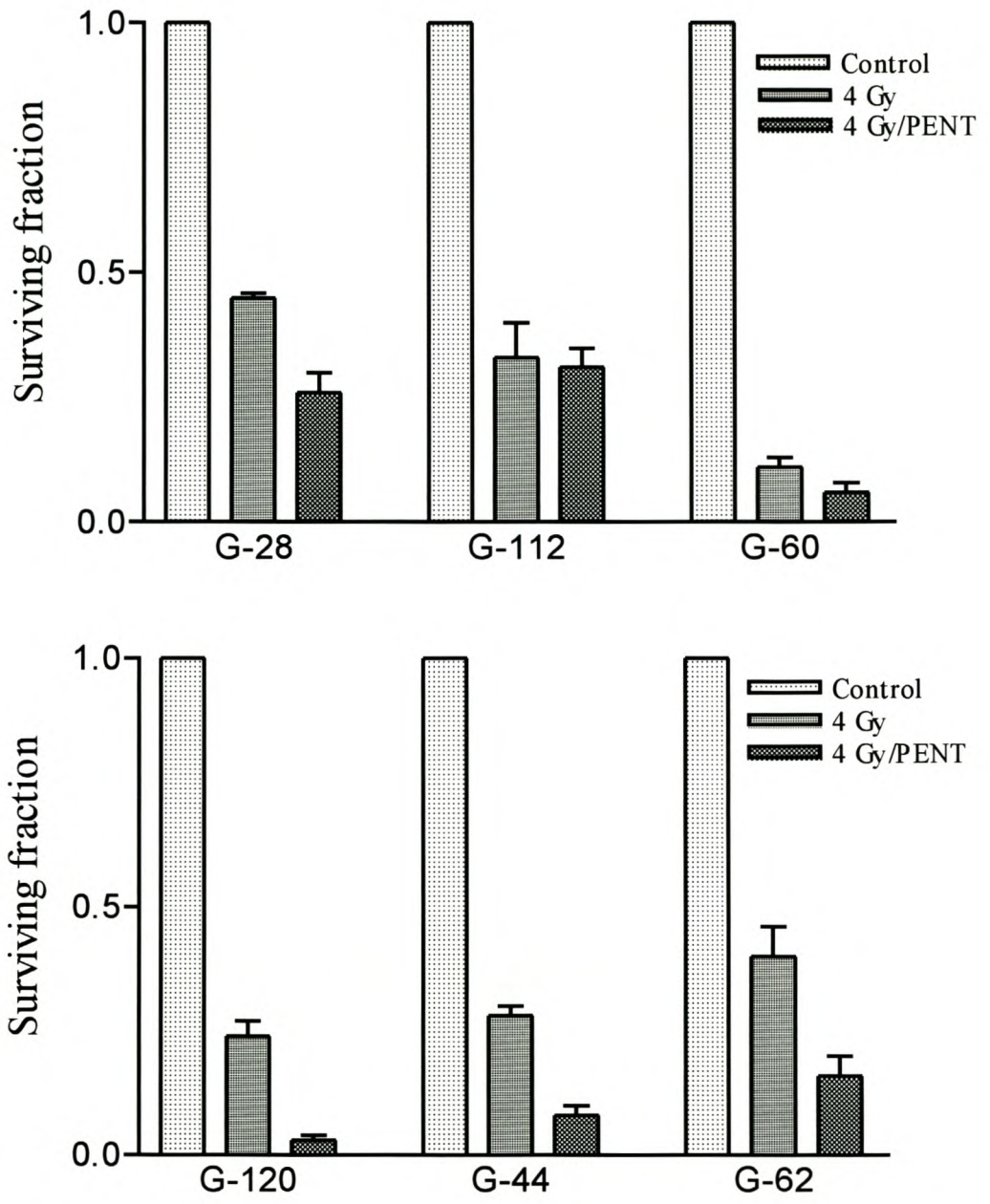


**FIGURE 3.30** The effect of pentoxifylline on cell survival in TP53 mutant (Upper panel) and TP53 wild-type (Lower panel) glioblastoma cell lines irradiated to 4 Gy with $^{60}Co$ γ-rays.

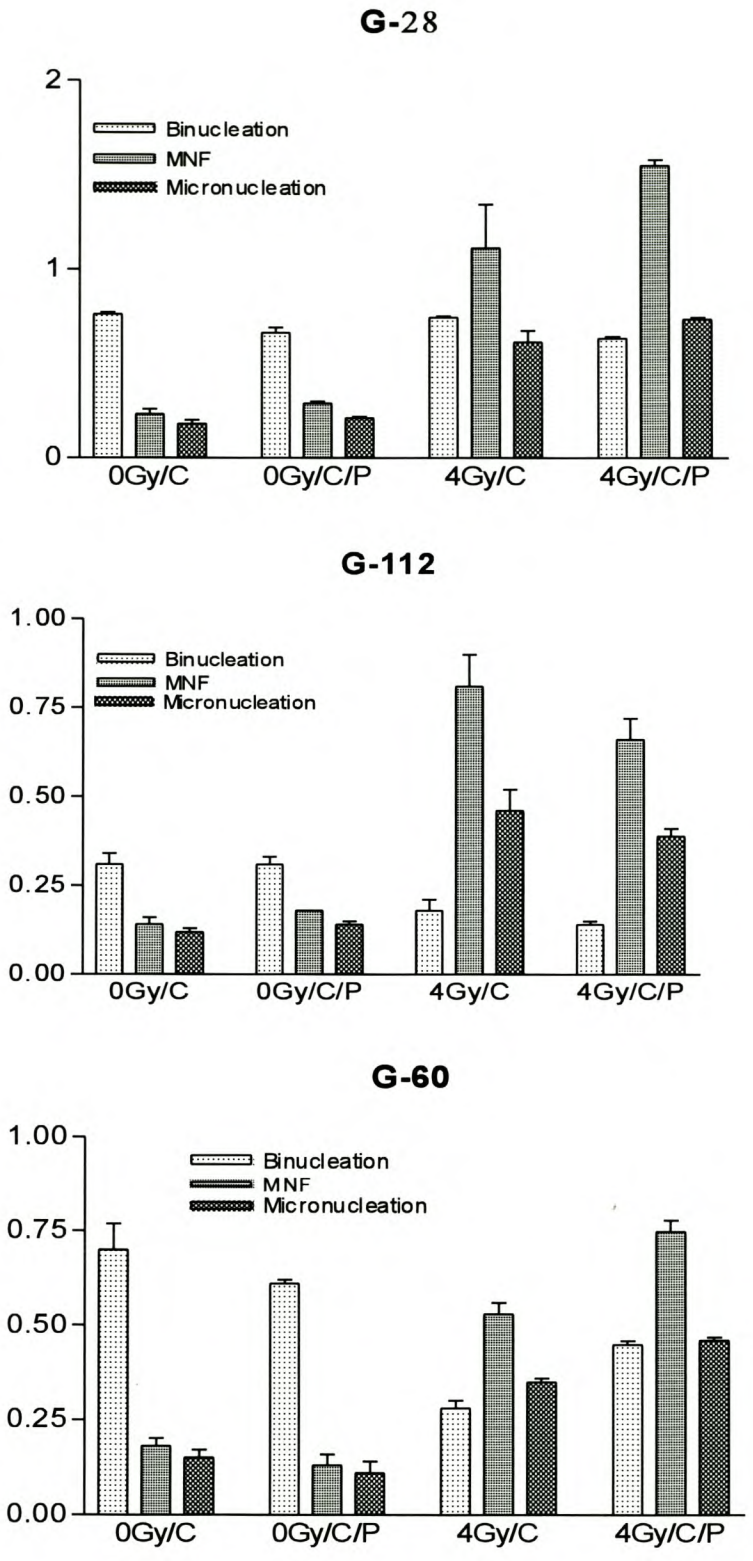


**FIGURE 3.31** Effect of pentoxifylline on binucleation, micronuclei frequency and the proportion of cells containing micronuclei irradiated in TP53 mutant human glioblastoma cell lines (P). In each mode of treatment, (C) represents treatment with cytochalasin B.

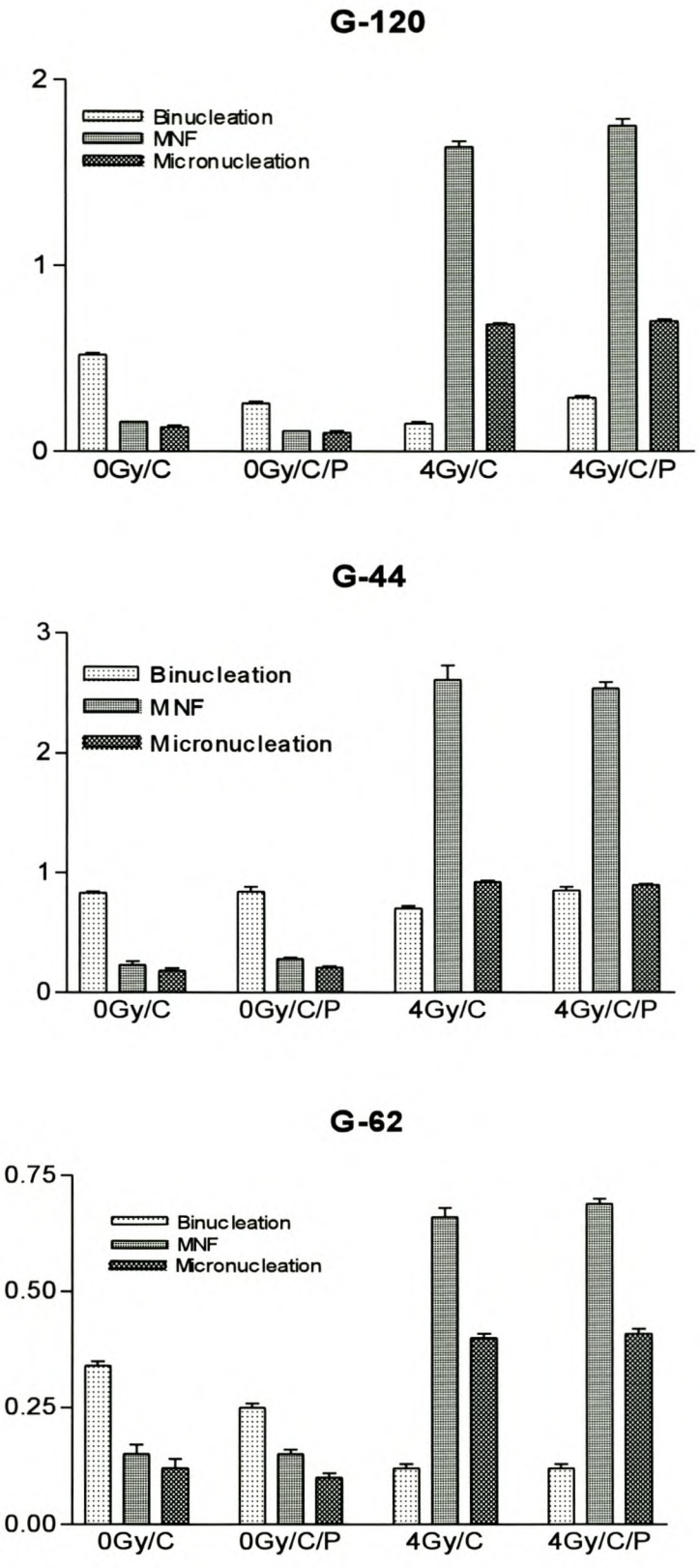


**FIGURE 3.32** Effect of pentoxifylline on binucleation, micronuclei frequency and the proportion of cells containing micronuclei in irradiated TP53 wild-type human glioblastoma cell lines (P). In each mode of treatment, (C) represents treatment with cytochalasin B.

**TABLE 3.6**

Effect of pentoxifylline (PENT) on cell survival, binucleation and micronuclei expression in TP53 mutant human glioblastoma cell lines. Values under each treatment mode are derived from figures 3.30 and 3.31, and represent the treated:control ratio for each parameter. PENT treated unirradiated samples were used as controls for PENT treated irradiated samples. The enhancement factors (EHFs) for binucleation, MNF and micronucleation represent the ratios for irradiation with to irradiation without PENT. EHF for cell survival was calculated from the relation: EHF = $SF_{4Gy}/SF_{4Gy/PENT}$.

| Cell Line | Parameter | PENT | 4 Gy | 4 Gy/PENT | EHF |
|---|---|---|---|---|---|
| | Binucleation | 0.87 | 0.97 | 0.95 | 0.98 |
| **G-28** | MNF | 1.25 | 4.83 | 5.35 | 1.11 |
| | MN | 1.16 | 3.39 | 3.38 | 1.03 |
| | SF | 0.97 | 0.45 | 0.26 | 1.72 |
| | Binucleation | 1.19 | 0.58 | 0.45 | 0.78 |
| **G-112** | MNF | 1.29 | 5.79 | 4.67 | 0.63 |
| | MN | 1.17 | 3.83 | 2.79 | 0.73 |
| | SF | 0.75 | 0.33 | 0.31 | 1.37 |
| | Binucleation | 0.87 | 0.40 | 0.74 | 1.85 |
| **G-60** | MNF | 0.72 | 2.94 | 5.77 | 1.96 |
| | MN | 0.73 | 2.33 | 4.18 | 1.79 |
| | SF | 0.71 | 0.11 | 0.06 | 1.82 |

**TABLE 3.7**

Effect of pentoxifylline (PENT) on cell survival, binucleation and micronuclei expression in TP53 wild-type human glioblastoma cell lines. Values under each treatment mode are derived from figures 3.30 and 3.32, and represent the treated:control ratio for each parameter. PENT treated unirradiated samples were used as controls for PENT treated irradiated samples. The enhancement factors (EHFs) for binucleation, MNF and micronucleation represent the ratios for irradiation with to irradiation without PENT. EHF for cell survival was calculated from the relation: EHF = $SF_{4Gy}/SF_{4Gy/PENT}$.

| Cell Line | Parameter | PENT | 4 Gy | 4 Gy/PENT | EHF |
|---|---|---|---|---|---|
| | Binucleation | 0.50 | 0.29 | 1.12 | 3.86 |
| **G-120** | MNF | 0.69 | 10.25 | 15.91 | 1.55 |
| | MN | 0.77 | 5.23 | 7.00 | 1.34 |
| | SF | 0.87 | 0.24 | 0.03 | 3.85 |
| | Binucleation | 1.05 | 0.84 | 1.01 | 1.20 |
| **G-44** | MNF | 1.25 | 11.35 | 9.07 | 0.80 |
| | MN | 1.15 | 5.11 | 4.29 | 0.84 |
| | SF | 0.96 | 0.28 | 0.08 | 3.13 |
| | Binucleation | 0.74 | 0.35 | 0.48 | 1.37 |
| **G-62** | MNF | 1.00 | 4.40 | 4.60 | 1.05 |
| | MN | 0.83 | 3.33 | 4.10 | 1.23 |
| | SF | 0.87 | 0.40 | 0.16 | 2.50 |

# CHAPTER 4

# DISCUSSIONS

## 4.1 CELL SURVIVAL AND MICRONUCLEI YIELD

The highest yield of binucleated cells (BNC) was achieved 1-2 days after incubation with cytochalasin B. This is in close agreement with results on other rodent cell lines which give 36-48 hours for EMT6 mouse mammary sarcoma cells (Shibamoto *et al.* 1992) and 24-48 hrs for the 4 murine cell lines Balb/C sarcoma, C3H/Hc squamous cell carcinoma, Balb/C melanoma and C57 BL adenocarcinoma (Shibamoto *et al.* 1991). The time point at which maximum binucleation was attained was used for the termination of cultures for subsequent micronucleus assessment.

Twelve of the thirteen cell lines used in this study showed a good correlation between MN formation and radiation dose (Figure 3.2). Similar results have been reported elsewhere (Shibamoto *et al.* 1991, 1994, Bush and McMillan 1993, Villa *et al.* 1994, Ono *et al.* 1994). There is however, no straightforward correlation between radiosensitivity derived by colony assay and micronucleus

frequency in binucleated cells evaluated under conditions of maximum binucleation. In fact, the number of micronuclei per Gy tends to be high in the more radioresistant cell lines (G-44, G-112, G-120, G-62, G-28 and N2α) and low in the radiosensitive cell lines OP-27 and SK-N-SH (Figures 3.2 and 3.5). Studies on other cell lines found radiosensitivity and MN frequency to be correlated, and the more radiosensitive cell lines producing more micronuclei at a given dose (Wandl *et al.* 1989, Shibamoto *et al.* 1991, 1994). However, an investigation of human primary ovarian carcinoma and malignant melanoma cell lines also reported that the micronucleus assay did not rank the cell lines in the order of radiosensitivity given by clonogenic survival (Villa *et al.* 1994). In a group of neuroblastoma, bladder and medulloblastoma cell lines, the more radioresistant cells produced higher levels of micronuclei per Gy of radiation (Bush and McMillan 1993).

Opinions regarding the potential usefulness of the MN assay as a predictive test of tumour cell radiosensitivity range from straightforward negative (Bush and McMillan 1993) through doubtful (Geard and Chen 1990, Villa *et al.* 1994) to advantageous (Shibamoto *et al.* 1991, 1994) in relation to colony formation. While the lack of a simple correlation between radiosensitivity and micronuclei frequency is widely acknowledged (Wandl *et al.* 1989, Bush and McMillan 1993, Shibamoto *et al* 1991, 1994, Villa *et al* 1994) no biological rationale has been advanced which would explain the finding that some radiosensitive cells are poor responders in terms of micronuclei formation. An answer may be in the relationship between the number of lethal lesions and micronuclei

frequency. Cells which exhibit high radiosensitivity in clonogenic assays clearly show very low micronucleus frequency in response to the number of lethal lesions and vice versa (Figure 3.3). In the radioresistant G-44, G-112, G-120, G-62, G-28 and N2$\alpha$ cell lines a single lethal lesion equates to 0.43-2.79 micronuclei per BNC, whereas in the radiosensitive KELLY, SK-N-SH and OP-27 cell lines one lethal lesion corresponds to as low as 0.05-0.23 micronuclei per BNC (Figure 3.3). One lethal event in a radioresistant cell line may equate to ten lethal lesions in a radiosensitive cell line. For any given irradiation dose, higher levels of lethality would be expected in radiosensitive cell lines. This may reduce the proportion of cells progressing into mitosis, and therefore affect the percentage of micronucleus bearing binucleated cells. On the other hand, a similar dose may not adversely affect the progression into mitosis in the radioresistant cell lines. Higher proportions of MN containing cells would thus be observed after the first post-irradiation mitosis. Alternatively, cells could be inherently inefficient in converting chromatid and chromosome fragments into micronuclei. Another possible explanation is that cells might express micronuclei only in subsequent divisions after the first post-irradiation mitosis as suggested elsewhere (Bush and McMillan 1993).

It has also been suggested that clonogenic survival and micronucleus formation could depend on the distribution of cells in the cell cycle during irradiation (Villa *et al.* 1994). This is because the distribution of cells in the various cell cycle stages may be different from cell line to cell line, and can affect cell survival and micronucleation. In cells irradiated in the $G_2$/M and late

S-phases, micronuclei could arise from only one daughter chromatid while the other may remain clonogenic and continue to form colonies. On the other hand, if cells are irradiated in $G_1$, micronuclei formation would lead to genetic deletions in both daughter cells at the first post-irradiation mitosis and adversely affect the clonogenicity in both cells and lead to low surviving fractions. Cell cycle effects cannot be the explanation for the results because the cell lines were not synchronized, and an influence on the relationship between MN formation and clonogenic survival from this source appears unlikely (Bush and McMillan 1993).

Another possibility for high MN frequency in radiation resistant cells could be ploidy. It has been shown that in diploid cells a micronucleus is equivalent to one lethal lesion whereas two micronuclei are required to form a lethal lesion in tetraploid cells (Revell 1983). In my data, a correlation between cellular DNA content and MN formation or clonogenic survival was not apparent (Figure 3.9).

The onset of radiation-induced apoptosis or programmed cell death is known to occur within hours after irradiation (Stephens *et al.* 1991, Mirkovic *et al.* 1994, Mathieu *et al.* 1996). This mode of cell death affects the correlation between MN formation and cell survival as reported by Abend *et al.* (1995) and Guo *et al.* (1998). Cell lines showing high levels of micronuclei might not exhibit high proportions of apoptosis, but inclusion of apoptotic and micronuclei data as total cell damage has been claimed to establish a cell line independent correlation with survival (Abend *et al.* 1995). Cell lines producing low levels of

micronuclei appear to be more susceptible to radiation-induced apoptosis, suggesting that both parameters may be required to predict cell survival (Abend *et al.* 1995, Guo *et al.* 1998). Concurrent determination of apoptotic propensity and micronuclei frequency indeed may improve the ranking of cell lines according to radiosensitivity and rationalise the observation that some radiosensitive cell lines show a very low micronuclei frequency.

In this panel of cell lines the cytokinesis-block micronucleus assay alone did not predict cellular radiosensitivity. It is also clear from these data that the selection of cell lines profoundly affects the results, and this may be the reason for the widely differing opinions on this issue (Wandl *et al.* 1989, Ono *et al.* 1989, 1994, Geard and Chen 1990, Shibamoto *et al.* 1991, Bush and McMillan 1993, Villa *et al.* 1994, Abend *et al.* 1995, Kinashi *et al.* 1997, Widel and Przybyszewski 1998, Guo *et al.* 1998, Akudugu *et al.* 2000). The essential lines of conclusion are that MN formation is a cell specific response which is not representative of the total cell damage. In this sense, micronuclei formation resembles apoptosis which is also cell specific and not alone an indication of total cell damage (Hendry and West 1997). Identification of the chromosomes responsible for micronuclei formation and the use of different irradiation modalities and hypoxia-induced radiation resistance could shed more light onto this problem.

## 4.2 INFLUENCE OF LET ON CORRELATION BETWEEN CELL SURVIVAL AND MICRONUCLEI YIELD

Radiation modalities of high linear energy transfer (LET) have been widely applied in the clinic to improve tumour control. These radiation types are of benefit in the treatment of radioresistant tumours such as those of the head and neck. It has been widely demonstrated that high LET irradiation causes high levels of cellular damage and subsequently leads to low levels of cell survival (Barendsen *et al.* 1960, Fertil *et al.* 1982, Chen *et al.* 1984, Fox and McNally 1988, Britten *et al.* 1992, Böhm *et al.* 1992, 1994, Slabbert *et al.* 1996).

In a study involving 2 neuroblastoma and 6 neuroepithelial cell lines with a wide spectrum of radiosensitivities, it was indeed found that p(66/$Be^{+}$) neutrons are more potent in inducing micronuclei than $\gamma$-rays. In fact, neutrons induced ~2.5 times more micronuclei than $\gamma$-rays (Figure 3.13). These results are in agreement with other findings on chromosome aberrations, micronuclei and DNA double strand breaks (Fox and McNally 1988, Tates *et al.* 1989, Darroudi *et al.* 1992, Huber *et al.* 1994, Heimers 1999), and illustrates the response of cells to different irradiation modalities. A high frequency of micronuclei could be an indication that that cell line in question is more deficient in repairing high LET damage. For peripheral blood lymphocytes, the high MN yield after neutron irradiation has been attributed to a high proportion of irreparable damage (Vral *et al.* 1994). Although DNA damage repair has not been

considered in this study, it is obvious from the higher MN frequencies induced by neutron irradiation that the cells are less capable of repairing damage responsible for the formation of micronuclei. There seems to be no marked difference between repair proficiency in low-LET and intermediate-LET irradiations (Britten and Murray 1997). In all the cell lines studied, the range of radiation sensitivities to photons determined by clonogenic survival narrows substantially after neutron irradiation (Figure 3.15). This is also supported by other studies which show that high-LET irradiation generates similar cell inactivation parameters irrespective of the responses to low-LET irradiation (Britten *et al.* 1992, Böhm *et al.* 1992, Slabbert *et al.* 1996). In this investigation, interestingly, the range of micronuclei frequencies, which is a reflection of the extent of damage, was much more pronounced after high LET irradiation (0.18-1.59 micronuclei per Gy) than after low LET irradiation (0.04-0.36 micronuclei per Gy) (Figure 3.13).

The correlation between the levels of irradiation-induced damage and cell survival is unclear. The widely varying susceptibility to micronuclei formation but similar survival after high LET irradiation may be explained by a number of phenomena. Differences in DNA content should lead to different interaction cross-sections for different cell lines and therefore varied amounts of damage induced per unit irradiation dose. DNA content cannot explain the wide variation in cellular response as indicated by micronucleation. These results show no correlation between DNA content and micronuclei frequency per unit dose. The DNA indices for G-62, G-120, G-28, G-44, KELLY, G-112 and SK-

N-SH are 2.42, 2.15, 1.75, 1.61, 1.17, 1.89 and 1.11, respectively. The marked difference in the micronuclei expression suggests that great differences exist in the way cells repair the damage reflected in micronuclei formation.

From these results, it is quite clear that higher susceptibility to micronuclei formation will not imply lower cell survival. Similar results have been reported elsewhere (Bush and McMillan 1993, Villa *et al.* 1994, Akudugu *et al.* 2000). The fact that cell lines vary widely in expressing micronuclei but show similar survival after neutron irradiation, suggests that other cell inactivation processes like apoptosis may play a crucial role. It can also be conjectured that when cells are irradiated with high LET radiation, a dose dependent but cell line independent sub-population does not sustain lethal damage and this sub-population then proceeds to form viable colonies. In conclusion therefore, a high expression of micronuclei does not imply high radiosensitivity. To explain the relationship between micronuclei formation and cell survival after high LET irradiation, other cell inactivation pathways or cell kinetics must be considered.

## 4.3 DETERMINATION OF RBE FROM THE MICRONUCLEUS ASSAY

The relative biological effectiveness (RBE) is a measure of the potency of a given radiation type in inactivating cells. This parameter is dependent upon the linear energy transfer (LET) of the radiation as well as the cell type. RBE's

have been derived from a variety of cell inactivation parameters, ie. the surviving fractions at given dose, $\alpha$-coefficients, mean inactivation doses, DNA strand breaks and chromosome aberrations (Fox and McNally 1988, Tates *et al.* 1989, Darroudi *et al.* 1992, Courdi *et al.* 1996, Slabbert *et al.* 1996, Heimers 1999, Frankenberg *et al.* 1999). For the induction of micronuclei by neutrons of varied LET, RBE's ranging from 3.0-12.0 have been reported for established cell lines and for human lymphocytes (Tates *et al.* 1989, Darroudi *et al.* 1992, Huber *et al.* 1994, Heimers 1999).

In this study, RBE's were derived from the areas under the normal nuclear division fraction-dose response curves ($\overline{NDF}$) and compared with RBE's obtained from clonogenic survival parameters (Figure 3.17). In the G-28 and G-120 cell lines, the $RBE_{\overline{NDF}}$ differed significantly from most of the RBE's determined from cell survival parameters. However in KELLY, G-60, G-44 and G-62 they compared rather well with RBE's obtained from cell survival parameters. In this panel of cell lines, the RBE's determined from SF2, $\alpha$-coefficient, $\alpha/\beta$ ratio and $\overline{D}$ ranged from 0.77 to 5.89. The RBE's determined from the normal nuclear number division fraction ranged from 0.99 to 2.42. The fact that $RBE_{\overline{NDF}}$ falls within the range of RBE's determined by the conventional survival assay suggest that the fraction of cells not containing micronuclei may indeed be useful for testing the toxicity of radiation modalities for cell inactivation. This potential of the micronucleus assay alone may not have been realized.

## 4.4 INTERRELATIONSHIP BETWEEN CELL SURVIVAL, MICRONUCLEI FORMATION AND APOPTOSIS

The reliability of the micronucleus assay as a predictor of radiosensitivity has been widely questioned. While some authors assert that the micronucleus frequency reflects intrinsic radiosensitivity (Masunaga *et al.* 1990, Ono *et al.* 1994, Khan *et al.* 1998), others see this as an oversimplification and caution against this interpretation (Geard and Chen 1990, Bush and McMillan 1993, Villa *et al.* 1994, Akudugu *et al.* 2000). The lack of correlation between the coefficient for radiation-induced micronucleation, $\mu_\gamma$, and the survival fraction at 2 Gy, $SF2_\gamma$, is consistent with the notion that micronucleation alone cannot adequately reflect radiosensitivity. Apoptosis is cell type specific and some cell types are not susceptible to this mode of death (Abend *et al.* 1995, Stephens *et al.* 1991, 1993, Guo *et al.* 1998, 1999). Data presented here for seven cell lines also show no correlation between apoptotic propensity and radiosensitivity. The lack of correlation between apoptosis and radiosensitivity strongly suggests that apoptotic propensity alone is inadequate in assessing the long-term response to radiation (Figures 3.18 and 3.19).

The apoptotic propensity depends on how rapidly apoptosis occurs after irradiation and how susceptible cells are to this mode of death. While some cells exhibit high apoptosis within hours after irradiation (Mirkovic *et al.* 1994, Weil *et al.* 1996), others express significant levels of apoptosis only after days

(Abend *et al.* 1995, 2000, Guo *et al.* 1998, 1999). The short-term response represents a direct effect while a delayed expression of apoptosis may be a response to mitotic failure.

The levels of binucleation that can be achieved in unirradiated cell lines by the cytokinesis-block assay usually range from 15 to 80% (Bush and McMillan 1993, Ono *et al.* 1994, Villa *et al.* 1994). The maximum binucleation indices achieved in our panel of cell lines within 40 hours are consistent with those found the literature, and as such validates the choice of for the micronucleus assay. Binucleation indices also tend to decline with increasing radiation dose (Table 3.3). The low proliferative activity of unirradiated G-120, G-62, KELLY and SK-N-SH cultures can be explained by their moderate to high radiosensitivity. This may be an indication of large proportions of cells stopped in the $G_0$ or $G_1$ phases during cell culture, resulting in only a small fraction cycling into mitoses. In the same vein, irradiation would only enhance this phenomenon and lead to low cell survival. The percentage of cells that are binucleated therefore may not be representative of the total cell population. The percentage of cells that are binucleated therefore may not be representative of the total cell population. The shortfall in matching micronucleation with survival may be explained by this reduction of cells going through mitosis. Ideally, the micronucleus assay should be applied to synchronised cultures but such models fall short of the requirement of heterogeneity usually exhibited by *in vivo* systems (Khan *et al.* 1998). Since some cell types express significant levels of micronuclei only after the second

or later post-irradiation divisions (Shibamoto and Streffer 1991, Bush and McMillan 1993, Widel and Przybyszewski 1998), cumulative micronucleation can be assessed in a time series over several days as described elsewhere (Geard and Chen 1990). This approach would be very tedious and cumbersome, and would present no special advantages over the conventional colony assay.

I have previously demonstrated that isolated measurements of micronucleation cannot rank the cell lines according to the radiosensitivity (Akudugu *et al.* 2000). Simultaneous assessment of apoptosis and micronucleation as modes of cellular damage has been shown to improve the predictability of radiosensitivity (Abend *et al.* 1995, Guo *et al.* 1998, 1999). The total proportions of non-apoptotic and non-micronucleated cells, assessed 40 hours after irradiation, seems to differ significantly from the cell population responsible for clonogenic survival (Table 3.3). Therefore, the sum of the damage assessed by apoptosis and micronucleation at this time point falls short of the total damage caused by irradiation. Other modes of cell death are likely to be involved in influencing radiosensitivity. The most likely candidate considered here is reproductive cell death or mitotic failure.

To date, no assays are available which can directly quantify the proportion of cells dying through reproductive failure. Although apoptosis is implicated as the ultimate route of cell death after irradiation-induced mitotic failure (Tauchi and Sawada 1994, Hu and Hill 1996, Olive *et al.* 1996), this is likely to occur

over several cell divisions. The assessment of apoptosis alone at a single time-point therefore may not be representative of the total irradiation response. Micronuclei and apoptosis scored at an early time point after irradiation may also not reflect all the damage that ultimately leads to loss of reproductive integrity. Cells which appear normal (non-micronucleated or non-apoptotic) at the time of observation may proceed to reproductive failure at subsequent mitoses and thus fail to form colonies. This could explain the large difference between the survival probability derived from micronucleation and apoptosis, $SF_{MA}$, and clonogenic survival, $SF_{COL}$ (Table 3.3). Other investigators, however, suggest that this disparity may be due to cell death through abnormal morphology (Abend *et al.* 2000).

The dose response for apoptosis and micronucleation cannot classify cell lines according to radiosensitivity (Figure 3.18). However, these measurements are useful in deriving a relationship between reproductive failure and dose (Figure 3.23). It is shown that radioresistant cell lines require threshold doses ranging from 0.87 to more than 6 Gy to exhibit reproductive failure, whereas radiosensitive cell lines go into reproductive cell death at very low doses just above 0 Gy. From the probability functions, a threshold dose of 3 Gy separates the 7 cell lines. Above this dose, the radiosensitive cell lines show a decline in the probability of entering reproductive failure, and the radioresistant cell lines show an increasing probability. It is demonstrated here that measurement of clonogenic survival, micronucleation and apoptosis leaves a variable cell specific parameter which accounts for the fact that

radiosensitivity (clonogenic survival) does not correlate with apoptotic propensity and micronucleus formation. This parameter is the probability of entering reproductive failure, and is relevant for the reconstruction of cellular responses to irradiation from micronucleation and apoptosis measurements.

## 4.5 CORRELATION BETWEEN CELL SURVIVAL, MICRONUCLEATION, APOPTOSIS AND REPAIR

The cytokinesis-block micronucleus and apoptosis assays are being widely discussed for their suitability as predictors of cellular sensitivity to cytotoxic agents (Masunaga *et al.* 1990, Geard and Chen 1990, Bush and McMillan 1993, Villa *et al.* 1994, Ono *et al.* 1994, Khan *et al.* 1998, Akudugu *et al.* 2000). These investigations show numerous inconsistencies and cannot correlate apoptosis and micronuclei data with radiosensitivity. Some authors propose that the assays could be reliable if additional factors including abnormal morphology (Abend *et al.* 2000) and cell death due to small deletions, chromosome aberrations, misrepair and late apoptosis (This thesis) are considered.

Differences in DNA repair proficiencies are widely known to affect cellular radiosensitivity (Weichselbaum 1986, Fox *et al.* 1988, Peak et al. 1991, Hu and Hill 1996, Britten *et al.* 1997, Dolling *et al.* 1998), but attempts to reconstruct clonogenic survival from micronuclei and apoptotic data often

ignore this fact. It is shown here in three glioblastoma cell lines with a moderately wide range of radiosensitivity that DNA dsb repair influences micronuclei formation and apoptosis, and ultimately cell survival. No significant difference was found in the initial DNA damage, but a clear correlation exists between damage repair after 20 hours and radiosensitivity, indicating that the more radioresistant cells exhibit better repair proficiency (Figure 3.24). This is in agreement with other reports (Whitaker *et al.* 1995, Dikomey *et al.* 1998, Theron *et al.* 2000).

It must be mentioned that some investigators found wide cell line dependent variations in the induction of DNA dsb damage (Zaffaroni *et al.* 1994, Ruiz de Almodovar *et al.* 1994). Other workers found no correlation at all between repair capacity and radiosensitivity (Smeets *et al.* 1993, Olive *et al.* 1994). These inconsistencies remain largely unexplained. In my panel of cell lines, the 2 hours repair data, elsewhere referred to as the fast repair component (Dikomey *et al.* 1998) correlates well with both apoptosis and micronuclei formation. The G-28 and G-120 cell lines which repaired more damage within the first 2 hours yielded more micronuclei per Gy but showed lower susceptibilities for the induction of apoptosis (Table 3.4). On the other hand, the more radiosensitive G-60 cells repaired less damage, expressed fewer micronuclei and were more susceptible to apoptosis. These results suggest that micronuclei and possibly apoptosis arise from failed DNA dsb damage repair within a couple of hours after irradiation. The better correlation between 20 hours repair (the sum of the fast and slow repair components) and

radiosensitivity seems to suggest that most of the repair that takes place later than 2 hours after irradiation is less error prone. A large extent of error-free repair would thus imply a high survival level.

Cellular DNA content has been shown to influence the yield of irradiation induced micronuclei frequency (Revell 1983). Since the magnitude of initial damage induced in these cell lines was independent of DNA content, cellular DNA content can only be implicated in radiosensitivity through its influence on repair. The cell lines containing more DNA repaired poorly and were thus more radiosensitive and vice versa. Conjecturally, this suggests that although comparable levels of DNA damage were induced, the repair rate would depend on the proficiency of repair enzymes to locate the damage. More time would be required to locate damage in a cell with high DNA content than in a cell with less DNA, a phenomenon analogous to searching for a friend in a crowd of 1000 people as compared to a group of 10 people. Differences in DNA content cannot explain this relationship since the ploidy of G-28 (SF2 = 0.69), G-120 (SF2 = 0.60) and G-60 (SF2 = 0.43) were found to be 1.75, 2.15 and 1.89, respectively. Consideration of chromatin structure also must play a role here.

## 4.6 CYTOTOXICITY OF AZADIRACHTIN A

The use of azadirachtin A as an insecticide is well documented (Rembold *et al.* 1989, Schmutterer 1995, Singh *et al.* 1996, Linton *et al.* 1997, Mitchell *et al.*

1997, Nogueira *et al.* 1997, Sayah *et al.* 1998, Guerrini and Kriticos 1998, Su and Mulla 1998, Kollien *et al.* 1998). Azadirachtin is known to affect feeding, metamorphosis and ultimately reproduction in insects, but little is known about its mode of action and the cellular targets (Rembold *et al.* 1989, Cohen *et al.* 1996, Nogueira *et al.* 1997, Sayah *et al.* 1998). There is, therefore, an enormous interest in agriculture and toxicology regarding the biological activity of azadirachtin and other neem toxins.

Azadirachtin toxicity in mammalian and insect cell lines is still not well characterized. Rembold and Annadurai have shown that 48-hour exposure of the *Spodoptera frugiperda* ovarian cell line, Sf 9, to ~1.4 $\mu$M azadirachtin was toxic (Rembold and Annadurai 1993). However, a hundred-fold higher dose of azadirachtin (i.e. >200 $\mu$M) was non-toxic to Sf 9, N1E-115 neuroblastoma (mouse), RAW 264.7 macrophages (mouse) and 143B.TK$^-$ osteosarcoma (human) cell lines, while a mild effect was observed in the *Drosophila melanogaster* KC cell line over 24 hours (Cohen *et al.* 1996). This suggests that the timing of endpoints after exposure to azadirachtin may play a critical role, and that it may be necessary to distinguish between endpoints reflecting target damage and endpoints reflecting cell damage.

The availability of a DNA damage assay (micronucleus assay) prompted me examine the curious observation that the neem toxin azadirachtin A should be insect specific and that much larger quantities of the toxin are required to inactivate mammalian cells (Cohen *et al.* 1996), and in particular human

tumour cell lines. The questions under investigation were: Does azadirachtin A induce any DNA damage in human cells and is the toxic dose indeed much higher than in insect cells?

In this study, six human glioblastoma cell lines with different TP53 status were used since insecticides often are neurotoxic. Differences in TP53 status could also lead to differences in cellular response to genotoxic agents. In a cytokinesis-block culture, binucleated cells are an indication of mitotic activity. Cultures with high binucleation, thus, have a high proliferation index (Geard and Chen 1990). The results in this study show that azadirachtin inhibits proliferation in G-28, G-60 and G-44 (Figures 3.27 and 3.28 and Table 3.5). When the induction of micronuclei was considered, all TP53 mutant cell lines and one TP53 wild-type cell line (G-62) exhibited elevated micronuclei frequencies. This implies that azadirachtin causes non-reparable DNA damage, which manifests itself as chromosome fragments in the form of micronuclei after mitosis.

The decrease in mitotic index which is evident from the binucleation parameter and low levels of micronucleation in the G-44 and G-120 cell lines can be explained by low survival. Mitotic index and micronucleation were determined after 40 hours. Cells which are very sensitive to the toxin may lose their reproductive integrity and, hence, do not progress into mitosis to form micronuclei (Akudugu *et al.* 2000). This would also explain the marked difference between the mitotic index and surviving fraction. Survival is

determined after 8 days, by which time most of the non-viable cells detected by the micronucleus assay would have died.

The results presented here permit a number of conclusions. In mammalian cells, nuclear DNA is a critical target for azadirachtin as evidenced by the formation of micronuclei. A period in excess of 40 hours (or at least one post-exposure mitosis) is required to detect the influence of azadirachtin on DNA. Other biological endpoints such as cell viability and morphological changes are known to be affected within minutes of contact with neem toxins (Cohen *et al.* 1996). When cell proliferation over 40 hours is considered, TP53 mutant human glioblastoma cell lines tend to be more sensitive to azadirachtin treatment. Interestingly, the higher susceptibility to DNA damage and the 2-3 fold higher MN frequency in TP53 mutant glioblastoma cells are coupled to better cell survival after 8 days than their TP53 wild-type relatives. This anomaly between toxin sensitivity and cell survival has also been noted in irradiated cells where the most resistant cells exhibit higher MN frequencies (Akudugu *et al.* 2000). The current explanation is that radioresistant cells can accumulate more DNA lesions and still go into mitosis whereas radiosensitive cells show greater lethality prior to the first post-irradiation mitosis (Akudugu *et al.* 2000). Whereas radiation induces DNA damage both by direct interaction and via free radicals. It is not known at this stage of our investigation whether azadirachtin causes DNA damage directly or through a cascade of other processes. However, there is a possibility that a cocktail effect in our preparation (91% azadirachtin A:~9% azadirachtin B) plays a synergistic role

in the relatively high toxic levels. In insects, it has been suggested that the susceptibility to toxins can be influenced by the reproductive potential (Stark *et al.* 1997). It is possible that the antifeedant and antimoulting effects of azadirachtin seen in insects are preceded by damage in critical targets. Investigations of these targets would be essential for a better understanding of the mechanisms of action of the neem toxins.

## 4.7 INFLUENCE OF PENTOXIFYLLINE ON CELL SURVIVAL, MITOTIC SUPPRESSION AND MICRONUCLEATION IN IRRADIATED CELLS

Pentoxifylline has been shown to exhibit sensitising effects in human and rodent cells in conjunction with ionising radiation (Kim *et al.* 1993, Vernimmen *et al.* 1994, Theron and Böhm 1998, 2000, Böhm *et al.* 1999). The drug is also known to rapidly abrogate the irradiation induced $G_2$ cell cycle checkpoint (Russell *et al.* 1996). The sensitising effect of pentoxifylline is thought to be due to an induction of early mitosis (Li *et al.* 1998), and as such cells do not have enough time for DNA repair (O'Connor 1997, Durante *et al.* 1999). This view has been questioned however, and it has been demonstrated that the drug does not enhance radiotoxicity when added at the $G_2$ block maximum, but only when present during irradiation (Theron *et al.* 2000). In the cytokinesis-block micronucleus assay the induction micronuclei after irradiation requires that cells pass through mitosis after irradiation since micronuclei are scored in binucleated cells.

In the six human glioblastoma cell lines of different TP53 status studied here, it was found that the toxicity of pentoxifylline itself varied from slight to moderate. At 2 mM PENT, the reduction in cell survival was found to be 3-29%. This toxicity range agrees well with other reports (Böhm *et al.* 1999, Theron and Böhm 2000, Theron *et al.* 2000). Pentoxifylline sensitises cells to $^{60}Co$ $\gamma$-irradiation giving cell kill enhancement factors ranging from 1.37 to 3.85 (Figure 3.30, Tables 3.6 and 3.7). Although these enhancement factors are well within the range reported by other investigations (Powell *et al.* 1995, Russell *et al.* 1995, 1996, Li *et al.* 1998, 1999, Theron *et al.* 2000), they contrast with the observation that the TP53 wild-type cell lines were more sensitised than their TP53 mutant homologues (Tables 3.6 and 3.7). The results presented here were obtained when pentoxifylline was added at the maximum expression of $G_2$ block. No enhanced radiotoxicity was seen in TP53 mutant and TP53 wild-type cells for application of the drug at this time point.

The enhanced cell kill found for glioblastoma cell lines is however consistent with the reduction of irradiation induced mitotic suppression as shown by the increase of the proportion of TP53 wild-type cells which have undergone mitosis (Table 3.7). Only one TP53 mutant cell line (G-60, Table 3.6) showed any significant increase in the proportion of cells that underwent mitosis. This phenomenon that pentoxifylline tends to preferentially sensitise TP53 wild-type cells cannot be due to the cytotoxicity of the drug alone since these cells showed better survival than their TP53 mutant homologues. Sensitisation of

the TP53 wild-type cells also cannot be explained by a possible accumulation of cells in an irradiation induced $G_1$ check-point, because the TP53 wild-type cells showed elevated proportions of cells undergoing mitosis as seen in the enhancement factors for binucleation (Table 3.7). Low EHF's for binucleation may imply either an increased radiotoxicity or cell blockage at the cell cycle check-points. It appears that the mode of action of pentoxifylline may be cell-type specific, and not only dependent on the TP53 status. To explain this phenomenon, apoptosis and DNA repair proficiencies in the presence of pentoxifylline would need to be considered.

# CONCLUSIONS

1. From a total of the 13 neuroblastoma and neuroepithelial cell lines, only the SH-SY5Y cell line did not express detectable levels of micronuclei in response to irradiation. It is not clear why this cell line failed to respond. Extreme radiosensitivity has been suggested as a reason for low micronuclei yield (Akudugu *et al.* 2000), however the SH-SY5Y cells are more radioresistant than the OP-27, SK-N-SH and KELLY cell lines, which expressed significant levels of micronuclei. Nevertheless, the cytokinesis-block micronucleus assay is suitable for testing sensitivity to cytotoxins. The major limitation however is that this assay does not rank cell lines according to radiosensitivity. This issue remains under investigation but is still unresolved.

2. Inclusion of apoptosis and cell death via pathways other than micronucleation could improve radiosensitivity ranking. Apoptosis and micronucleation are dose dependent and interrelated by an exponential function. Cell death due to processes like small deletions, misrepair and chromosome aberrations is a variable and cell type-specific parameter which appears to be a component of cell survival. This mode of cell death occurs even at very low doses in radiosensitive cell lines, while radioresistant cell lines require moderate to high threshold doses for cell death from processes other than apoptosis and micronucleation. A clear

understanding of the interrelationship between these cell inactivation pathways would help to resolve anomalies in radiosensitivity ranking.

3. Results on DNA dsb repair in 3 cell lines of differing radiosensitivity suggest that both micronucleation and apoptosis may be influenced by DNA dsb damage repair. It is shown that the fast repair component tends to strongly correlate with the induction of micronuclei and apoptosis. This furthermore suggests that micronucleation and apoptosis are a consequence of early repair, and that a high repair activity in the first 2 hours may signal a high micronuclei frequency and a depression of apoptosis.

4. In the human glioblastoma (neuroepithelial) cell lines, the TP53 wild-type cells are significantly radiosensitised when pentoxifylline was added 18 hours after irradiation, while no sensitisation was observed in the TP53 mutant cell lines. This result is in contrast with several reports showing that the radiation sensitisation of pentoxifylline occurs only in TP53 mutant cell lines and only when the drug is added at the time of irradiation (Russell *et al.* 1995, 1996, Li *et al.* 1998, 1999, Theron *et al.* 2000). Clinical applications of pentoxifylline in glioblastoma therapy are consistent with the unusual behaviour of glioblastoma cells (NIH Clinical Research Studies, Protocol no: 95-C-0069). TP53 wild-type glioblastoma lines also show enhanced proportions of cells undergoing mitosis. This confirms abrogation

of a $G_2$-phase block. The enhanced radiosensitivity is therefore not a consequence of a $G_1$-phase arrest in the TP53 wild-type cells.

5. The micronucleus assay and other damage assays are not exclusively suitable for comparing cytotoxic responses between cell types. Damage assays tend to be cell specific and cannot predict the ultimate cell survival. The MN assay however shows great potential in assessing radiotoxicity and drug toxicity in individual cell systems. This assay is sensitive to low levels of damage and should be useful in studying the effects of microenvironmental changes on the induction of damage in tissue. Studies of this nature would be useful in the areas of biological dosimetry (in the event of patient overdose or accidental exposure of radiation workers) and toxicology e.g. the food industry.

6. The micronucleus assay is capable of distinguishing between radiation modalities. It is shown here that the assay sharply differentiates low-LET irradiation from high-LET irradiation, and can identify photon-resistant cells which are neutron sensitive. The RBE of p(66/$Be^+$) neutrons determined by the micronucleus assay compares favourably with those determined by conventional survival parameters (Fox and McNally 1988, Tates *et al.* 1989, Darroudi *et al.* 1992, Courdi *et al.* 1996, Slabbert *et al.* 1996, Heimers 1999, Frankenberg *et al.* 1999). This assay would also be capable in

assessing drug toxicity and therefore may be suitable in pharmaceutical and agricultural industry.

7. Limitations of applying the micronucleus assay exist. Some cells may not express micronuclei as seen in the case of the SH-SY5Y cell line (Akudugu *et al.* 2000). Established cell lines tend to show high background MN frequencies, which can result in low MN reponses to irradiation or drugs. The fact that the MN response to dose is not infinitely linear but shows saturation kinetics, limits it application to low doses. Scoring of micronuclei in cells with little or no cytoplasm is error prone, however a low nuclear:cytoplasmic ratio helps in detecting cells from which micronuclei originate. Cell lines which tend to clump are difficult to score. Therefore, great caution must be taken in applying the MN assay to cell toxicity studies.

## PUBLISHED AND UNPUBLISHED PAPERS FROM THIS THESIS

1. Akudugu JM, Slabbert JP, Serafin A, Böhm L. Frequency of radiation-induced micronuclei in neuronal cells does not correlate with clonogenic survival. *Radiat. Res.* **153:** 62-67, 2000.

2. Akudugu JM, Böhm L. Measurement of mocronucleation and apoptosis in human neuroblastoma and neuroepithelial cell lines and the role of cell death via other pathways in the reconstruction of radiosensitivity. *Radiat. Res.* (Under revision).

3. Akudugu JM, Gäde G, Böhm L. Cytotoxicity of azadirachtin A in human glioblastoma cell lines. *Life Sciences.* (In Press).

4. Akudugu JM, Böhm L. Dose response relationships of p(66/$Be^{+}$) neutron and $^{60}Co$ $\gamma$ induced micronuclei in human neuroblastoma and neuroepithelial cell lines. *Radiat. Res.* (Submitted).

5. Akudugu JM, Theron T, Böhm L. Influence of DNA double-strand break repair on micronuclei yield. *Radiat. Res.* (Submitted).

# BIBLIOGRAPHY

Abend M, Rhein A, Gilbertz K-P, Blakely WF, van Beuningen D. Correlation of micronucleus and apoptosis assays with reproductive cell death. *Int. J. Radiat. Biol.* **67:** 315-326, 1995.

Abend M, Kehe K, Kehe K, Riedel M, van Beuningen D. Correlation of micronucleus and apoptosis assays with reproductive cell death can be improved by considering other modes of death. *Int. J. Radiat. Biol.* **76:** 249-259, 2000.

Ager DD, Dewey WC, Gardiner K, Harvey W, Johnson RT, Waldren CA. Measurement of radiation-induced DNA double-strand breaks by pulsed-field gel electrophoresis. *Radiat. Res.* **122:** 181-187, 1990.

Akudugu JM, Slabbert JP, Serafin A, Böhm L. Frequency of radiation-induced micronuclei in neuronal cells does not correlate with clonogenic survival. *Radiat. Res.* **153:** 62-67, 2000.

Arlett CF, Harcourt SA. Survey of radiosensitivity in a variety of human cell strains. *Cancer Res.* **40:** 926-932, 1980.

Bache M, Dunst J, Würl P, Fröde D, Dietzel M, Meye A, Schmidt H, Rath F-W, Wohlrab W, Dralle H, Taubert H. Radiation induced $G_2$/M block and apoptosis in two human sarcoma cell lines with different p53 gene status. *Int. J. Radiat. Oncol.* **11:** 993-997, 1997.

Barendsen GW, Beusker TLJ, Vergroesen AJ, Budke L. Effects of different ionizing radiations on human cells in tissue culture. II. Biological experiments. *Radiat. Res.* **13:** 841-819, 1960.

Barranco SC, Romsdahl MM, Humphrey RM. The radiation response of human malignant melanoma cells grown *in vitro*. *Cancer Res.* **31:** 830-833, 1971.

Begg AC, Hofland I, Moonen L, Bartelink H, Schraub S, Bontemps P, Le Fur R, van der Bogaert W, Caspers R, van Glabbeke M, Horiot JC. The predictive value of cell kinetic measurements in a European trial of accelerated fractionation in advanced head and neck tumours: an interim report. *Int. J. Radiat. Oncol. Biol. Phys.* **19:** 1449-1453, 1990.

Belloc F, Dumain P, Boisseau MR, Jalloustre C, Reiffers J, Bernard P, Lacombe F. A flow cytometric method using Hoechst 33342 and PI for simultaneous cell cycle analysis and apoptosis determination in unfixed cells. *Cytometry* **17:** 59-65, 1994.

Biedler JL, Helson L, Spengler BA. Morphology and growth, tumourigenicity, and cytogenetics of human neuroblastoma cells in continuous culture. *Cancer Res.* **33:** 2643-2652, 1973.

Biedler JL, Spengler BA. A novel chromosome abnormality in human neuroblastoma and antifolate-resistant Chinese Hamster cell lines in culture. *J. Natl. Cancer Inst.* **57:** 683-695, 1976.

Birnboim HC, Jevcak JJ. Fluorometric method for rapid detection of DNA strand breaks in human white blood cells produced by low doses of radiation. *Cancer Res.* **41:** 1889-1892, 1981.

Böhm L, Blekkenhorst G, Slabbert JP, Verheye F, Jones DT, Yudelev M. RBE and OER measurements on the p(66/$Be^{+}$) neutron beam at Faure, South Africa. *Strahlenther. Onkol.* **168:** 42-47, 1992.

Böhm L, Theron T, Binder A. Pentoxifyline inhibits the irradiation induced $G_2$/M block and alters DNA synthesis in p53 mutant and repair deficient cells. In *Fundamentals for the Assessment of Risk from Environmental Radiation* (C. Baumstark-Khan, S. Kozubek and G. Horneck, eds.) pp. 305-310. Kluwer Academic Press, Netherlands, 1999.

Boller K, Schmid W. Chemische Mutagenese beim Säuger. Das Knochenmark des Chinesishen Hamster als *in vivo* Testsystem. Hämatologische Befunde nach Behandlung mit Trenimon. *Humangenetik* **11:** 35-54, 1970.

Bradley MO, Kohn KW. X-ray induced DNA double-strand break production and reapir in mammalian cells as measured by neutral filter elution. *Nucleic Acids Res.* **7:** 793-804, 1979.

Brenneke H. Strahlenschädigung von Mäuse- und Rattensperma beobachtet an der Frühentwicklung der Eier. *Strahlentherapie* **60:** 214-238, 1937.

Britten RA, Warenius HM, Parkins C, Peacock JH. The inherent cellular sensitivity to 62.5 MeV ($p \rightarrow Be^{+}$) neutrons of human cells differing in photon sensitivity. *Int. J. Radiat. Biol.* **61:** 805-812, 1992.

Britten RA, Murray D. Constancy of the relative biological effectiveness of 42 MeV ($p \rightarrow Be^{+}$) neutrons among cell lines with different DNA repair proficiencies. *Radiat. Res.* **148:** 308-316, 1997.

Brock WA, Baker FL, Wike JL, Sivon SL, Peters LJ. Cellular radiosensivity of primary head and neck squamous cell carcinoma and tumour control. *Int. J. Radiat. Oncol. Biol. Phys.* **18:** 1283-1286, 1990.

Budach W, Gioioso D, Taghian A, Stuschke M, Suit HD. Repopulation capacity during fractionated irradiation of squamous cell carcinomas and glioblastomas *in vitro*. *Int. J. Radiat. Oncol. Biol. Phys.* **39:** 743-750, 1997.

Busciglio J, Yankner BA. Apoptosis and increased generation of reactive oxygen species in Down's syndrome neurons *in vitro*. *Nature.* **378:** 776-779, 1995.

Bush C, McMillan TJ. Micronucleus formation in human tumour cells: lack of correlation with radiosensitivity. *Br. J. Cancer* **67:** 102-106, 1993.

Carrano AV. Chromosome aberrations and radiation induced cell death. I. Transmission and survival parameters of aberrations. II. Predicted and observed cell survival. *Mutat. Res.* **17:** 341-353, 355-366, 1973.

Chen DJ, Strniste GF, Tokita N. The genotoxicity of alpha particles in human embryonic skin fibroblasts. . *Radiat. Res.* **100:** 321-327, 1984.

Coco Martin JM, Mooren E, Ottenheim C, Burrill W, Nunez MI, Sprong D, Bartelink H, Begg AC. Potential of radiation-induced chromosome aberrations to predict radiosensitivity in human tumour cells. *Int. J. Radiat. Biol.* **75:** 1161-1168, 1999.

Cohen E, Quistad GB, Casida JE. Cytotoxicity of nimbolide, epoxyazadiradione and other limonoids from neem insecticides. *Life Sciences* **58:** 1075-181, 1996.

Countryman PI, Heddle JA. The production of micronuclei from chromosome aberrations in irradiated cultures of human lymphocytes. *Mutat. Res.* **41:** 321-332, 1976.

Courdi A, Brassart N, Herault J, Mari D, Chauvel P. The RBE of fast neutrons for *in vitro* inactivation of human tumour cells determined by the ratio of mean inactivation doses. *Acta Oncol.* **35:** 237-242, 1996.

Courtenay VD, Mills J. An *in vitro* colony assay for human tumours grown in immune-suppressed mice and treated *in vivo* with cytotoxic agents. *Br. J. Cancer* **37:** 261-268, 1978.

Cullen BM, Evans NTS, Walker HC, Emery EW, Boag JW. Cell survival at low oxygen tension and dose build-up in argon. *Int. J. Rdaiat. Biol.* **37:** 19-23, 1980.

Cunniffe S, O'Neill P. The complexity of radiation-induced DNA damage as revealed by exposure to cell extracts. *Radiat. Res.* **152:** 421-427, 1999.

Darroudi F, Farouqi Z, Benova D, Natarajan AT. The mouse splenocyte assay, an *in vivo/in vitro* system for biological monitoring: studies with X-rays, fission neutrons and bleomycin. *Mutat. Res.* **272:** 237-248, 1992.

Deacon J, Peckham MJ, Steel GG. The radioresponsiveness of human tumours and the initial slope of the cell survival curve. *Radiother. Oncol.* **2:** 317-323, 1984.

Dertinger H, Guichard M, Malaise EP. Relationship between intercellular communication and radiosensitivity of human tumour xenografts. *Eur. J. Cancer. Clin. Oncol.* **20:** 561-566, 1984.

Dikomey E, Dahm-Daphi J, Brammer I, Martensen R, Kaina B. Correlation between cellular radiosensitivity and non-repaired double strand breaks studied in nine mammalian cell lines. *Int. J. Radiat. Biol.* **73:** 269-278, 1998.

Discombe G. L'origine des corps de Howell-Jolly et des anneaux de Cabot. *Sang.* **19:** 262-264, 1948.

Dolling J-A, Boreham DR, Brown DL, Mitchel REJ, Raaphorst GP. Modulation of radiation-induced strand break repair by cisplatin in mammalian cells. *Int. J. Radiat. Biol.* **74:** 61-69, 1998.

Durante M, George K, Yang TC. Biodosimetry of ionizing radiation by selective painting of prematurely condensed chromosomes in human lymphocytes. *Radiat. Res.* **148:** S45-S50, 1997.

Durante M, George K, Wu H-L, Yang TC. Rejoining and misrejoining of radiation-induced chromatin breaks. III. Hypertonic treatment. *Radiat. Res.* **149:** 68-74, 1998.

Durante M, Furusawa Y, Majima H, Kawata T, Gotoh E. Association between $G_2$-phase block and repair of radiation-induced chromosome fragments in human lymphocytes. *Radiat. Res.* **151:** 670-676, 1999.

Elkind MM, Sutton H. Radiation response of mammalian cells grown in culture. I. Repair of x-ray damage in surviving Chinese hamster cells. *Radiat. Res.* **13:** 556-593, 1960.

Evans HJ, Neary GJ, Williamson FS. The relative biological efficiency of single doses of fast neutrons and gamma-rays on *Vicia faba* roots and the effect of oxygen. Part II. Chromosome damage: the production of micronuclei. *Int. J. Radiat. Biol.* **3:** 216-229, 1959.

Falkvoll KH. The occurrence of apoptosis, abnormal mitoses, cells dying in mitosis and micronuclei in a human melanoma xenograft exposed to single dose irradiation. *Strahlenther. Onkol.* **166:** 487-492, 1990.

Fenech F, Morley AA. Solutions to the kinetic problem in the micronucleus assay. *Cytobios.* **43:** 233-246, 1985.

Fertil B, Deschavanne PJ, Gueulette J, Possoz A, Wambersie A, Malaise EP. *In vitro* radiosensitivity of six human cell lines II. Relation to the RBE of 50 MeV neutrons. *Radiat. Res.* **90:** 526-537, 1982.

Fertil B, Dertinger H, Courdi A, Malaise EP. Mean inactivation dose: a useful concept for intercomparison of human cell survival curves. *Radiat. Res.* **99:** 73-84, 1984.

Fertil B, Malaise EP. Intrinsic radiosensitivity of human cell lines is correlated with radioresponsiveness of human tumours: Analysis of 101 published survival curves. *Int. J. Radiat. Oncol.* **11:** 1699-1707, 1985.

Fornace JR, Nagasawa AJ, Little JB. Relationship of DNA repair to chromosome aberrations, sister chromatid exchanges and survival during liquid-holding recovery in X-irradiated mammalian cells. *Mutat. Res.* **70:** 323-336, 1980.

Fowler JF. Potential for increasing the differential response between tumours and normal tissues: can proliferation rate be used? *Int. J. Radiat. Oncol. Biol. Phys.* **12:** 641-645, 1986.

Fox JC, McNally NJ. Cell survival and DNA double-strand break repair following X-ray or neutron irradiation of V79 cells. *Int. J. Radiat. Oncol. Biol. Phys.* **54:** 1021-1030, 1988.

Frankenberg D, Brede HJ, Schrewe UJ, Steinmetz C, Frankenberg-Schwager M, Kasten G, Pralle E. Induction of DNA double-strand breaks by $^{1}H$ and $^{4}H$ ions in primary human skin fibroblasts in the LET range of 8 to 124 keV/μm. *Radiat. Res.* **151:** 540-549, 1999.

Geard CR, Chen CY. Micronuclei and clonogenicity following low- and high-dose-rate γ irradiation of normal human fibroblasts. *Radiat. Res.* **124:** S56-S61, 1990.

Giese A, Rief MD, Loo MA, Berens ME. Determinants of human astrocytoma migration. *Cancer Res.* **54:** 3897-3904, 1994.

Greinert R, Thieke C, Detzler E, Boguhn O, Frankenberg D, Harder D. Chromosome aberrations induced in human lymphocytes by 3.45 MeV alpha

particles analyzed by premature chromosome condensation. *Radiat. Res.* **152:** 412-420, 1999.

Guerrini VH, Kriticos CM. Effect of azadirachtin on *Ctenocephalides felis* in the dog and the cat. *Vet. Parasitol.* **74:** 289-297, 1998.

Guo M, Chen C, Vidar C, Marino S, Dewey WC, Ling CC. Characterization of radiation-induced apoptosis in rodent cell lines. *Radiat. Res.* **147:** 295-303, 1997.

Guo GZ, Sasai K, Oya N, Takagi T, Shibuya K, Hiraoka M. Simultaneous evaluation of radiation-induced apoptosis and micronuclei in five cell lines. *Int. J. Radiat. Biol.* **73:** 297-302, 1998.

Guo GZ, Sasai K, Oya N, Shibata T, Shibuya K, Hiraoka M. A significant correlation between clonogenic radiosensitivity and the simultaneous assessment of micronucleus and apoptotic cell frequency. *Int. J. Radiat. Biol.* **75:** 857-864, 1999.

Hall EJ, Marchese MJ, Astor MB, Morse T. Response of cells of human origin, normal and malignant, to acute and low dose rate irradiation. *Int. J. Radiat. Oncol. Biol. Phys.* **12:** 655-659, 1986.

Halperin EC, Burger PC, Bullard DE. The fallacy of the localized supretentorial malignant glioma. *Int. J. Radiat. Oncol. Biol. Phys.* **15:** 505-509, 1988.

Hartsell WF, Gajjar A, Heideman RL, Langston JA, Sanford RA, Walter A, Jones D, Chen G, Kun LE. Patterns of failure in children with medulloblastoma: Effects of preirradiation chemotherapy. *Int. J. Radiat. Oncol. Biol. Phys.* **39:** 15-24, 1997.

Heddle JA. Rapid *in vivo* test for chromosomal damage. *Mutat. Res.* **18:** 187-190, 1973.

Heimers A. Cytogenetic analysis in human lymphocytes after exposure to simulated cosmic radiation which reflects the inflight radiation environment. *Int. J. Radiat. Biol.* **75:** 691-698, 1999.

Hendry JH, West CW. Apoptosis and mitotic cell death: their relative contribution to normal-tissue and tumour radiation response. *Int. J. Radiat. Biol.* **71:** 709-719, 1997.

Howard-Flanders P, Alper T. The sensitivity of microorganisms to irradiation under controlled gas conditions. *Radiat. Res.* **7:** 518-540, 1957.

Howell WH. The life-history of the formed elements of the blood, especially the red blood corpuscles. *J. Morphol.* **4:** 57-116, 1891.

Hu Q, Hill RP. Radiosensitivity, apoptosis and repair of DNA double-strand breaks in radiation-sensitive Chinese hamster ovary cell mutants treated at different dose rates. *Radiat. Res.* **146:** 636-645, 1996.

Huber R, Schraube H, Nahrstedt U, Braselmann H, Bauchinger M. Dose-response relationships of micronuclei in human lymphocytes induced by fission neutrons and by low LET radiation. *Mutat. Res.* **306:** 135-141, 1994.

Jalava AM, Heikkilä J, Åkerlind G, Pettit GR, Åkerman KEO. Effects of Bryostatins 1 and 2 on morphological and functional differentiation of SH-SY5Y human neuroblastoma cells. *Cancer Res.* **50:** 3422-3428, 1990.

Jolly J. Recherches sur la formation des globules rouges des mammifères. *Arch. Anat. Microsc.* **9:** 133-314, 1907.

Juckett MB, Shadley JD, Zheng Y, Klein JP. Desferrioxamine enhances the effect of gamma radiation on clonogenic survival and the formation of chromosomal aberrations in endothelial cells. *Radiat. Res.* **149:** 330-337, 1998.

Kallman RF, Dorie MJ. Tumour oxygenation and reoxygenation during radiation therapy: Their importance in predicting tumour response. *Int. J. Radiat. Oncol. Biol. Phys.* **12:** 681-685, 1986.

Kerr JFR, Wyllie AH, Currie AR. Apoptosis: a basic biological phenomenon with wide-ranging implications in tissue kinetics. *Brit. J. Cancer* **26:** 239-257, 1972.

Khan MA, Hill RP, Dyk JV. Partial volume rat lung irradiation: An evaluation of early DNA damage. *Int. J. Radiat. Oncol. Biol. Phys.* **40:** 467-476, 1998.

Kim SH, Khil MS, Ryu S, Kim JH. Enhancement of radiation response on human carcinoma cell lines in culture by pentoxifylline. *Int. J. Radiat. Oncol. Biol. Phys.* **25:** 61-65, 1993.

Kim HE, Han SJ, Kasza T, Han R, Choi H-S, Palmer KC, Kim H-R. Platelet-derived growth factor (PDGF)-signaling mediates radiation-induced apoptosis in human prostate cancer cells with loss of *p53* function. *Int. J. Radiat. Oncol. Biol. Phys.* **39:** 731-736, 1997.

Kinashi Y, Ono K, Abe M. The micronucleus assay of lymphocyte is a useful predictive assay of the radiosensitivity of normal tissue: A study of three inbred strains of mice. *Radiat. Res.* **148:** 341-347, 1997.

Kohn KW, Ewig RAG, Erickson LC, Zwelling LA. Measurement of strand breaks and cross-links by alkaline elution. In *DNA repair: A Laboratory Manual of Research Procedures* eds. Friedberg EC, Hanawalt PC. Part B, Vol. 1, pp. 379-401. Dekker, New York, 1981.

Kollien AH, Goncalves TC, De-Azambuja P, Garcia ES, Schaub GA. The effect of azadirachtin on fresh isolates of *Trypanosoma cruzi* in different species of triatomines. *Parasitol. Res.* **84:** 286-290, 1998.

Koutcher JA, Alfieri AA, Devitt ML, Rhee JG, Kornblith AB, Mahmood U, Merchant TE, Cowburn D. Quantitative changes in tumour metabolism, partial pressure of oxygen, and radiobiological oxygenation status postradiation. *Cancer Res.* **52:** 4620-4627, 1992.

Lartigau E, Lespinasse F, Vitu L, Guichard M. Does the direct measurement of oxygen tension in tumours have any adverse effects? *Int. J. Radiat. Oncol. Biol. Phys.* **22:** 949-951, 1992.

Lee H-S, Park HJ, Lyons JC, Griffin RJ, Auger EA, Song CW. Radiation-induced apoptosis in different pH environments *in vitro*. *Int. J. Radiat. Oncol. Biol. Phys.* **38:** 1079-1087, 1997.

Li Y-X, Weber-Johnston K, Sun L-Q, Paschoud N, Mirimanoff R-O, Coucke PA. Effect of pentoxifylline in radiation-induced $G_2$-phase delay and radiosensitivity of human colon and cervical cancer cells. *Radiat. Res.* **149:** 338-342, 1998.

Li Y-X, Sun L-Q, Weber-Johnston K, Paschoud N, Coucke PA. Potentiation of cytotoxicity and radiosensitisation of (E)-2-deoxy-2'-(fluoromethylene) cytidine by pentoxifylline *in vitro*. *Int. J. Cancer* **80:** 155-160, 1999.

Ling CC, Chen CH, Fuks Z. An equation for the dose response of radiation-induced apoptosis: possible incorporation with the LQ model. *Radiother. Oncol.* **33:** 17-22, 1994.

Linton YM, Nisbet AJ, Mordue-Luntz AJ. The effect of azadirachtin on the testes of the desert locust, *Schistocerca gregaria*. *J. Insect Physiol.* **43:** 1077-1084, 1997.

Littbrand B, Revesz L. The effect of oxygen on cellular survival and recovery after radiation. *Br. J. Radiol.* **42:** 914-924, 1969.

Loeffler JS, Alexander III E, Hochberg FH, Wen PY, Morris JH, Schoene WC, Siddon RL, Morse RH, Black PM. Clinical patterns of failure following stereotactic interstitial irradiation for malignant gliomas. *Int. J. Radiat. Oncol. Biol. Phys.* **19:** 1455-1462, 1990.

Lucas JN, Awa A, Straume T, Poggensee M, Kodama Y, Nakano M, Ohtaki K, Weier H-U, Pinkel D, Gray J, Littlefield G. Rapid translocation frequency analysis in humans decades after exposure to ionizing radiation. *Int. J. Radiat. Biol.* **62:** 53-63, 1992.

Lucas JN. Dose reconstruction for individuals exposed to ionizing radiation using chromosome painting. *Radiat. Res.* **148:** S33-S38, 1997.

Mantyla M, Toivanen JT, Pitkanen MA, Rekonen AH. Radiation-induced changes in regional blood flow in human tumours. *Int. J. Radiat. Oncol. Biol. Phys.* **8:** 1711-1717, 1982.

Masunaga S, Ono K, Wandl EO, Fushiki M, Abe M. Use of the micronucleus assay for the selective detection of radiosensitivity in BudR-unincorporated cells after pulse-labelling of exponentially growing tumour cells. *Int. J. Radiat. Biol.* **58:** 303-311, 1990.

Mathieu J, Ferlat S, Ballester B, Platel S, Herodin F. Radiation-induced apoptosis in thymocytes: Inhibition by diethyldithiocarbamate and zinc. *Radiat. Res.* **146:** 652-659, 1996.

Meyn RE, Stephens LC, Kian Ang K, Hunter NR, Brock WA, Milas L, Peters LJ. Heterogeneity in the development of apoptosis in irradiated murine tumours of different hitologies. *Int. J. Radiat. Biol.* **64:** 583-591, 1993.

Mirkovic N, Meyn RE, Hunter NR, Milas L. Radiation-induced apoptosis in a murine lymphoma *in vivo*. *Radiother. Oncol.* **33:** 11-16, 1994.

Mitchell MJ, Smith SL, Johnson S, Morgan ED. Effect of the neem tree compounds azadirachtin, salannin, nimbin and 6-desacetylnimbin on ecdysone 20-monooxygenase activity. *Arch. Insect Biochem. Physiol.* **35:** 199-209, 1997.

Mottram JC. Factor of importance in radiosensitivity of tumours. *Br. J. Radiol.* **9:** 606-614, 1936.

Müller W-U, Streffer C. Distribution of micronuclei among single cells of pre-implantation mouse embyos after X-irradiation *in vitro*. *Mutat. Res.* **125:** 65-70, 1984.

Müller W-U, Streffer C. Change in frequency of radiation induced micronuclei during interphase of four-cell mouse embyos *in vitro*. *Radiat. Environ. Biophys.* **25:** 195-199, 1986.

Müller W-U, Streffer C. Biological indicators for radiation damage. *Int. J. Radiat. Biol.* **59:** 863-873, 1991.

Neumann E. Ueber die Bedeutung des Knochenmarkes für die Blutbildung. *Arch. Heilkd* **X:** 68-102, 1869.

NIH Clinical Research Studies. A phase I study of combined radiation response modifiers employing pentoxifylline and hydroxyurea for treatment of glioblastoma. Protocol No: 95-C-0069.

Nogueira NF, Gonzales M, Garcia EM, de Souza W. Effect of azadirachtin A on the fine structure of the midgut of *Rhodnius prolixus*. *J. Invertebr. Pathol.* **69:** 58-63, 1997.

Nordsmark M, Høyer M, Keller J, Nielsen OS, Jensen OM, Overgaard J. The relationship between tumour oxygenation and cell proliferation in human soft tissue sarcomas. *Int. J. Radiat. Oncol. Biol. Phys.* **35:** 701-708, 1996.

O'Connor PM. Mammalian $G_1$ and $G_2$ phase checkpoints. *Cancer Surv.* **29:** 151-182, 1997.

Ogiu T, Fukami H, Nishimura M. DNA strand breaks and death of thymocytes induced by *N*-methyl-*N*-nitrosourea. *J. Cancer Res. Clin. Oncol.* **118:** 23-29, 1992.

Olive PL, Banáth JP, Macphah HS. Lack of a correlation between radiosensitivity and DNA double strand break induction of rejoining in six human tumour cell lines. *Cancer Res.* **54:** 3939-3946, 1994.

Olive PL, Banáth JP, Durand RE. Development of apoptosis and polypoidy in human lymphoblast cells as a function of position in the cell cycle at the time of irradiation. *Radiat. Res.* **146:** 595-602, 1996.

Olive PL, Durand RE. Apoptosis: an indicator of radiosensitivity in *vitro? Int. J. Radiat. Biol.* **71:** 695-707, 1997.

Ono K, Wandl E, Tsutsui K, Sasai K, Abe M. The correlation between cell survival curve and dose-response curve of micronucleus (MN) frequency. *Strahlenther. Onkol.* **165:** 824-827, 1989.

Ono K, Masunaga S, Akaboshi M, Akuta K. Estimation of the initial slope of the cell survival curve after irradiation from micronucleus frequency in cytokinesis-blocked cells. *Radiat. Res.* **138:** S101-S104, 1994.

Ormerod MG, Sun XM, Brown D, Snowden RT, Cohen GM. Quantification of apoptosis and necrosis by flow cytometry. *Acta Oncol.* **32:** 417-424, 1993.

Palcic B, Skarsgard LD. Reduced oxygen enhancement ratio at low doses of ionizing radiation. *Radiat. Res.* **100:** 328-339, 1984.

Palcic B, Faddegon B, Skarsgard LD. The effect of misonidazole as a hypoxic sensitizer at low dose. *Radiat. Res.* **100:** 340-347, 1984.

Parker L, Skarsgard LD, Emmerson PT. Sensitization of anoxic mammalian cells to x-rays by triacetoneamine-*N*-oxyl. Survival and Toxicity Studies. *Radiat. Res.* **38:** 493-500, 1969.

Peacock JH, Cassoni AM, McMillan TJ. Radiosensitive human tumour cell lines may not be recovery deficient. *Int. J. Radiat. Biol.* **54:** 945-952, 1988.

Peak MJ, Wang L, Hill CK, Peak JG. Comparison of repair of DNA double-strand breaks caused by neutron or gamma radiation in cultured human cells. *Int. J. Radiat. Biol.* **60:** 891-898, 1991.

Peters LJ, Brock WA, Johnson T, Meyn RE, Tofilon PJ, Milas L. Potential methods for predicting tumour radiocurability. *Int. J. Radiat. Oncol. Biol. Phys.* **12:** 459-467, 1986.

Peters LJ, Brock WA. Cellular radiosensitivity as predictors of treatment outcome: where do we stand? *Int. J. Radiat. Oncol. Biol. Phys.* **25:** 147-148, 1992.

Pettersen EO, Christensen T, Bakke O, Oftebro R. A change in the oxygen effect throughout the cell-cycle of human cells of the line NHIK 3025 cultivated *in vitro*. *Int. J. Radiat. Biol.* **31:** 171-184, 1977.

Pinkel D, Landegent J, Collins C, Fuscoe J, Segraves R, Lucas J, Grya J. Fluorescence *in situ* hybridization with human chromosome-specific libraries: Detection of trisomy 21 and translocations of chromosome 4. *Proc. Natl. Acad. Sci. USA* **85:** 9138-9142, 1988.

Pourreau-Schneider N, Malaise EP. Relationship between surviving fractions using the colony method, $LD_{50}$ and the growth delay after irradiation of human melanoma cells grown as multicellular spheroids. *Radiat. Res.* **85:** 321-332, 1981.

Powell SN, DeFrank JS, Connell P, Eogan M, Preffer F, Dombkowski D, Tang W, Friend S. Differential sensitivity of $p53^-$ and $p53^+$ cells to caffeine induced radiosensitisation and override of $G_2$ delay. *Cancer Res.* **55:** 1643-1648, 1995.

Puck TT, Marcus PI. Action of X-rays on mammalian cells. *J. Exp. Med.* **103:** 653-666, 1956.

Rabbitts TH. Chromosomal translocations in human cancer. *Nature.* **372:** 143-149, 1994.

Radford IR, Murphy TK. Radiation response of mouse lymphoid and myeloid cell lines. Part III. Different signals can lead to apoptosis and may influence sensitivity to killing by DNA double-strand breakage. *Int. J. Radiat. Biol.* **65:** 229-239, 1994.

Radford IR, Murphy TK, Radley JM, Ellis SL. Radiation response of mouse lymphoid and myeloid cell lines. Part II. Apoptotic death is shown by all lines examined. *Int. J. Radiat. Biol.* **65:** 217-227, 1994.

Ramakrishnan N, McClain DE, Catravas GN. Membranes as sensitive targets in thymocyte apoptosis. *Int. J. Radiat. Biol.* **63:** 693-701, 1993.

Rasey JS, Nelson NJ, Mahler P, Anderson K, Krohn KA, Menard T. Radioprotection of normal tissues against gamma-rays and cyclotron neutrons with WR2721: $LD_{50}$ studies and $^{35}S$-WR2721 biodistribution. *Radiat. Res.* **97:** 598-607, 1984.

Rembold H, Subrahmanyam B, Müller T. *Experientia.* **45:** 361-363, 1989.

Rembold H. The Azadirachtins - Their potential for insect control. *Economic and Medical Plant Res.* **3:** 57-72, 1989.

Rembold H, Annadurai RS. Azadirachtin inhibits proliferation of Sf 9 cells in monolayer. *Z. Naturforsch.* **48c:** 495-499, 1993.

Revell SH. Relationship between chromosome damage and cell death. In *Radiation-Induced Chromosome Damage in Man,* eds Ishihara T, Sasaki MS. pp 215-233. Alan R. Liss: New York, 1983.

Rockwell SC, Kallman RF. Cellular radiosensitivity and tumour radiation response in the EMT6 tumour cell system. *Radiat. Res.* **53:** 281-284, 1973.

Rockwell SC. Effect of clumps and clusters on survival measurements with clonogenic assay. *Cancer Res.* **45:** 1601-1607, 1985.

Rofstad EK, Brustad T. Radiation response *in vitro* of cells from five human malignant melanoma xenografts. *Int. J. Radiat. Biol.* **40:** 677-680, 1981.

Roos WP, Binder A, Böhm L. Determination of the initial DNA damage and the residual DNA damage remaining after 12 hours of repair in eleven cell lines at low doses of irradiation. *Int. J. Radiat. Biol.* **76:** 1493-1500, 2000.

Ruiz de Almodovar JM, Nunez MI McMillan TJ, Olea N, Mort C, Villalobos M, Pedraza V, Steel GG. Initial radiation-induced DNA damage in human tumour cell lines: a correlation with intrinsic cellular radiosensitivity. *Br. J. Cancer* **69:** 457-462, 1994.

Russell KJ, Wiens LW, Demers GW, Galloway DA, Plon SE, Groudine M. Abrogation of the $G_2$ checkpoint results in differential radiosensitisation of $G_1$ checkpoint-deficient and $G_1$ checkpoint-competent cells. *Cancer Res.* **55:** 1639-1642, 1995.

Russell KJ, Wiens LW, Demers GW, Galloway DA, Le Tiep BA, Rice GC, Bianco JA, Singer JW, Groudine M. Preferential radiosensitisation of $G_1$ checkpoint-deficient cells by methylxanthines. *Int. J. Radiat. Oncol. Biol. Phys.* **36:** 1099-1106, 1996.

Sayah F, Idaomar M, Soranzo L, Karlinsky A. Endocrine and neuroendocrine effects of azadirachtin in adult females of the earwig *Labidura riparia*. *Tissue Cell* **30:** 86-94, 1998.

Schmid E, Zitzelsberger H, Braselmann H, Gray JW, Bauchinger M. Radiation-induced chromosome aberrations analysed by fluorescence *in situ* hybridization with a triple combination of composite whole chromosome-specific DNA probes. *Int. J. Radiat. Biol.* **62:** 673-678, 1992.

Schmutterer H. The neem tree. Source of unique natural products for integrated pest management, medicine, industry and other purposes. *VCH Verlagsgesellschaft*, Weinheim, Germany, 1995.

Schwab M, Alitalo K, Klempnauer K-H, Varmus HE, Bishop JM, Gilbert F, Brodeur G, Golstein M, Trent J. Amplified DNA with limited homology to *myc* cellular oncogene is shared by human neuroblastoma cell lines and a neuroblastoma tumour. *Nature* **305:** 245-248, 1983.

Schwartz JL, Vaughan ATM. Association between DNA/chromosome break rejoining rates, chromatin structure alterations and radiation sensitivity in human tumour cell lines. *Cancer Res.* **49:** 5054-5057, 1989.

Schwartz JL, Cowan J, Grdina DJ, Weichselbaum RR. Attenuation of $G_2$-phase cell cycle checkpoint control is associated with increased frequencies of unrejoined chromosome breaks in human tumour cells. *Radiat. Res.* **146:** 139-143, 1996.

Scott D, Zampetti-Bosseler. The relationship between cell killing, chromosome aberration, spindle defects and mitotic delay in mouse lymphoma cells of different sensitivity to X-rays. *Int. J. Radiat. Biol.* **37:** 33-47, 1980.

Selby PJ, Courtenay D. In vitro cellular radiosensitivity of human malignant melanoma xenografts. *Int. J. Radiat. Oncol. Biol. Phys.* **8:** 1235-1237, 1982.

Sigma: Product brochure. Biochemicals and reagents for life science research, 1999.

Singh K, Singh A, Singh DK. Molluscicidal activity of neem (*azadirachtin indica A. Juss*). *J. Ethnopharmacol.* **52:** 35-40, 1996.

Shibamoto Y, Nishimoto S, Mi F, Sasai K, Kagiya T, Abe M. Evaluation of various types of new hypoxic cell sensitizers using the EMT6 single cell-spheroid-solid tumour system. *Int. J. Radiat. Biol.* **52:** 347-357, 1987.

Shibamoto Y, Nishimoto S, Shimokawa K, Hisanaga Y, Zhou L, Wang J, Sasai K, Takahashi M, Abe M, Kagiya T. Characteristics of fluorinated nitroazoles as hypoxic cell radiosensitizers. *Int. J. Radiat. Oncol. Biol. Phys.* **16:** 1045-1048, 1989.

Shibamoto Y, Streffer C. Estimation of the dividing fraction and potential doubling time of tumours using cytochalasin B. *Cancer. Res.* **51:** 5134-5138, 1991.

Shibamoto Y, Streffer C, Fuhrmann C, Budach V. Tumour radiosensitivity prediction by the cytokinesis-block micronucleus assay. *Radiat. Res.* **128:** 293-300, 1991.

Shibamoto Y, Streffer C, Sasai K, Oya N, Abe M. Radiosensitization efficacy of KU-2285, RP-170 and etanidazole at low radiation doses: assessment by *in vitro* cytokinesis-block micronucleus assay. *Int. J. Radiat. Biol.* **61:** 473-478, 1992.

Shibamoto Y, Shibata T, Miyatake S, Oda Y, Manabe T, Ohshio G, Yagi K, Streffer C, Takahashi M, Abe M. Assessment of the proliferative activity and radiosensitivity of human tumours using the cytokinesis-block assay. *Br. J. Cancer* **70:** 67-71, 1994.

Skarsgard LD, Harrison I, Durand RE, Palcic B. Radiosensitization of hypoxic cells at low doses. *Int. J. Radiat. Oncol. Biol. Phys.* **12:** 1075-1078, 1986.

Skarsgard LD, Skwarchuk MW, Wouters BG. The survival of asynchronous V79 cell at low radiation doses: modelling the response of mixed cell populations. *Radiat. Res.* **138:** S72-S75, 1994.

Skarsgard LD, Skwarchuk MW, Wouters BG, Durand RE. Substructure in the radiation survival response at low dose in cells of human tumour cell lines. *Radiat. Res.* **146:** 388-398, 1996.

Slabbert JP, Theron T, Serafin A, Jones DTL, Böhm L, Schmitt G. Radiosensitivity variations in human tumour cell lines exposed *in vitro* to p(66/$Be^{+}$) neutrons or $^{60}Co$ $\gamma$-rays. *Strahlenther. Onkol.* **172:** 567-572, 1996.

Smeets MFHA, Mooren EHM, Begg AC. Radiation-induced DNA damage and repair in radiosensitive and radioresistant human tumour cells measured by field inversion gel electrophoresis. *Int. J. Radiat. Biol.* **63:** 703-713, 1993.

Smith SB, Aldridge PK, Callus JB. Observation of individual DNA molecules undergoing gel electrophoresis. *Science* **243:** 203-206, 1989.

Stark JD, Tanigoshi L, Bounfour M, Antonelli A. Reproductive potential: its influence on the susceptibility of a species to pesticides. *Ecotoxicol. Environ. Saf.* **37:** 273-279, 1997.

Steel GG, Courtenay VC, Beckham MJ: The response to chemotherapy of a variety of human tumour xenografts. *Br. J. Cancer* **47:** 1-113, 1983.

Stephens LC, Ang KK, Schultheiss TE, Milas L, Meyn RE. Apoptosis in irradiated murine tumours. *Radiat. Res.* **127:** 308-316, 1991.

Stephens LC, Hunter NR, Ang KK, Milas L, Meyn RE. Development of apoptosis in irradiated murine tumours as a function of time and dose. *Radiat. Res.* **135:** 75-80, 1993.

Stratford IJ, Adams GE, Hardy C, Hoe S, O'Neill P, Sheldon PW. Thiol reactive nitroimidazoles: radiosensitization studies *in vitro* and *in vivo*. *Int. J. Radiat. Biol.* **46:** 731-745, 1984

Stuschke M, Budach V, Klaes W, Sack H. Radiosensitivity, repair capacity, and stem cell fraction in human soft tissue tumours: An *in vitro* study using multicellular spheroids and colony assay. *Int. J. Radiat. Oncol. Biol. Phys.* **23:** 69-80, 1992.

Stuschke M, Budach V, Kalff RL, Sack H, Bamberg M, Reinhardt V, Feldmann HJ. Spheroid control of malignant glioma cell lines after fractionated irradiation: relation to survival fraction at 2 Gy and colony forming deficiencies in soft agar clonegenic assay. *Radiother. Oncol.* **27:** 245-251, 1993.

Su T, Mulla MS. Ovicidal activity of neem products (azadirachtin) against *Culex tarsalis* and *Culex quinquefasciatus* (*Diptera: Culicidae*). *J. Am. Mosq. Control Assoc.* **14:** 204-209, 1998.

Sutherland RM, Inch WR, McCredie JA, Kruuv J. A multi-component radiation survival curve using an *in vitro* tumour model. *Int. J. Radiat. Biol.* **18:** 491-495, 1970.

Sutherland RM, McCredie JA, Inch WR. Growth of multicell spheroids in tissue culture as a model of nodular carcinomas. *J. Natl. Cancer Inst.* **46:** 113-120, 1971.

Sutherland RM, Sordat B, Bamat J, Gabbert H, Bourrat B, Mueller-Klieser W. Oxygenation and differentiation in multicellular spheroids of human colon carcinomas. *Cancer Res.* **46:** 5320-5329, 1986.

Tates AD, de Vogel N, Rotteveel AH, Leupe F, Davids JA. The response of spermatogonia and spermatocytes of the Northern vole *Microtus oeconomus* to the induction of sex-chromosome nondisjunction, diploidy and chromosome breakage by X-rays and fast fission neutrons. *Mutat. Res.* **210:** 173-189, 1989.

Tauchi H, Sawada S. Analysis of mitotic cell death caused by radiation in mouse leukaemia L5178Y cells: apoptosis is the ultimate form of cell death following mitotic failure. *Int. J. Radiat. Biol.* **65:** 449-455, 1994.

Taylor YC, Brown JM. Radiosensitization in multifraction schedules. II. Greater sensitization by 2-nitroimidazoles than by oxygen. *Radiat. Res.* **112:** 134-145, 1987.

Theron T, Böhm L. Cyclin B1 expression in response to abrogation of the radiation-induced $G_2$/M block in HeLa cells. *Cell Prolif.* **31:** 49-57, 1998.

Theron T, Böhm L. Influence of the $G_2$ cell cycle block abrogator pentoxifylline on the expression and subcellular location of cyclin B1 and $p34^{cdc2}$ in HeLa cervical carcinoma cells. *Cell Prolif.* **33:** 39-50, 2000.

Theron T, Binder A, Verheye-Dua F, Böhm L. The role of $G_2$-block abrogation, DNA double-strand break repair and apoptosis in the radiosensitisation of melanoma and squamous cell carcinoma cell lines by pentoxifylline. *Int. J. Radiat. Biol.* **76:** 1197-1208, 2000.

Thoday JM. The effect of ionizing radiation on the broad bean root. Part IX. Chromosome breakage and the lethality of ionizing radiations to the root meristem. *Br. J. Radiol.* **2:** 572-576, 622-628, 1951.

Tofilon PJ, Vines CM, Bill CA. Enhancement of radiation-induced DNA double-strand breaks and micronuclei in human colon carcinoma cells by *N*-methylformide. *Radiat. Res.* **119:** 166-175, 1989.

Tsuboi K, Tsuchida Y, Nose T, Ando K. Cytotoxic effect of accelerated carbon beams in glioblastoma cell line with p53 mutation: clonogenic survival and cell cycle analysis. *Int. J. Radiat. Biol.* **74:** 71-79, 1998.

Utley JF, Marlowe C, Waddell WJ. Distribution of $^{35}$S-labeled WR-2721 in normal and malignant tissues of the mouse. *Radiat. Res.* **68:** 284-291, 1976.

van Beuningen D, Streffer C, Bertholdt G. Mikronukleusbildung im Vergleich zur Überlebensrate von menschlichen Melanomzellen nach Röntgen-, Neutronenbestrahlung und Hyperthermie. *Strahlentherapie* **157:** 600-606, 1981.

Vaupel P, Kallinowski F, Okunieff P. Blood flow, oxygenation and nutrient supply, and metabolic microenvironment of human tumours: A review. *Cancer Res.* **49:** 6449-6465, 1989.

Vernimmen F, Verheye-Dua F, du Toit H, Böhm L. Effect of pentoxifylline on radiation damage and tumour growth. *Strahlenther. Onkol.* **10:** 595-601, 1994.

Villa R, Zaffaroni N, Gornati D, Costa A, Silvestrini R. Lack of correlation between micronucleus formation and radiosensitivity in established and primary cultures of human tumours. *Br. J Cancer* **70:** 1112-1117, 1994.

Vral A, Verhaegen F, Thierens H, De-Ridder L. Micronuclei induced by fast neutrons versus $^{60}Co$ gamma-rays in human peripheral blood lymphocytes. *Int. J. Radiat. Biol.* **65:** 321-328, 1994.

Wandl EO, Ono K, Kain R, Herbsthofer T, Hienert G, Höbarth K. Linear correlation between surviving fraction and the micronucleus frequency. *Int. J. Radiat. Biol.* **56:** 771-775, 1989.

Warenius HM, Britten RA, Browning PG, Morton IE, Peacock JH. Identification of human *in vitro* cell lines with greater intrinsic cellular radiosensitivity to 62.5 MeV ($p \rightarrow Be^{+}$) neutrons than 4 MeV photons. *Int. J. Radiat. Oncol. Biol. Phys.* **28:** 913-920, 1994.

Washburn LC, Carlton JE, Hayes RL. Distribution of WR-2721 in normal and malignant tissues of mice and rats bearing solid tumours: dependence on tumour type, drug dose, and species. *Radiat. Res.* **59:** 475-483, 1974.

Weichselbuaum RR. Radioresistant and repair proficient cells may determine radiocurability in human tumours. *Int. J. Radiat. Oncol. Biol. Phys.* **12:** 637-639, 1986.

Weichselbuaum RR, Rotmensch J, Ahmed-Swan S, Beckett MA. Radiobiological characterization of 53 human tumour cell lines. *Int. J. Radiat. Biol.* **56:** 553-560, 1989.

Weil MM, Amos CI, Mason KA, Stephens LC. Genetic basis of strain variation in levels of radiation-induced apoptosis of thymocytes. *Radiat. Res.* **146:** 646-651, 1996.

West CML, Davidson SE, Roberts SA, Hunter RD. Intrinsic radiosensitivity and prediction of patient response to radiotherapy for carcinoma of the cervix. *Brit. J. Cancer* **68:** 819-823, 1993.

Westphal M, Hansel M, Müller D, Laas R, Kunzmann R, Rohde E, Koenig A, Holzel F, Herrmann H-D. Biological and karyotypic characteristics of a new cell line drived from human gliosarcoma. *Cancer Res.* **48:** 731-740, 1988.

Whillans DW, Rauth AM. An experimental and analytical study of oxygen depletion in stirred cell suspensions. *Radiat. Res.* **84:** 97-114, 1980.

Whitaker SJ, Ung YC, McMillan TJ. DNA double strand break induction and rejoining as determinants of human tumour cell radiosensitivity: A pulsed field gel electrophoresis study. *Int. J. Radiat. Biol.* **67:** 7-18, 1995.

Widel M, Przybyszewski WM. Inverse dose-rate effect for the induction of micronuclei in Lewis lung carcinoma after exposure to cobalt-60 gamma rays. *Radiat. Res.* **149:** 98-102, 1998.

Wlodek D, Hittelman WN. The repair of double-strand DNA breaks correlates with radiosensitivity of L5178Y-S and L5178Y-R cells. *Radiat. Res.* **112:** 146-155, 1987.

Wlodek D, Hittelman WN. The relationship of DNA and chromosome damage to survival of synchronized x-irradiated L5178Y cells. I. Initial Damage. *Radiat. Res.* **115:** 550-565, 1988a.

Wlodek D, Hittelman WN. The relationship of DNA and chromosome damage to survival of synchronized x-irradiated L5178Y cells. II. Repair. *Radiat. Res.* **115:** 566-575, 1988b.

Yuhas JM, Tarleton AE, Molzen KB: Multicellular tumour spheroid formation by breast cancer cells isolated from different sites. *Cancer Res.* **38:** 2486-2491, 1978.

Yuhas JM. Active versus passive absorption kinetics as the basis for selective protection of normal tissues by S-2-(3-aminopropylamino)-ethyl-phosphorothioic acid. *Cancer Res.* **40:** 1519-1524, 1980.

Yuhas JM, Blake S, Weichselbaum RR. Quantitation of the response of human tumour spheroids to daily radiation exposures. *Int. J. Radiat. Oncol. Biol. Phys.* **10:** 2323-2327, 1984.

Zaffaroni N, Orland L, Villa R, Bearzatto A, Rofstad EK, Silvistrini R. DNA double strand break repair and radiation response in human tumour primary cultures. *Int. J. Radiat. Biol.* **66:** 279-285, 1994.

Zywietz F. Vascular and cellular damage in a murine tumour during fractionated treatment with radiation and hyperthermia. *Strahlenther. Onkol.* **166:** 493-501, 1990.

Zywietz F, Reeker W, Kochs E. Tumour oxygenation in a transplanted rat rhabdomyosarcoma during fractionated irradiation. *Int. J. Radiat. Oncol. Biol. Phys.* **32:** 1391-1400, 1995.